Modelling and Control Techniques for Patient General Anaesthesia

Novais Carvalho Araujo, Hugo Filipe

Awarding institution:
King's College London

Modelling and Control Techniques for Patient General Anaesthesia

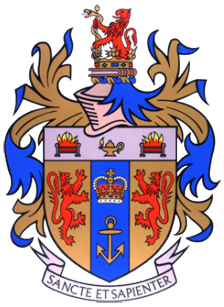

Hugo Filipe Novais Carvalho Araujo

Department of Informatics

King's College London

A thesis submitted for the degree of

Doctor of Philosophy

April 2014

Acknowledgements

This work would not have been possible without the help of many people.

I am grateful to my supervisor, Dr. Hak-Keung Lam, for his support and guidance since he become my principal supervisor, having always a word of advice when I felt lost throughout this research project. I also thank Dr. Catarina Nunes for her support and advise upon my research with her knowledge and experience. I will be forever thankful for her help in applying for this opportunity and start the supervision of my PhD.

I also thank Dr. David Green from King's College Hospital who always had kind words of encouragement. His help in gathering all the clinical data and his constant availability to always give feedback on clinical experience can not be understated. Thank you to all the anaesthesiologist trainees I had the opportunity to work with during my visits to King's College Hospital who always have been so helpful.

I would like to thank Fundação para a Ciência e Tecnologia, the Portuguese Foundation for Science and Technology, for their financial support during the course of this research through their PhD studentship (grant number SFHR/BD/44162/2008) which is co-financed

by the European Social Fund in the POPH framework.

My gratitude to colleague at King's at Embankment office which throughout the years have become friends, especially to Andreas, Angela, Ankur, Dimitris, João, Neil and Vahid which always had a word of encouragement during our lunch breaks. I thank Natalia for her help in proof reading this thesis.

Lastly, but not least, I thank my parents and brother Helder who have been truly exceptional in their support and encouragement throughout my entire life. If it were not for their support many opportunities in my life would not have been taken.

Abstract

This thesis aim is to purpose the design of an automatic close-loop control system for general anaesthesia. General anaesthesia is achieved through the administration of pharmaceutical drugs, which produce an effect on patients undergoing surgery.

To achieve the aim of this research clinical data obtained from a set-up assembled at King's College Hospital and used for estimation and optimization of Pharmacodynamic (PD) models associating effect-site concentrations of propofol, remifentanil and cardiac output to BIS readings. These models were estimated using two techniques, Hill equation and support vector regressors (SVRs) based models. The use of SVRs as a modelling technique allows the incorporation of additional biological signals The SVR technique may produce a non-parametric model which does not guarantee total adequacy of the estimated model as a PD model, therefore a Model Adequacy Index was proposed to assess compliance of the estimated models based on the expected clinical behaviour.

PD models considering both pharmaceutical drugs estimated through the SVR technique and Gaussian radial basis kernel presents a considerably higher performance when compared to the estimated multi-drug Hill model.

Three proportional-integral-differential (PID) controllers are employed, namely linear PID controller, type-1 (T1) fuzzy PID controller and interval type-2 (IT2) fuzzy PID controller, to regulate the bispectral index using the nominal patient's model. The PID gains and membership functions are obtained using genetic algorithm (GA) by minimizing a cost function measuring the control performance. The best trained PID controllers are tested under different scenarios and compared in terms of control performance. Simulation results show that the IT2 fuzzy PID controller offers the best control strategy regulating the BIS index while the T1 fuzzy PID controller comes second.

Statement of contributions

According to the knowledge of the author, this thesis has the following contributions which are asserted to be original.

- Setup of clinical platform for synchronized clinical data at King's College Hospital, presented on Chapter 2. Clinical data has been recorded for a high number patients undergoing surgery and 42 of these cases was used in this thesis.
- Development of pharmacodynamic models using support vector regression techniques with the consideration of different kernel functions reported in Chapter 3.
- Application of non-parametric modelling technique to the pharmacodynamic modelling allowing the incorporation of additional variables. Pharmacodynamic model incorporation nominal cardiac output performance is reported in Chapter 3.
- Development of an index assessing the validity and adequacy of a SVR-based model as pharmacodynamic model based on clinical knowledge is discussed in Chapter 3.
- Design and testing of controllers for BIS index regulation including traditional PID controller, type-1 fuzzy PID controller and

interval type-2 fuzzy PID controller for administration of propofol and remifentanil based on estimated PK/PD models. These results are reported in Chapter 4.

List of Publications

Journals

1. H. Araujo, B. Xiao, C. Liu, Y. Zhao and H. K. Lam, "Design of type-1 and interval type-2 fuzzy PID control for anesthesia Using genetic algorithms", Journal of Intelligent Learning Systems and Applications, 2014, 6, 70-93.

2. H.K. Lam, U. Ekong, H. Liu , B. Xiao, H. Araujo, S.H. Ling and K.Y. Chan, "A study of neural-network-based classifiers for material classification", Neurocomputing, 2014, Volume 144, p. 367-377.

3. H. Araujo, H.K. Lam, D. Green and C. S. Nunes, "Support vector regressors: a novel approach for pharmacodynamic modelling during general anaesthesia", Medical & Biological Engineering & Computing, April 2014 (Submitted).

Conference Proceedings

1. H. Araujo, J. Gill, D.W. Green and E. Mills, "Pre-emptive strategy for haemodynamic optimization minimizes incidence of Triple Low in high risk vascular surgical patients", Proceedings of the 2014 Annual Meeting of the American Society Anesthesiologists, A1164, New Orleans, 11-15 October 2014, http://www.asaabstracts.com.

2. H. Araujo, D. Green, N. Ferreira, D. Amoako and G. Kunst, "Relationship between cardiac output, bispectral index and cerebral oxygen saturations in cardiac surgery", The 28th Annual Meeting of the European Association of Cardiothoracic Anaesthesiologists - Applied Cardiopulmonary Pathophysiology, Vol. 17, No. 2-2013, O-17, Barcelona, 6-8 June 2013.

3. H. Araujo, D. Green, C.S. Nunes, "Propofol requirements during BIS monitored total intravenous anaesthesia. The influence of cardiac output (CO) on the pharmacokinetic model", Proceedings of the 3rd World Congress of Total Intravenous Anesthesia and Target Controlled Infusion (TIVA-TCI 2011), Singapore, 31 March-2 April 2011.

4. H. Araujo, D. Green, C.S. Nunes, "Relationship between BIS, cardiac output and cerebral oxygenation during general anesthesia", Proceedings of the 2010 Annual Meeting of the American Society Anesthesiologists, A054, San Diego, 16-20 October 2010, http://www.asaabstracts.com.

Contents

List of Figures

List of Tables

Nomenclature

k_{ij}	Rate constants for distribution and elimination of drug
N	Negative
P	Positive
Z	Zero
BIS	Bispectral Index
DIA	Diastolic blood pressure
DOA	Depth of anaesthesia
ECG	Electrocardiograph
EEG	Electroencephalogram
EMG	Electromyography
FOU	Footprint of uncertainty
GA	Genetic algorithm
HR	Heart rate

LOC Loss of consciousness

MAE Mean absolute error

MAI Model adequacy index

MAP Mean arterial pressure

nCO Nominal cardiac ouput

NIBP Non invasive blood pressure

PD Pharmacodynamics

PID Proportional-integral-differential controller

PK Pharmacokinetics

PPV Pulse pressure variation

rSO_2 Cerebral regional oxygen saturation

SR Suppression ratio

SV Stroke volume

SVR Support vector regressors

SVV Stroke volume variation

SYS Systolic blood pressure

TCI Target controlled infusion

TIVA Total intravenous anaesthesia

TTPE Time to peak effect

ZOH Zero-order-hold

Chapter 1

Introduction

Anaesthesiologists provide an adequate general anaesthesia by continuously assessing and judging the state of patients based on various observations. Anaesthesia commonly depends on a combination of various drugs which presents a variety of interactions. Additionally patients' intra and inter-individual variability is also present as all these processes take place on a complex biological system, the human body, often throughout several hours. Due to all these characteristics, anaesthesiology is a complex control task which would benefit from an automatic control system which automatically adjusted the amounts of drugs infused to achieve a desired clinical effect. A reliable and robust patient model is required to design and develop such a system. Such a model would also prove beneficial for the understanding of drugs interactions and their effect upon the patient being anaesthetised.

1.1 General Anaeshtesia

The first public demonstration of general anaesthesia during surgery can be traced back to 16 October 1846; ether anaesthesia administrated by William T. G. Morton in the Massachusetts General Hospital in Boston [44]. After this event the word anaesthesia, which is derived from Greek for without-perception, was suggested to describe the effect observed. Ether anaesthesia was rapidly adopted around the world, having been successfully administrated in London two months following Morton's public demonstration. This event is widely considered the starting point of the anaesthesiology speciality.

1.1.1 Defining general anaesthesia

General anaesthesia is a reversible state where patients undergoing surgery are temporarily deprived of consciousness with the purpose of undergoing an operation without pain and creating good operating conditions for the surgeon. General anaesthesia is defined by three main components: unconsciousness, analgesia and muscle relaxation, which is conveyed through various behavioural effects such as amnesia, hypnosis, analgesia, immobility and dimmed automatic reflexes. Additionally homoeostasis and prevention of injuries are achieved through pharmacological manipulation of major organ systems. The clinical aim of general anaesthesia is to achieve an adequate mix of various drugs concentrations to produce the desired clinical effect while remaining below unsatisfactory toxicity levels [44].

Unconsciousness in general anaesthesia, also mentioned as hypnotic component of general anaesthesia, consists of a person being unaware, i.e. not having

perception, of himself/herself and unable to receive and process external information. Patients under general anaesthesia are expected to be in a state of unrousable unconsciousness, i.e. unable to be awoken despite applied stimulus. The depth of anesthesia (DOA) represents the level of consciousness [48]. Awareness during general anaesthesia, which consists of patients' consciousness during intra-operative events and following explicit recall, is a clinical complication that may have a serious impact on patients who experience it, such as post-traumatic stress disorder.

Analgesia, i.e. pain relief, is widely achieved during general anaesthesia through use of opioid drugs as they are able to block nociceptive information resulting from several noxious stimulus, such as skin incision, which patients are subjected to during surgical procedures. In the absence of an adequate analgesia component, the various noxious stimulus will prompt an undesired patients' nociceptive response. Additionally, the use of opioid in general anaesthesia can reduce somatic and autonomic responses.

Additional muscle relaxation is commonly achieved during general anaesthesia via administration of neuromuscular blockers ensuring patients paralysis. Patients' immobility needs are dependent on surgical procedures which should be taken into account in the administration of neuromuscular blockers in order to minimize its cardiovascular and respiratory side effects. Neuromuscular blockers are a value auxiliary drug in general anaesthesia however as neuromuscular blockers do not present amnesic nor analgesic properties there is a high risk of awareness during surgery with possible serious psychological consequences for the patients. In order to minimize this risk, depth of anaesthesia and level of analgesia should be continuously monitored and ensured. Muscle relaxation facilitate

tracheal intubation and provides optimal conditions for the surgeon having a important impact on the development of various surgeries.

Even through a single drug can be used to achieve general anaesthesia satisfying the three components, it may require doses which produce high haemodynamic depression. A balanced anaesthesia is the common practice where a combination of different drugs is used to provide the required levels for each of the anaesthetic components, such as an opioid and a neuromuscular blocker for the analgesia and muscle relaxation components respectively. However the use of a balanced anaesthesia introduces a drug interactions problem where the effect of a certain drug might be modified by the presence of another drug, amplifying or reducing its effect.

General anaesthesia is usually divided into three phases: induction, maintenance and recovery [16]. Induction is the first phase of anaesthesia where the aim is to produce an unrousable unconsciousness state in the patient in preparation to the surgical procedure. Maintenance phase follows induction and it is during this phase that the surgical procedure takes place. The last phase is recovery where a safe and comfortable return of consciousness is expected following the surgery.

A combination of pharmaceutical drugs of different classes, such as hypnotic, opioid and neuromuscular blockers, is used by anaesthesiologists to induce general anaesthesia during surgery with the aim of producing a balanced anaesthesia. Each administrated drug has an expected clinical effect due to its interactions with the patient under surgery. These interactions can be divided into pharmacokinetics (PK), the relation between the administrated dose and its concentration, and pharmacodynamics (PD), the relation between its concentration and

the clinical effect [1].

During induction a combined dose of pharmaceutical drugs high enough to obtain an unrousable unconsciousness state and achieve safe and comfortable conditions to perform endotracheal intubation or laryngeal mask airway insertion should be administrated to the patient. Induction is a critical phase of general anaesthesia where profound changes to patients' central nervous, respiratory and cardiovascular systems may occur and as such needs to be closely monitored and administration of the various pharmaceutical drugs performed in accordance with their evolution. Severe respiratory depression occurs during anaesthesia induction which creates the need for mechanical ventilation. Cardiovascular depression is also a common occurrence if no steps are taken to avoid it.

Following induction of anaesthesia, the anaesthesiologist maintains an adequate anaesthesia for the surgical procedure managing the levels of hypnotic, analgesic and muscle relaxation components while ensuring patient's overall homoeostasis though administration of various drugs, intravenous infusion of fluid or blood as required to maintain and manipulate haemodynamic stability and essential functions of major organ systems. Depending on the surgical procedure, this phase of anaesthesia may last several hours throughout which the anaesthesiologist's strategy might need to change and adapt to changes in the patient's condition.

Recovery is the last phase of general anaesthesia at the end of surgical procedure where the aim is a safe and comfortable return to consciousness and to normal bodily functions, such as spontaneous ventilation and reversal of muscle relaxation. Titration of hypnotic and neuromuscular blocker are stopped, however analgesia is still maintained in order to cope with the pain arising from the

performed surgical procedure. Depending on the surgical procedure recovery may occur in the operating theatre just after the end of surgery or hours later in a recovery unit. Various drugs are available to facilitate and reduce recovery time [5].

1.1.2 Propofol, Remifentanil and their effect

As mentioned in the previous section, a balanced anaesthesia is the standard practice for general anaesthesia. This entails the administration of various pharmaceutical drugs via inhalation or intravenous infusion or a combination both. Inhalational anaesthesia has been used since the mid-19th century with, for instance, nitrous oxide, isoflurane, and halothane as commonly used drugs [47]. Total intravenous anaesthesia (TIVA) is the practise of induction and maintenance of general anaesthesia solely recurring pharmaceutical drugs administrated to the patient through intravenous infusion with the following advantages[27]: provision of anesthesia separate from ventilation, reduced atmospheric pollution, rapid and clear-headed recovery, and so on. While inhalational anaesthesia is still frequently used, intravenous anaesthesia has become increasingly popular due to the rapid and safe transition [62].

Propofol, a drug with hypnotic properties, is the most commonly used intravenous anaesthetic drug today with the aim of providing the unconsciousness component of general anaesthesia. During TIVA the analgesic component is provided by the intravenous infusion of an opioid in addition to propofol, commonly remifentanil [33].

As previously mentioned, co-administration of more than one drug may pro-

duce additive, synergistic or infra-additive interactions producing a distinct clinical effect for the drugs combination. Mathematical models representing the drugs' joint pharmacodynamics can be used to describe these pharmacological interactions [46]. These interactions can also potentiate the side-effects of anaesthetic drugs, such as a decrease in the patient's haemodynamic parameters. Propofol and remifentanil have a synergistic interaction when jointly administrated.

The effect of the anaesthetic drugs on the central nervous system can be obtained by analysing the electroencephalogram (EEG) with measurements such as Bispectral Index (BIS) which is a processed EEG parameter calculated with the BIS algorithm [31]. Using time domain, frequency domain and bispectral analysis, the BIS algorithm combines various EEG features, which are highly correlated with hypnosis in the EEGs from more than 5000 adults subjects, to provide a reliable parameter for anaesthetic hypnosis. BIS index is a dimensionless number between 0 and 100 which correlates with the clinical state of the patient and is a good indicator of the the patient's cortical surpression [2, 31, 39]. There are several monitors such as BIS, all based in the EEG and using different signal processing techniques, but it is worth mentioning that they do not fully describe the state of conscious or unconsciouness, they are representative of the effect of the drugs on the EEG, which is in turn is used to assess the brain's activity.

1.2 Modelling and control for drug administration

The study of drug interactions is of major importance as it can provide guidelines to optimize drug administration during general anaesthesia and therefore reduces the amount of drug necessary and its recovery time. Modelling the effects of anaesthetic drugs would also enable anaesthetists to access simulation training through Human Patient Simulators which incorporated PK and PD models. Additionally, a better understanding of the anaesthetic drugs interactions and their effects on patients would provide useful information for the design of an automatic controller system for induction and maintenance of general anaesthesia, potentiating further improvements in patient safety.

Using population pharmacodynamic analysis, PD models [10, 21, 46, 61] for anaesthetic drugs have been estimated, but due to inter and intra-individual variability and the change in conditions caused by surgery, these may not reflect the most accurate assessment of the state of patient. During surgery, various surgical stimulus and perturbations, such as incision and blood loss, can occur which may have an impact on the drugs' potency and interaction power. These PD models are based on a defined sigmoid curve and cannot contemplate the surgical stimulus and perturbations nor other variables which may impact upon them. The incorporation of other factors and techniques may therefore be advisable.

The main difficulties involved in modelling are the determination of PD model parameters and the selection of the output index. In general, the parameters of PK and PD models need to be determined beforehand. For the PK model, parameters can be estimated depending on the sex, age, and weight of patients.

Nonetheless, for the PD model, it is not possible to estimate the parameters for certain patient. Accordingly, it requires the controller to be robust in a domain of PD model parameters [23]. Although PK model parameters are varied with patients and PD model parameters can change for just one patient, a general index can be designed to evaluate the DOA for all patients [34].

In general, control strategies can be categorized into two classes: open-loop control and closed-loop control. In the anaesthetic field, open-loop control is based on the knowledge and experience of anaesthetists who manually adjust the drug dosage to maintain the DOA assisted by some clinical indices of patients. In closed-loop control, the drug dosage is automatically adjusted according to some indices of DOA, which makes control input continuous and responsive [51]. Closed-loop control is also expected to avoid over- and under-dosage and suppress the adverse effect of inter-individual differences [32]. Despite its advantages, the stability of closed-loop control needs to be ensured due to the automated process without supervision [58].

To achieve the stabilization based on closed-loop control, the following components are required [59]: (1) a patient model, with an output as the index of DOA; (2) a controller for stabilization, such as proportional-integral-differential (PID) controllers. Therefore, to begin with, an estimated patient model is required to represent real patients supporting the control design and performance evaluation. A widely employed mathematical model consists of a linear PK model and a non-linear PD model [8]. The PK model uses the drug dosage as the input and the drug concentration as the output. In what follows, the PD model exploits the drug concentration as the input and exports the index of DOA.

With regard to the controllers for stabilization, several control problems are

faced with the closed-loop control of anesthesia: stability, which is the basic control objective; robustness, which overcomes the uncertainty of PD model parameters, measurement noise, surgical stimulation, and so forth; adaptiveness, which makes the controller adaptable to different patients rather than only one patient. Commonly used controllers include PID controllers, model-based controllers, and knowledge-based controllers [59].

To close the loop of control systems, the classical PID controller is undoubtedly option due to its successful applications in other areas. For stabilization, it is necessary to tune the parameters of PID controllers for a certain patient model. While the tuning process is an empirical manner, some tuning schemes have been developed to guarantee the robustness [19, 52]. Combined with patient model identification from the induction phase of anesthesia [57], the adaptiveness can be further achieved. In addition, combined with genetic algorithm (GA), the parameters of PID controllers can also be online optimized [55].

Despite various causes of the changes in PK and PD model parameters, the model-based controller relies on the current model which reflects the patient's current pharmacological behavior. For this reason, the patient model needs to be updated through the overall process of anesthesia. This online adaptation can be achieved by several approaches such as Kalman filter algorithm [53], Bayesian-based adaptive control [17], and adaptive genetic fuzzy clustering algorithm [55]. Alternatively, the variability of PK and PD models between individuals as well as surgical stimulation and anesthetic-analgesic interaction can be explicitly considered offline such that the stability is mathematically guaranteed [26]. Additionally, a Lyapunov-based adaptive controller has been developed to attain partial asymptotic regulation [24].

Unlike model-based controllers, knowledge-based controllers do not require a known mathematical model. In fuzzy logic controllers, for example, decisions are made based on fuzzy rules predefined by expert knowledge and experience. Compared with linear PID controllers and model-based controllers, knowledge-based controllers are easier to implement without tuning PID parameters or mathematical derivation. A hybrid control scheme, namely fuzzy-PID control, was developed to combine the merits of both control strategies [3]. Moreover, a multivariable neural-fuzzy controller was proposed to simultaneously administrate both propofol and remifentanil [40]. However, one problem of knowledge-based controllers is that the interaction of each piece of knowledge makes the controller less transparent and makes it difficult to achieve adaptive control [59]. To deal with this problem, a direct adaptive interval type-2 (IT2) fuzzy logic controller was proposed for multivariable anesthesia systems [20] and a genetic fuzzy logic controller was developed to adjust fuzzy rules using GA [55].

1.3 Project aims and objectives

This project aims to design a close-loop control system for general anaesthesia. To achieve this aim two objective were establish. A robust and reliable PK/PD model describing anaesthetic drugs interactions, namely hypnotic propofol and analgesic remifentanil using real clinical data from patients needs to be developed and to design a controller to administrate the drugs automatically to regulate the BIS index. To realize the project aim and objectives, the following step have been considered.

- Set up a clinical platform consisting of laptop running a data synchroniza-

tion and recording software developed by our research team, connected to various medical devices including *Alaris PK* infusion pumps, *BIS Vista* monitor, *LiDCOrapid* monitor and *INVOS* monitor.

- Collect patients' data for investigation. The data include BIS, propofol and remifentanil infusion rates and predicted concentration, brain regional oxygen saturation (rSO_2) and various haemodynamic parameters such as heart rate, blood pressures, nominal cardiac ouput (nCO) and stroke volume (SV).

- Determine the parameters of Hill's PD model using patient's data for comparison purposes. Genetic algorithm using different cost functions and least squares methods fitting were employed.

- Develop a more accurate PK/PD model using support vector regression techniques with the consideration of different kernel functions.

- Design an evaluation function to measure the modelling performance and validity of the developed support vector regressors (SVR)-based models.

- Based on the PK/PD model with the patient's parameters, control methodologies are designed to administrate the drugs for the regulation of BIS index. Various controllers including traditional PID controller, type-1 fuzzy PID controller and interval type-2 fuzzy PID controller are considered.

- Design a fitness function to measure the regulation performance of BIS index value.

- Apply genetic algorithm to determine the controller gains by optimizing the fitness function.

To summarize, the PK/PD model is employed to describe the dynamics of patient's body responding to the hypnotic propofol and analgesic remifentanil. By investigating the closed-loop system formed by the PK/PD model and a controller, a control methodology is proposed to administrate the drugs controlling its inflow to the patient's body such that BIS index regulation can be regulated.

1.4 Thesis structure

This thesis is divided into five chapters, one appendix and references. A brief explanation of the contents of each chapter is presented below.

Chapter 2 discuss the set up implemented at King's College Hospital for data collection, a description of the clinical protocol followed by the anaesthesiologist to induce general anaesthesia. Technical details for published PK/PD models are also explained in the chapters with the description of PK models implementation in MATLAB for the porpuse of simulation for support of this project.

Chapter 3 introduces the estimation of PD models from clinical data. Two approaches are studied in this thesis, a parametric technique based on the Hill equation and a non-parametric one based on the use of SVRs. Using SVRs to develop a PD model enables the incorporation of additional biological variables into the PD model. However adequacy of the estimated models needs to be assessed, and a index is described in order to measure adequacy.

In chapter 4, various proposed control methodologies such as, linear PID controller, type-1 (T1) fuzzy PID controller and interval type-2 (IT2) fuzzy PID

controller, are discussed and the results obtained in simulation environment supported by estimated PD model on the previous chapter are presented.

The final chapter presents the conclusion of the research and sets recommendations for future work.

In the appendix an initial continuous in time simulink implementation of the 3-compartmental PK model in MATLAB is presented.

Chapter 2

Anaesthesia Protocol and Clinical Setup

2.1 Introduction

Administration of an adequate general anaesthesia is a complex art that requires the anaesthesiologist to continuously analyse and make judgements about the state of the patient based upon a variety of observations, clinical monitors and drugs administrated to the patient. A system allowing continuous collection of clinical data observed by the anaesthesiologist is therefore an invaluable tool for this research project.

2.2 Clinical Protocol

Before induction of anaesthesia, intravenous access with a plastic cannula is obtained. Various anaesthetic drugs and fluids are administrated through it during

the surgery. Standard anaesthetic monitoring is also initiated pre-induction which includes pulse oximeter, non invasive blood pressure (NIBP), electrocardiograph (ECG), airway gases and pressure. In addition to standard anaesthetic monitoring, right cerebral regional oxygen saturation, BIS index and various haemodynamic parameters obtained from *LiDCOrapid* monitor (LiDCO PLC, London, UK) are also monitored pre-induction. Details of non-standard anaesthetic monitoring is discussed on Section 2.3.

Patients receive TIVA with propofol and remifentanil target controlled infusion (TCI) by two *Alaris*® *PK* infusion pumps using Marsh [41] and Minto [45] PK models respectively. For details of TCI refer to Section 2.4.1.2.

Induction starts with a remifentanil plasmatic concentration (Cp_{remi}) target of 3 ng/ml. When remifentanil effect-site concentration (Ce_{remi}) of 2 ng/ml is reached, Cp_{remi} target is adjusted to 2 ng/ml and propofol infusion is started with a propofol plasmatic concentration (Cp_{prop}) target of 3 μg/ml and adjusted therefore according to BIS index readings in order to BIS reach the interval 40 to 60. Loss of consciousness (LOC), i.e. the patient stops responding to verbal commands and mechanical stimulus, is expected to have happened by this point. A neuromuscular blocker, usually cisatracurium, is also simultaneously manually infused.

Once BIS index below or around value 50 is achieved for a period of 2 minutes, laryngeal mask airway insertion takes place. Therefore, propofol and remifentanil plasma concentration targets are manually adjusted by the anaesthetist during surgery according to readings of the various clinical monitoring equipments, the expected effect of administrated anaesthetic drugs and noxious stimulus expected to take place in order to provide an adequate general anaesthesia.

Throughout surgery additional drugs or fluids are administrated to maintain homoeostasis according to the judgement of the anaesthesiologist. For example, nCO is monitored during all stages of surgery, and the anaesthetist takes the necessary steps, such as performing a fluid challenge which involves a rapid infusion of 250 ml of colloid fluid to ensure the nCO is maintained at a stable condition at or near pre-induction level.

Once the end of surgery is approaching, additional analgesic drugs are administrated to the patient to ensure analgesia is present when the patient recovers consciousness to cope with the pain arising from the surgical wound. These depend on the degree of pain anticipated from the surgery and might be intravenous paracetamol or morphine, for example.

Once the state of general anaesthesia is no longer necessary, the infusion of propofol and remifentanil are stopped and the anaesthesiologist ensures that a smooth, safe and comfortable recovery takes place.

2.3 Setup at King's College Hospital

One of the essential components of this project is recording data from the patient immediately before, during and immediately after the administration of general anaesthesia in the operating theatre. The analysis of collected data will enable the extraction of information showing signals that are relevant to establish the state of the patient. The data recorded during surgery is also indispensable to develop and establish accurate and robust PK/PD models and assist with the design and simulation of an automatic controller.

To achieve this target, a system (Figure 2.1) was assembled at King's Col-

lege Hospital comprising of a laptop connected to various medical devices for continuous data collection during the entire duration of general anaesthesia.

Figure 2.1: Data recording set-up system at King's College Hospital operating theatre.

ASYS (Anesthesia Synchronization Software) [9] (Figure 2.2), a data acquisition software developed by our research team, runs on the laptop recording the values it receives from various medical devices it is connected to every 5 seconds, two *Alaris PK* infusion pumps, *BIS Vista* monitor, *LiDCOrapid* monitor and *INVOS* monitor (Figure 2.3). None of these devices is controlled or its behaviour is in any way affected by ASYS as it only records the data provided by these

devices and the anaesthetist has complete access and control over all monitoring equipment.

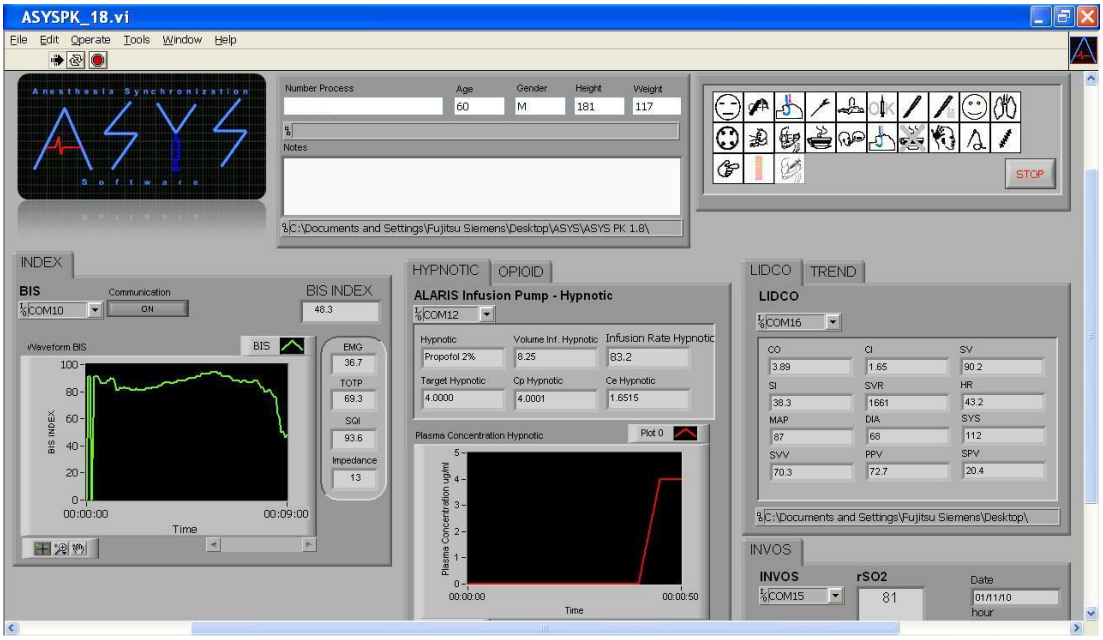

Figure 2.2: Data record software ASYS.

The *Alaris PK* infusion pumps are the devices which regulate the infusion of anaesthetic drugs propofol and remifentanil with the built-in TCI algorithm. From the infusion pumps, ASYS records the current plasma target concentration (Cp_t) defined by the anaesthetist, the current plasma concentration and effect-site concentration estimated by the pump PK model, the current infusion rate and the amount of drugs administrated since the beginning of infusion.

BIS Vista monitor provides BIS index which is a processed EEG parameter calculated by BIS algorithm. Using time domain, frequency domain and bispectral analysis, the BIS algorithm combines various EEG features which are highly

Figure 2.3: Medical devices that comprise setup for data recording at King's College Hospital. *Alaris PK* infusion pump (left upper image) [11]. *BIS Vista* monitoring system (left bottom image) [15]. *LiDCOrapid* monitor (right upper image) [38]. *INVOS* monitor (right bottom image)[14].

correlated with hypnosis in the EEGs from more than 5000 adults subjects. The BIS index is a dimensionless number between 0 and 100 which correlates with the clinical state of the patient and is a good indicator of patients' unconsciousness (Figure 2.4) [2, 31]. ASYS records the BIS index, electromyography (EMG) and suppression ratio (SR) of EEG from this device.

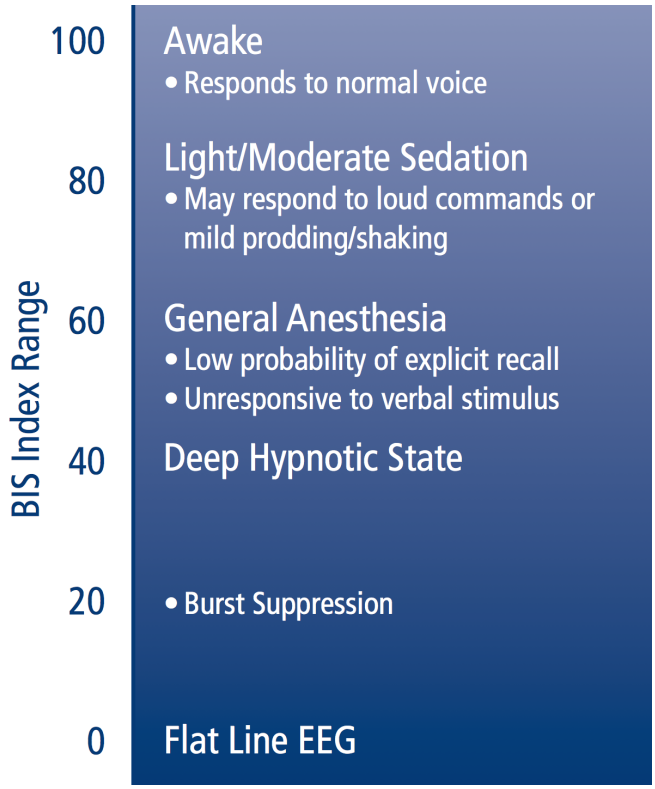

Figure 2.4: BIS range guidelines [31].

LiDCOrapid monitors patient's fluid and hemodynamic status by analyzing and processing the continuous arterial pressure waveform obtained from an radial arterial line placed pre-induction. Patient's fluid and hemodynamic status is showed by various cardio-vascular parameters, such as heart rate (HR), systolic (SYS), mean (MAP) and diastolic (DIA) blood pressure, SV, nCO, pulse pressure

variation (PPV) and stroke volume variation (SVV). All these cardio-vascular parameters are recorded with ASYS throughout surgery including pre-induction baselines.

INVOS is a regional oxymetry monitor which provides the regional blood oxygen saturation (varies between 0 and 100%) in cerebral and somatic tissue. The measurement follows a non-invasive method where a sensor is placed in the patient. For this research project right-side oxygen saturation (rSO_2) is assessed on the right side of the brain as the brain is susceptible to oxygen deprivation. rSO_2 provides tangible information about cerebral perfusion which can be used in conjunction with other variables to avoid cerebral ischemia. Only the saturation value is recorded by ASYS. Pre-induction *INVOS* and *BIS* 4 electrode sensors are attached to the right and left sides of the patient's forehead, respectevely, to obtain baseline readings on all clinical monitors.

During the installation and configuration of the system, the anaesthetist Dr David Green made some suggestions and gave advice on which features would be useful to include in the system. A close contact was maintained with the ASYS developer to adjust these features throughout this research project.

Data records are compiled of patients undergoing surgery under general anaesthesia administrated by Dr David Green. Usually, data are collected every week with my presence in the operating theatre from one or two patients undergoing vascular surgery. ASYS automatically records the data from the connected devices every five seconds and the laptop user has the responsibility of registering on ASYS any event which may have any importance on the patients state, like the start of incision or the administration of other drugs, for example ephedrine. The data recording process does not interfere in any way with the usual and standard

practise of the anaesthetist. Local ethical committee approval was sought but was not deemed necessary as the procedures carried out were normal practice at King's College Hospital.

2.4 Pharmacokinetic / Pharmacodynamic Model - Technical details

2.4.1 Pharmacokinetic Model

The pharmacokinetics of a drug is the relation between the dose administered and its concentration in the blood. Pharmacokinetics is usually defined as what the body does to the drug. A PK model is a mathematical model of this relationship, which describes the process of drug distribution and elimination. It can be used to predict the blood/plasma concentration and effect-site concentration profile of a drug after its administration whether by bolus or infusion [1].

The PK models for most of the drugs are multi-compartmental. The one- and two-compartment models can be used to describe the pharmacokinetics behaviour of drugs within a large therapeutic window. However for a PK model of the hypnotic and analgesic drugs administrated intravenously for general anaesthesia, particularly propofol and remifentanil, a three-compartmental structure is usually used (Figure 2.5) [22].

Drug metabolism and distribution rates can be expressed by rate constants, which represent the proportion of drug suffering elimination or distribution during a unit of time. The drug is infused in the patient at a rate $r(t)$ (mg/min). By convention the compartment into which the drug is injected is called central

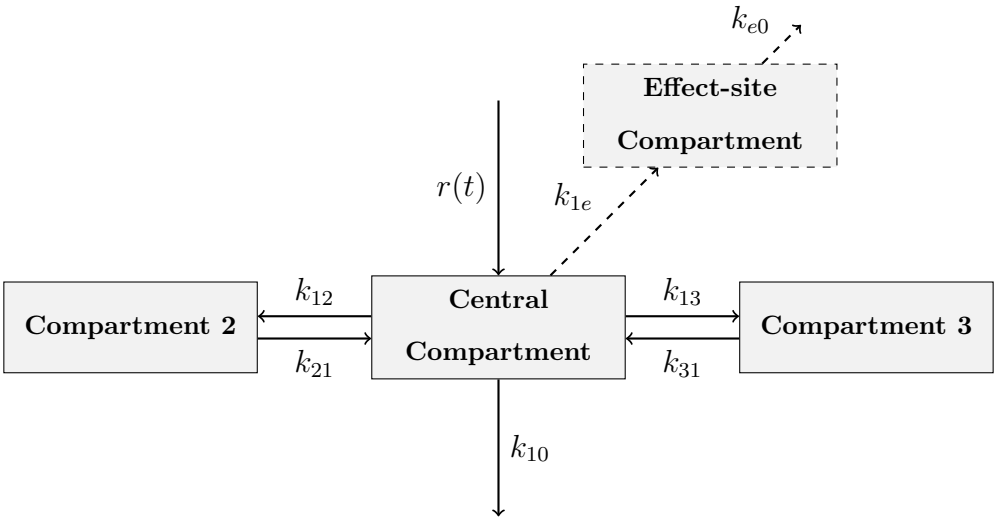

Figure 2.5: Structure of a three-compartmental with effect-site compartment pharmacokinetic model. $r(t)$ is the infusion rate of the drug, k_{10}, k_{12}, k_{13}, k_{21}, k_{31}, k_{1e} and k_{e0} are rate constants for distribution and elimination of the drug.[1]

compartment and its volume, V_1 (l), is the initial volume of distribution. There is a rapid drug re-distribution between the central compartment and compartment 2 defined by the rate constants k_{12} (min^{-1}) and k_{21} (min^{-1}) and a slower drug distribution between the central compartment and compartment 3 described by the rate constants k_{13} (min^{-1}) and k_{31} (min^{-1}). The volumes of compartment 2 and 3 are represented by V_2 (l) and V_3 (l), respectively. The rate constant k_{10} (min^{-1}) represents the drug elimination from the central compartment [1].

The effect-site compartment is a hypothetical compartment, without volume by definition, used to describe the delay between the blood/plasma concentration and the effect-site concentration. Because of the definition of the effect-site compartment as a volume-less compartment, the rate constants k_{1e} and k_{e0} are equal. This subject will be further explained later. The changes in the amount of

drug in each of the three compartments can be described by the next differential equations [4]:

$$\begin{aligned} \frac{dm_1}{dt} &= r(t) - (k_{10} + k_{12} + k_{13})m_1(t) + k_{21}m_2(t) + k_{31}m_3(t) \\ \frac{dm_2}{dt} &= k_{12}m_1(t) - k_{21}m_2(t) \\ \frac{dm_2}{dt} &= k_{13}m_1(t) - k_{31}m_3(t) \end{aligned} \quad , \tag{2.1}$$

where $m_1(t)$ is mass of drug in the central compartment (mg); $m_2(t)$ is mass of drug in the compartment 2 (mg); $m_3(t)$ is mass of drug in the compartment 3 (mg); $r(t)$ is infusion rate (mg/min); k_{10}, k_{12}, k_{13}, k_{21}, k_{31} are rate constants for the transfer of drug (min^{-1}).

The blood/plasma concentration of the drug can be calculated dividing the mass of drug in the central compartment by its volume ($C_p(t) = (m_1(t)/V_1)$. The volumes of the compartments on the three-compartment model are theoretical volumes which are used to calculate the blood/plasma concentration of a drug, and they can not be associated with any anatomical or physiological meaning.

As referred to previously, there is a delay in time between the equilibration of the effect-site concentration and the blood/plasma concentration, time to peak effect (TTPE). Factors like cardiac output, cerebral blood flow and pharmacological properties of the drug influence the rate of equilibration between blood/plasma and effect-site. The parameter k_{e0} can describe the delay of the blood and effect-site equilibration, and the effect-site concentration can be obtained from the blood/plasma concentration using the following differential equation [50]:

$$\frac{dC_e}{dt} = k_{e0}C_p(t) - k_{e0}C_e(t), \tag{2.2}$$

where $C_p(t)$ is blood/plasma drug concentration (g/ml); $C_e(t)$ is effect-site drug concentration (g/ml) and k_{e0} is rate constant.

Since the PK of most anaesthetics appear to be linear, i.e. the shape of drug concentration decay and the derived pharmacokinetic parameters are unaffected by the dose, within clinical dosage, the pharmacokinetic parameters can be used to calculate the blood/plasma concentration generated by any bolus or infusion scheme [22].

2.4.1.1 Discretization of Pharmacokinetic (PK) models

One of the objective of this research project is to develop a digital controller and as the devices which it will be controlling work in a discrete time domain, discretization of the PK model is needed.

From the differential equations which describe the changes in the amount of drug in each of the three compartments and relate to the plasma concentration with the effect/site concentration, and converting time from minutes to seconds, a state space representation for the continuous time PK models, equation (2.3) can be obtained.

$$\begin{aligned} \dot{x}(t) &= Fx(t) + Gr(t) \\ y(t) &= Cx(t) \end{aligned}, \tag{2.3}$$

where $y(t) = \begin{bmatrix} C_p(t) \\ C_e(t) \end{bmatrix}$, $x(t) = \begin{bmatrix} m_1(t) \\ m_2(t) \\ m_3(t) \\ C_e(t) \end{bmatrix}$,

$$F = \frac{1}{60}\begin{bmatrix} -k_{10}-k_{12}-k_{13} & k_{21} & k_{31} & 0 \\ k_{12} & -k_{21} & 0 & 0 \\ k_{13} & -k_{31} & 0 & 0 \\ \frac{k_{e0}}{V_1} & 0 & 0 & -k_{e0} \end{bmatrix},$$

$$G = \frac{1}{60}\begin{bmatrix} 1 \\ 0 \\ 0 \\ 0 \end{bmatrix}, C = \begin{bmatrix} \frac{1}{V_1} & 0 & 0 & 0 \\ 0 & 0 & 0 & 1 \end{bmatrix}$$

k_{e0} (min^{-1}) is a parameter describing the delay in time of the plasmatic-effect-site drug concentration equilibration.

A zero order hold assumption for the PK models, this is, the input signal, infusion rate, does not experience any alteration during the sampling interval can be made. Also assuming that uniform sampling intervals, Ts, the state space representation for the discrete time PK models can be represented by equation (2.4) [49].

$$\begin{aligned} x_{[n+1]} &= Ax_{[n]} + Bu_{[n]} \\ y_{[n]} &= Cx_{[n]} + Du_{[n]} \end{aligned}, \tag{2.4}$$

where $y_{[n]} = \begin{bmatrix} C_p(nT_s) \\ C_e(nT_s) \end{bmatrix}$, $x_{[n]} = \begin{bmatrix} m_1(nT_s) \\ m_2(nT_s) \\ m_3(nT_s) \\ C_e(nT_s) \end{bmatrix}$, $u_{[n]} = r(nT_s)$,

$A = e^{FT_s}$, $B = \left[\int_0^{T_s} e^{Ft}dt\right] G = F^{-1}(A - I)G$

2.4.1.2 TCI Target controlled infusion

Using the PK models of the drug, TCI systems calculate the infusion rate necessary to obtain and maintain a desired blood/plasma concentration. The TCI systems follow an infusion scheme designated as BET (bolus-elimination-transfer). Initially a bolus is administrated to achieve the blood/plasma target concentration (Cpt) on the central compartment equation (2.5), following a continuous infusion with a rate of r(t), to compensate for the loss of the drug by the elimination process and replace the drug transferred between the central and peripheral compartments equation (2.6).[4]

$$LD = V_1 Cpt \tag{2.5}$$

$$r(t) = LD(k_{10} + k_{12}e^{-k_{21}t} + k_{13}e^{-k_{31}t}), \tag{2.6}$$

When the target concentration increases, the TCI system calculates a new initial bolus to increase the drug concentration in the central compartment from the previous blood/plasma target concentration to the new one equation (2.7), and recalculates the infusion rates associated with the elimination and transfer processes for the new target, considering the amount of the drug already present in the peripheral compartments equation (2.8).[60]

$$ADDLD = V_1(NCpt - Cpt), \tag{2.7}$$

$$r(t) = V_1 NCpt(k_{10} + k_{12}e^{-k_{21}(t-\tau)} + k_{13}e^{-k_{31}(t-\tau)}) \\ -(k_{21}m_2(\tau)e^{-k_{21}(t-\tau)} + k_{31}m_3(\tau)e^{-k_{31}(t-\tau)}) \quad , \tag{2.8}$$

where τ is the time of Cpt change; $m_2(\tau)$ (mg) is the amount of anaesthetic drug in the second compartment at the time of target change and $m_3(\tau)$ (mg) is the amount of anaesthetic drug in the third compartment at the time of target change.

If the target concentration decreases, the TCI system will stop the infusion until the new blood/plasma target concentration is achieved and restart the infusion at that moment with the new infusion rate obtained from equation (2.8).[4] However in the real world, it is necessary to consider the limitation of the infusions devices, such as a lack of infinity precision and the maximum infusion rate, and so continuous adjustments to the infusion rates are necessary.

2.4.2 Pharmacodynamic Modelling

The PK models described on the previous Subsection allows us to predict the effect-site concentrations of administrated anaesthetic drugs from their infusion profiles. In this Subsection the PD models are introduced which will relate the effect-site concentration with the effect that the anaesthetic drug exhibits over the patient, which is assessed as the degree of depression of the EEG (in the case of this research project measured by the *BIS Vista* monitor). It can be described as what the drug does to the body. The effect-site compartment refers to the PK model can also be considered as part of the PD model.

The typical method to describe the PD model is through a single variable Hill curve which is used to estimate a single drug parametric PD model using

optimization techniques. A multi variable Hill curve is also introduced which is used to estimate a two drugs PD model considering the drugs interactions.

2.4.2.1 Hill Model - One Drug

The pharmacodynamics of individual drugs are often modeled by a sigmoid E_{max} model called Hill curve described by the following equation [28]:

$$Effect(Ce) = E_0 + (E_{max} - E_0)\frac{Ce^{\gamma}}{Ce_{50}^{\gamma} + Ce^{\gamma}} \tag{2.9}$$

where E_0 is the clinical effect when no drug is present, E_{max} is the maximum drug effect, Ce_{50} is the effect-site drug concentration associated with 50% maximal drug potency, γ is the steepness of the concentration-response curve and Ce is the effect-site drug concentration.

For the case considered in this research project, where the effect of the anaesthetist is assessed though *BIS Vista* monitor, E_0 and E_{max} will have a value of 100 and 0, respectively. Ce_{50} and γ are the patient's dependent parameters to which there are no widely accepted parameters. In the project, these parameters are estimated from the clinical data recorded at King's College London using least square curve fitting and genetic algorithms optimization.

2.4.2.2 Hill Model - Two Drugs

In 2000, Minto *et al.* proposed [46] a response surface model, based on the Hill curve, to describe drugs' interaction when more than one drug is administrated. A joint pharmacodynamic model for the co-administration of propofol

and remifentanil can be described by the following equation [10]:

$$Effect(Ce_{prop}, Ce_{remi}) = E_0 + (E_{max} - E_0)\frac{\left(\frac{U_{prop}+U_{remi}}{U_{50}(\theta)}\right)^{\gamma}}{1+\left(\frac{U_{prop}+U_{remi}}{U_{50}(\theta)}\right)^{\gamma}} \tag{2.10}$$

where θ is the ratio of the two drugs defined by equation (2.11); and U_{prop} and U_{remi} are the normalized effect-site drug concentrations of propofol and remifentanil, respectively, defined in equation (2.12). $U_{50}(\theta)$ is defined by equation (2.13).

$$\theta = \frac{U_{prop}}{U_{prop} + U_{remi}} \tag{2.11}$$

$$U_{prop} = \frac{Ce_{prop}}{Ce_{50,prop}} \quad U_{remi} = \frac{Ce_{remi}}{Ce_{50,remi}} \tag{2.12}$$

$$U_{50}(\theta) = 1 - \beta\theta + \beta\theta^2 \tag{2.13}$$

Such as in the PD model of individual drugs, E_0 and E_{max} will have a value of 100 and 0, respectively. $Ce_{50,prop}$, $Ce_{50,remi}$, β and γ are patient's dependent parameters.

2.5 Implementation of the Pharmacokinetic model in MATLAB

During this research, a three-compartment pharmacokinetic model with effect-site compartment was implemented for use in simulation studies. Initially, it was

implemented using MATLAB and Simulink on its continuous representation using the differential equations which describe the changes of the amount of drug in each of the three compartments and relate to the plasma concentration with the effect/site concentration, see Appendix A. This model was implemented with the model parameters as variables, which permit the simulation of the PK behaviour of different drugs, and with the possibility to define up to 4 different infusion rates.

Two different well-known PK models for propofol, Marsh and Schnider models (tables 3.1 and 3.2), can predict different blood/plasma drug concentrations and effect-site drug concentrations (Figure 2.6 and 2.7) even using the same infusion scheme for the same patient. Therefore it is important to analyze these models and propose adjustments if justified, since the blood/plasma drug concentrations are related to the effect of anaesthetic agents [60].

Analyzing Figure 2.6 and 2.7, it is possible to observe that the changes in the infusion rate are reproduced faster in the plasma concentration and effect-site concentration of propofol with the Schnider model [54] than with the Marsh model [41]. When a high infusion rate was used for a short time the peak of blood/plasma concentration of propofol was much higher in the simulation using Schnider model. This also happens in the effect-site concentration.

Over all the simulation time, it is possible to observe that the plasma and effect-site concentration of propofol is higher when a Schnider model is used to estimate the drug concentrations. This is not true only after a decrease of the infusion rate where the plasma concentration and effect-site concentration is higher in simulation with the Marsh model. This is due to the slower time of response in the Marsh model, which makes the decrease of drug concentrations

slower.

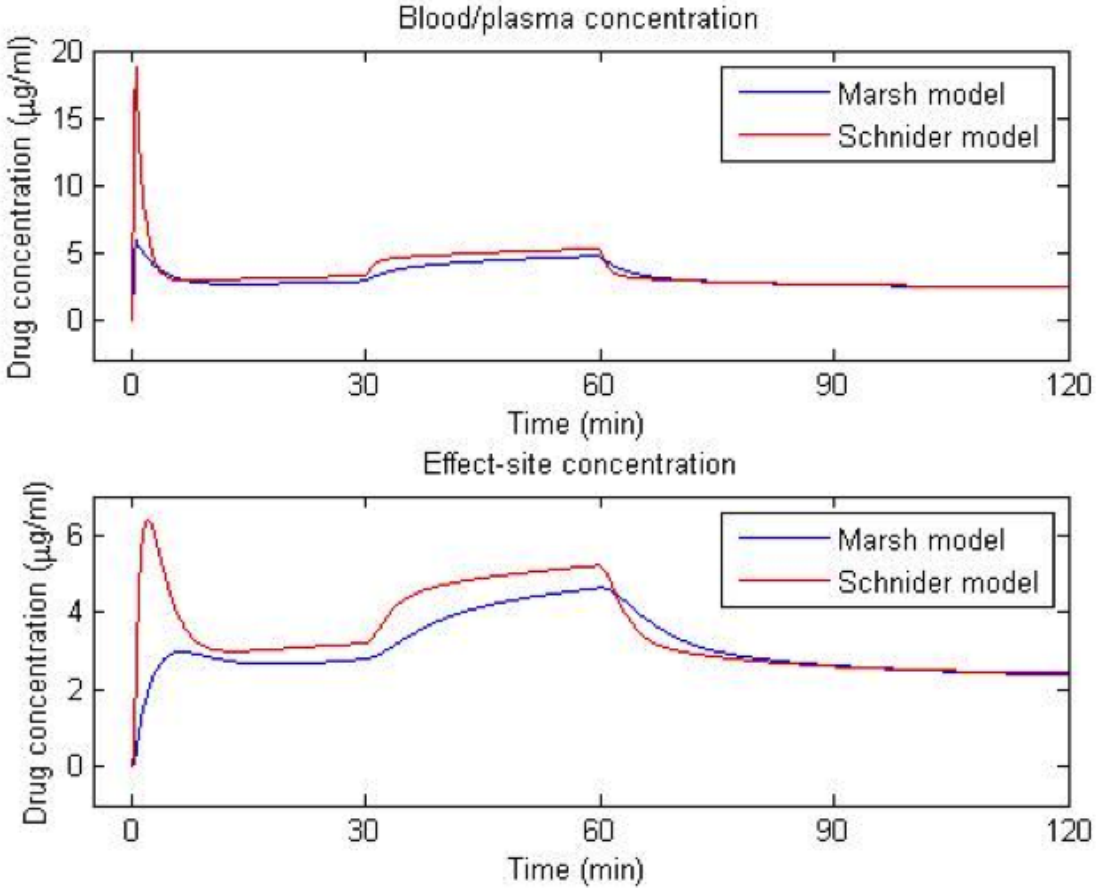

Figure 2.6: Simulated blood/plasma drug concentration (upper graph) and effect-site drug concentration (bottom graph) for the infusion of propofol 2% (20 mg/ml) in a patient 50 years old, male, height of 175 cm and weight of 70 kg, with Marsh and Schnider model with the same infusion scheme. Infusion at 600 ml/h until second 30, 25 ml/h between second 30 and minute 30, 40 ml/h between minute 30 to 60 and 15 ml/h from minute 60 until the end, with a total propofol administrated of 1046 mg.

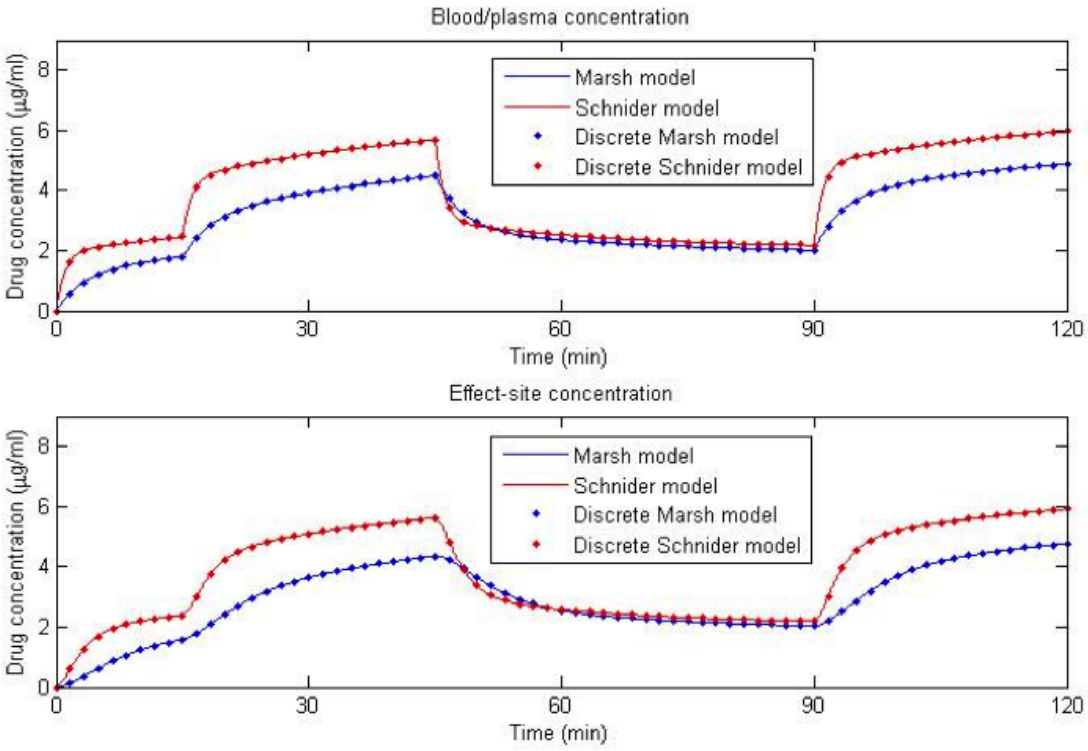

Figure 2.7: Simulated blood/plasma drug concentration (upper graph) and effect-site drug concentration (bottom graph) for the infusion of propofol 2% (20 mg/ml) in a patient 50 years old, male, height of 185 cm and weight of 85 kg, with Marsh and Schnider models in continuous and discrete (sampling time of 100 seconds) time with the same infusion scheme. Infusion at 25 ml/h until minute 15, 50 ml/h between minute 15 and minute 45, 15 ml/h between minute 45 to 90 and 50 ml/h from minute 90 until the end, with a total propofol administrated of 1350 mg.

2.5.1 Implementation of discrete PK model

Following the implementation of the pharmacokinetic model using MATLAB and Simulink on its continuous time representation using the differential equations, an implementation on discrete time was needed to support the simulations of the controller to be developed, as the aim of this project is to design a automatic close-loop control system for general anaesthesia to be implemented on a digital computer. This implementation was achieved using MATLAB routines.

An object representing the continuous time state space model for the PK model was created in MATLAB. The discretization of the PK model was accomplished using the MATLAB function c2d with the method of zero hold order and a sampling time specified by the user. A study was carried out to verify that the function c2d converts the continuous time models according to the rules defined in Subsection 2.4.1.1.

The representation of the simulated concentrations obtained when using the continuous (lines in blue and red) and discrete (points in blue and red) time PK model can be observed in Figure 2.7. For the discrete time PK model simulation a sampling time of 100 seconds was used. It is possible to observe that the concentrations on the sampling points are exactly the same as those obtained with the continuous time PK model simulation.

A user interface (Figure 2.8) was created to enable easy access to the PK and TCI discrete implementations. These tools enable the verification and correction of inconsistencies in the data recorded at the King's College Hospital due to occasional communication issues between ASYS and the infusion pumps.

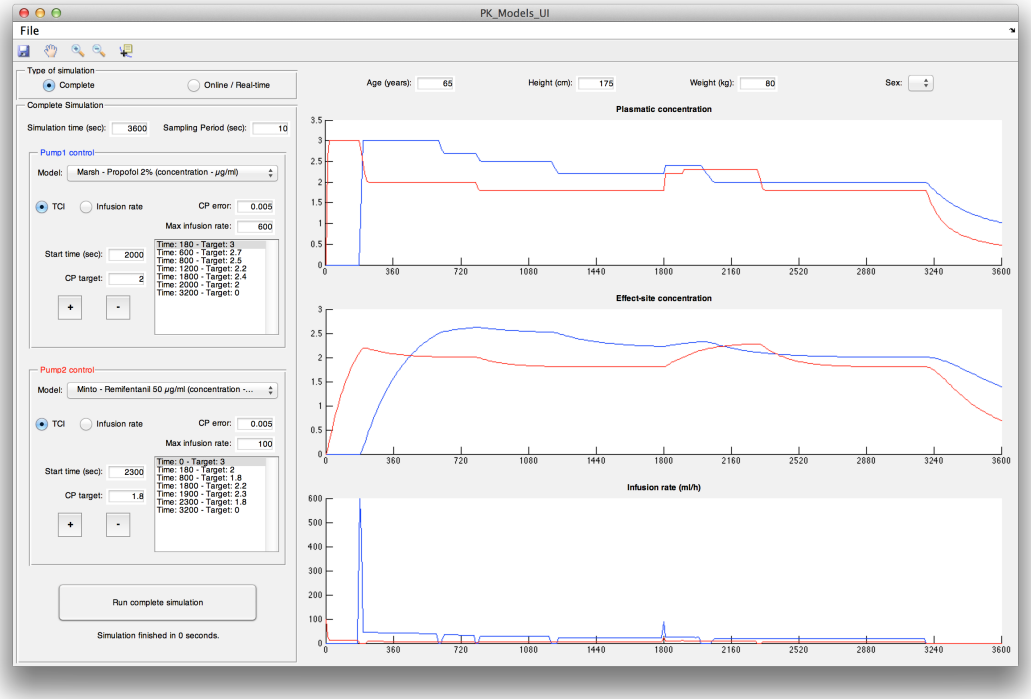

Figure 2.8: User interface for PK models and TCI implementations.

2.6 Summary

In this chapter an overview of the clinical protocol during surgeries used at King's College Hospital is presented followed by a description of the clinical setup implemented for data collection. A brief literature review of pharmacological modelling is presented with the implementation and simulation of a pharmacokinetic models.

Chapter 3

SVR-based PD modelling

3.1 Introduction

As mentioned in Section 1.2, the existing populational PD models present a variety of challenges and the importance of PD models in drug administration motivates the development of an accurate PD model. Patients' data (BIS and haemodynamic parameters) collected at King's College Hospital are used to support this investigation. Some published parametric PD models structures based on the Hill equation and modelling techniques (such as least-squares and genetic algorithm on data fitting) are studied and their performance compared in terms of modelling error.

PD modelling for the co-administration of propofol and remifentanil using BIS as a measure of the drugs' effect is investigated. SVR, a non-parametric modelling technique, and the incorporation of patients' haemodynamic parameters in PD modelling are also explored. Three PD models implemented by SVRs [56] are proposed for BIS estimation. The first SVR-based PD model is with single-

drug input (propofol) while the second one is with two-drug input (propofol and remifentanil). A third SVR-based PD model considers nCO as an additional input, as nCO plays an important role in PK/PD modelling [7, 35].

The three SVR-based PD models are trained with the patients' data in the induction stage. An algorithm is proposed to model the induction stage of a given patient's data. The modelling performance of the three SVR-based PD models are compared with Hill equation based PD models.

PD models are continuous non-dynamic models, which aim to map PK predicted effect-site concentrations with clinical effect of the anaesthetic drugs. The dynamic behaviour of the system is represented by the PK models defined on section 2.4.1.

3.2 Clinical Data

Clinical data recorded with ASYS as described in Chapter 2 from 42 elderly patients undergoing major vascular surgery of the lower limbs was used to perform PD modelling. This population was comprised of 35 males and 7 females, age of 72 ± 8 years, height of 169 ± 10 cm and weight 73 ± 14 kg. Values are presented as mean $\pm$ SD.

The clinical data recorded with ASYS provides predicted effect-site concentration for anaesthetic drugs according to pharmacokinetic models descrived on section 2.4.1. The PK model's parameters for a specific drug are usually estimated using statistical approaches by measuring the arterial or venous blood concentration of the drug after a bolus or infusion, in a group of patients or volunteers. These parameters are presented on tables 3.1, 3.2 and 3.3 with *age* in

years, *height* in cm and *weight* in Kg for the PK models of the hypnotic drug propofol and the analgesic drug remifentanil. LBM is defined as:

- Males: $LBM = 1.1weight - 128(weight/height)^2$
- Females: $LBM = 1.07weight - 148(weight/height)^2$

Table 3.1: Parameters for Propofol - Marsh model[41]

Parameter	**Value**
$V_1(l)$	$0.228weight$
$V_2(l)$	$0.463weight$
$V_3(l)$	$2.893weight$
$k_{10}(min^{-1})$	0.119
$k_{12}(min^{-1})$	0.112
$k_{13}(min^{-1})$	0.042
$k_{21}(min^{-1})$	0.55
$k_{31}(min^{-1})$	0.0033
$k_{e0}(min^{-1})$	0.26

3.3 Pharmacodynamic Modelling

The PK model described in Section 2.4.1 allows us to predict the effect-site concentrations of administrated anaesthetic drugs from their infusion profiles. Predicted effect-site concentrations evaluated by the infusion pumps are available on the clinical data recorded through ASYS.

Table 3.2: Parameters for Propofol - Schnider model[54]

Parameter	**Value**
$V_1(l)$	4.27
$V_2(l)$	$18.9 - 0.391(age - 53)$
$V_3(l)$	238
$k_{10}(min^{-1})$	$0.443 + 0.0107(weight - 77) - 0.0159(LBM - 59) + 0.0062(height - 177)$
$k_{12}(min^{-1})$	$0.302 - 0.0056(age - 53)$
$k_{13}(min^{-1})$	0.196
$k_{21}(min^{-1})$	$[1.29 - 0.024(age - 53)]/[18.9 - 0.391(age - 53)]$
$k_{31}(min^{-1})$	0.0035
$k_{e0}(min^{-1})$	0.456

Table 3.3: Parameters for Remifentanil - Minto model[45]

Parameter	**Value**
$V_1(l)$	$5.1 - 0.0201(age - 40) + 0.072(LBM - 55)$
$V_2(l)$	$9.82 - 0.0811(age - 40) + 0.108(LBM - 55)$
$V_3(l)$	5.42
$k_{10}(min^{-1})$	$[2.6 - 0.0162(age - 40) + 0.0191(LBM - 55)]/V_1$
$k_{12}(min^{-1})$	$[2.05 - 0.0301(age - 40)]/V_1$
$k_{13}(min^{-1})$	$[0.076 - 0.00113(age - 40)]/V_1$
$k_{21}(min^{-1})$	$k_{12}V_1/V_2$
$k_{31}(min^{-1})$	$k_{13}V_1/V_3$
$k_{e0}(min^{-1})$	$0.595 - 0.007(age - 40)$

Hill equation based PD models described on Section 2.4.2 are estimated for the 42 clinical data records through least square curve fitting method and GA optimization.

3.3.1 Support Vector Machine/Regression Model

The problem with PD modelling of the effect of anaesthetic drugs can also be approached as a non-parametric regression problem. Having this approach in mind, SVR, a technique based on support vector machine (SVM), was applied to the clinical data. The basic concept of this technique is to project the input data using a kernel function into a higher dimensional *feature space* where a linear regression problem is obtained [56]. In this work a standard ε-insensitive loss function was used for the SVR algortihm.

Considering a training dataset $S = \{(x_1, y_1) \dots (x_m, y_m)\}$, where $x_i \in \mathbb{R}^d$ is the input sample and $y_i \in \mathbb{R}$ is the observed output value, the ε-insensitive SVR technique for linear functions aims to find function $f(x) = \langle w, x \rangle + b$ which has at most ε deviation from y for all data points S, where w is the parameter defining the hyperplane, b is the bias and $\langle ., . \rangle$ is the inner product operator. However, sometimes such function $f(x)$ does not exist and the introduction of slack variables (ξ_i, ξ_i^*) is necessary to allow certain data points to violate the constraints at a cost $C \in \mathbb{R}$. A solution to the described problem is achieved by

solving the following optimization problem:

$$\begin{aligned} \text{minimize} \quad & \frac{1}{2}\|w\|^2 + C\Sigma_{i=1}^{m}(\xi_i + \xi_i^*) \\ \text{subject to} \quad & \begin{cases} y_i - \langle w, x_i \rangle - b \leqslant \varepsilon + \xi_i \\ \langle w, x_i \rangle + b - y_i \leqslant \varepsilon + \xi_i^* \\ \xi_i, \xi_i^* \geqslant 0 \end{cases} \end{aligned} \tag{3.1}$$

As shown by Smola and Schölkopf [56], by solving optimization equation (3.1) comes:

$$f(x) = \sum_{i=1}^{m}(\alpha_i - \alpha_i^*)\langle x_i, x \rangle + b, \tag{3.2}$$

where α_i and α_i^* are the Lagrangian multipliers obtained by solving the problem described by equation (3.1). The subset of the training data points for which $\alpha_i - \alpha_i^* \neq 0$, are called the support vectors and they are enough to completely describe the SVR solution, decreasing the computational requirements this way.

This ε-insensitive SVR technique for linear functions can be extended to non-linear functions by applying a kernel mapping to project the input data into a higher dimension *feature space* where the problem has linear characteristics and can be approached by the described method. As all the described method can be expressed in terms of inner-product between the training dataset, a kernel function ($K(x_i, x_j)$) matching the inner-product on the *feature space* is enough to solve the problem. Therefore equation (3.2) can be written, for nonlinear case, as:

$$f(x) = \sum_{i=1}^{m}(\alpha_i - \alpha_i^*)K(x_i, x) + b, \tag{3.3}$$

To a kernel function ($K(x_i, x_j)$) matching the inner-product on the *feature*

space, it needs to obey Mercer's Theorem [56].

3.4 Model Adequacy Index

As the SVR modelling technique is a non-parametric modelling method, analysing the modelling performance only in terms of the mean absolute error (MAE) on the testing dataset is not enough. The modelling performance should be analysed in terms of error, in training and testing datasets, and in terms of the adequacy of the output signal of the generated model as an estimator of the clinical effect of the anaesthetic drugs. Taking these points into consideration, a new measure of Pharmacodynamic modelling performance should be created to evaluate and compare the different modelling techniques.

To ensure the adequacy of the output signal of the generated model as an estimator of the clinical effect of the anaesthetic drugs, both signals, the model estimated output and the BIS signal, should have similar behaviour. In this study the clinical effect of the anaesthetic drugs is evaluated by the BIS signal which ranges from 0 to 100, and it decreases with the increase in the anaesthetic drugs concentration, when no other factors are taken in consideration. The expected value for the BIS signal on a fully awake patient without the presence of anaesthetic drugs is near 100.

From these known behaviours the following index was created to evaluate pharmacodynamic modelling performance.

3.4.1 Empirical knowledge of the effect signal

To assess the adequacy and performance of the estimated pharmacodynamic models the known characteristics and expected behaviour of the BIS signal should be taken into account and verified against the estimated models.

As previously described BIS signal ranges from 0 to 100 and is expected to be near 100 when no anaesthetic drug is present and the patient is awake, and to decrease up to 0 as anaesthetic drug presence increases, *i.e.* BIS index should be a decreasing function of the concentration of anaesthetic drug. As such it is expected for a BIS value to be 0 for high concentrations of anaesthetic drug. The hypnotic drug used in this study was propofol to which an estimated effect-site concentration of 18 $\mu g/l$ has an expected BIS value of 0 as it is well above usual doses [44].

3.4.2 Description of Model Adequacy Index

To validate the estimated models though the SVRs technique as adequate pharmacodynamic models each estimated model was evaluated in 4096 points in the range range 0 and 20 for the various possible inputs. For example, in the models estimated using the single-drug SVR technique which only has propofol effect-site concentration as input, the effect of the propofol was evaluated with the output of the estimated PD model on 4096 points for the propofol effect-site concentrations between 0 and 20 $\mu g/ml$, uniformly spaced. However, in the case of the the models estimated using the nCO adjusted multi-drug SVR technique which has propofol, remifentanil effect-site concentration and nCO as input, the effect of the anaesthetic drugs was evaluated with the estimated PD model on 4096 points,

uniformly spaced on a grid sense, i.e. for all the possible combinations of 16 values of propofol effect-site between 0 and 20 $\mu g/ml$, 16 values of remifentanil effect-site between 0 and 20 ng/ml and 16 values of nCO between 0 and 20 l/min, uniformly spaced. From these 4096 obtained values a Model Adequacy Index (MAI) was proposed to evaluate the performance and validity of the SVR-based PD model.

The MAI tests various statistics obtained from the 4096 points, which test the adequacy of the models' outputs as BIS signal. These statistics are percentages of the number of estimated points without output below 0 and -10 and above 100 and 110. Another statistic used is the percentage of points with an output within the range of 0 to 100 which satisfy the condition of BIS being a decreasing function of the concentration of propofol, i.e. the percentage of points for which the estimated effect is lower than the estimated effect for the immediate previous point with higher propofol effect-site concentration and the same remifentanil effect-site concentration and nCO, if applicable. The last statistic used is the Deviation, which assess the deviation from the expected BIS value of 0 on high concentrations of propofol. The absolute average output (AAO) is the absolute average of the estimated effect for the points with the 10% higher values of the evaluated propofol effect-site concentration, which will consist of the absolute average of the the estimated effect for all the validation points obtained from a propofol effect-site concentration between 18 and 20 $\mu g/ml$. *Deviation* is calculated by assessing the displacement of AAO against the expected value of 0 using equation (3.4). *Deviation* value was expressed as a percentage for the

evaluation of MAI.

$$Deviation = \frac{1}{1 + AAO} \tag{3.4}$$

Table 3.4 presents the weights used for each component of the model adequacy index.

Table 3.4: Weights of the Model Adequacy Index statistics.

Condition	**Weight**
% of points $\not< 0$	1
% of points $\not< -10$	10
% of points $\not> 100$	1
% of points $\not> 110$	10
% of points where BIS becomes a decreasing function of the concentration of propofol	5
Deviation	20
Total	**47**

3.5 Experiment/Simulation Results

Clinical data from 42 vascular surgeries under general anaesthesia were collected. Collected BIS index, propofol and remifentanil concentrations trends were visually analyzed to access times for stable pre-induction baseline readings, i.e. marking an interval of stable clinical signals before starting the infusion of anaesthetic drugs. From the observations of the visual analysis, it was also decided to

mark the end of induction 8 minutes and 20 seconds (100 samples) after the first reading of BIS index below 60. The data recorded up to this mark will constitute the training dataset, while the remaining surgery data will be the testing dataset.

Average BIS index on pre-induction baselines was 93.2 $\pm$ 7.3 and nCO was 6.9 $\pm$ 2.7 l/min. Average duration of induction was 15.2 $\pm$ 3.2 minutes and total amount of propofol and remifentanil infused during induction were 2.55 $\pm$ 0.67 mg/kg and 1.5 $\pm$ 0.37 $\mu g/kg$, respectively.

Most of the considerable changes in BIS index were verified during the induction period, maintaining a stable reading during maintenance phase as this was the main control variable used by the anaesthetist as it can be observed on Figure 3.1. At pre-induction baseline, before drugs infusion, BIS index presents a high value, between 90 and 100. With the infusion of anaesthetic drugs and their effect-site concentration increase, BIS values start to decline to the 40 to 60 interval, where they are maintained after induction. A 5 fold variation in inter-patient propofol and remifentanil effect-site concentrations requirements was needed to maintain BIS within target as shown by Figure 3.1.

From Figures 3.2 and 3.3 which present signal traces from two surgeries, it is observed that dissimilar anaesthetic drugs effect-site concentrations might be necessary to maintain a BIS signal within the target boundary of 40 to 60. It is also observed that even though the anaesthetist was aiming to maintain BIS within 40 to 60 limit it was not always possible to achieve and there were a few periods where BIS value was outside these. This is particularly noticeable on Figure 3.3 from minute 120 where BIS show higher variation.

Simultaneously with the decrease in BIS values, a decrease in nCO is verified in most of the 42 analysed cases. This can be easily observed for case 1 in Figure

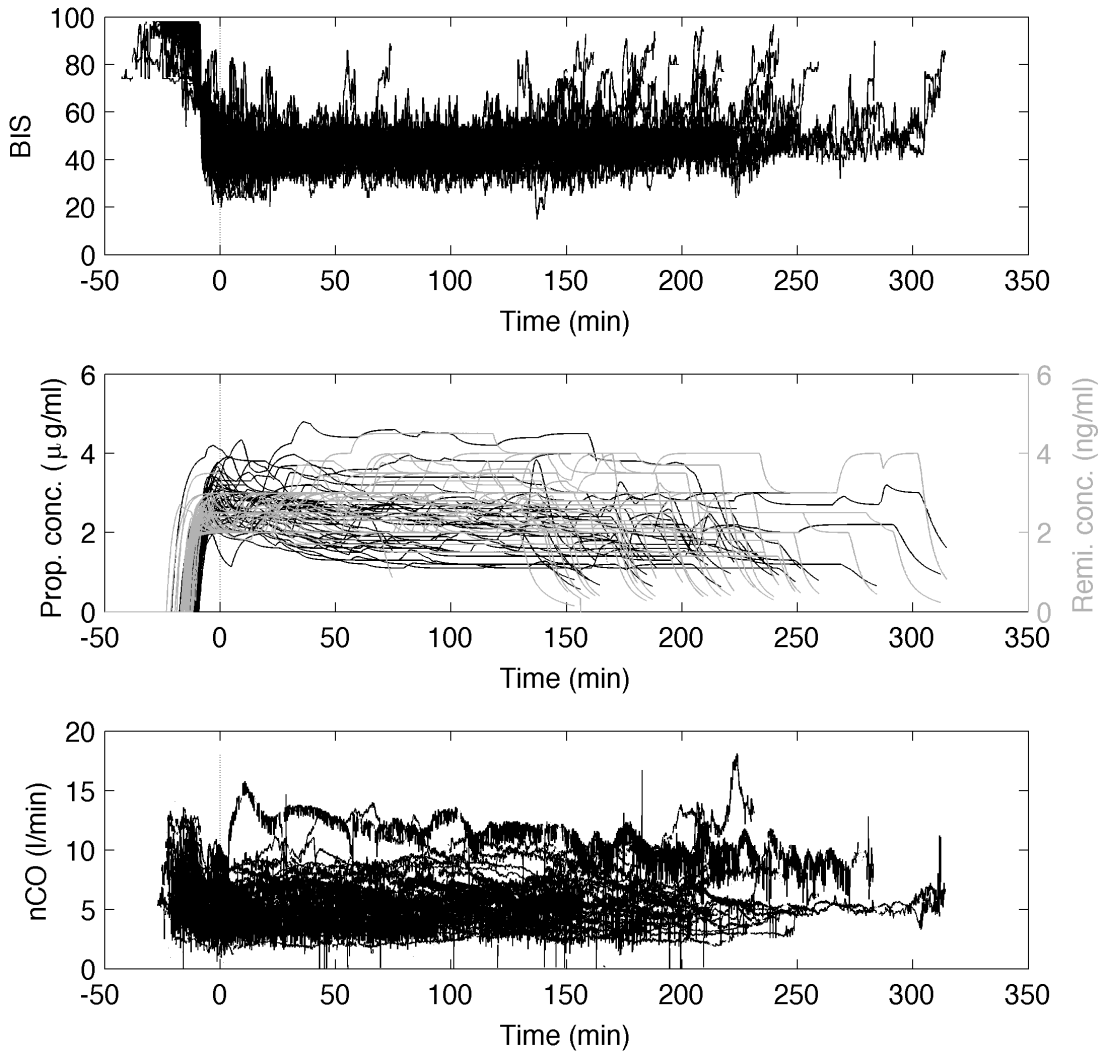

Figure 3.1: Clinical data traces for all 42 vascular surgeries. Zero minute was set 100 samples (8 minutes and 20 seconds) following BIS first reading below 60. Top: BIS values; Middle: Propofol (Prop.) and remifentanil (Remi.) effect-site concentrations; Bottom: nCO values.

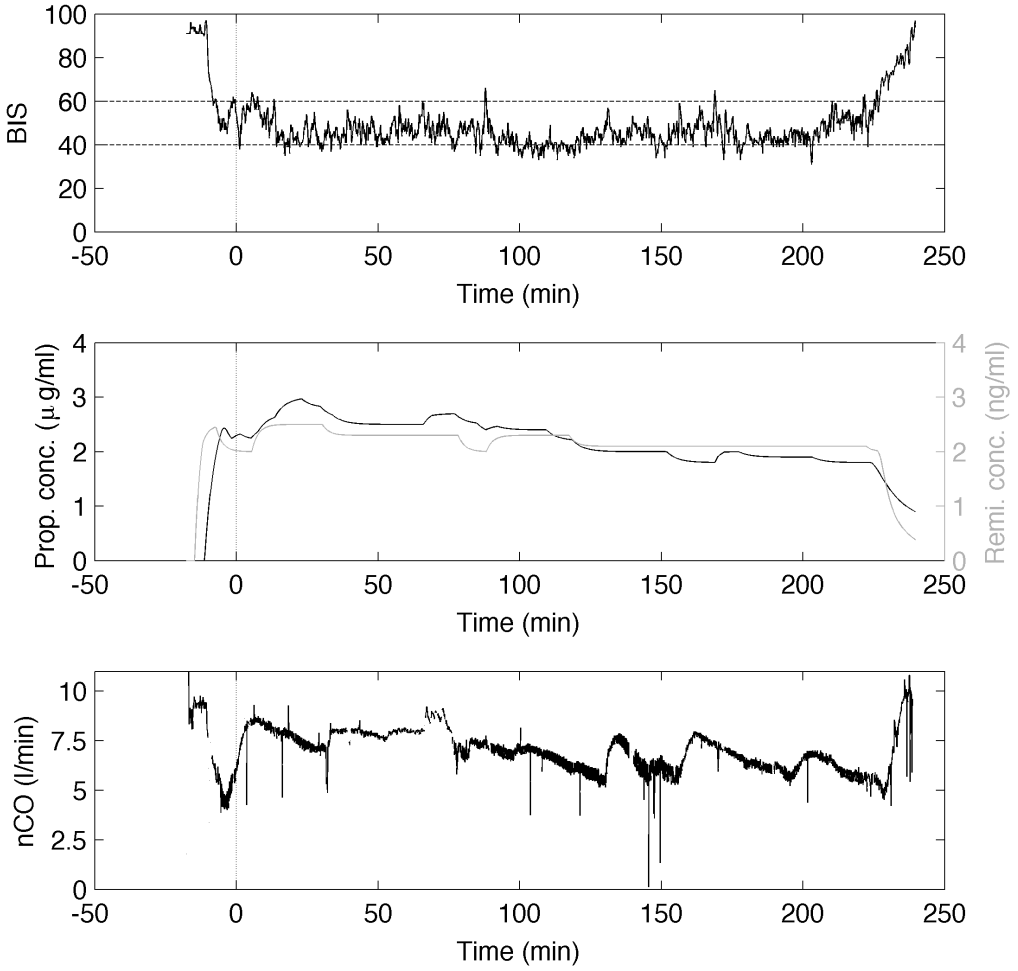

Figure 3.2: Clinical data trace for case 1. Zero minute was set 100 samples (8 minutes and 20 seconds) following BIS first reading below 60. Top: BIS values; Middle: Propofol and remifentanil effect-site concentrations; Bottom: nCO values.

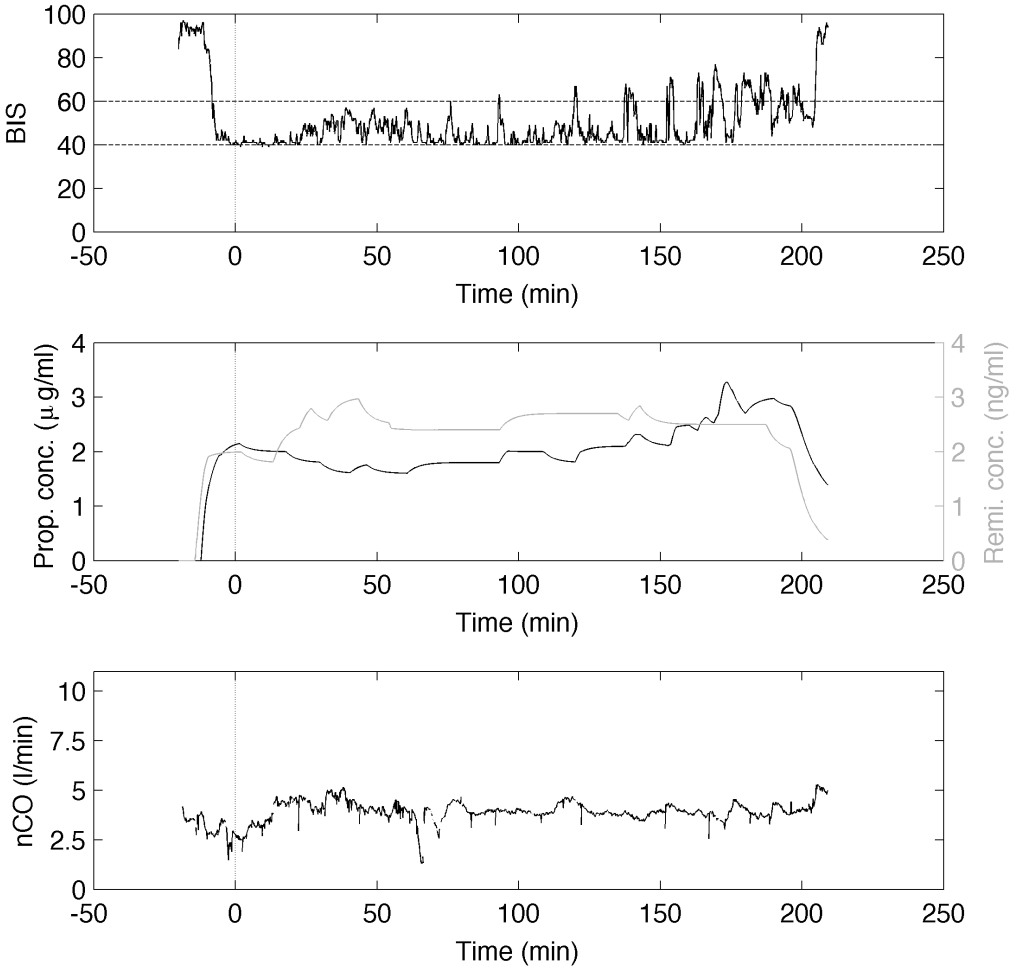

Figure 3.3: Clinical data trace for case 2. Zero minute was set 100 samples (8 minutes and 20 seconds) following BIS first reading below 60. Top: BIS values; Middle: Propofol and remifentanil effect-site concentrations; Bottom: nCO values.

3.2.

3.5.1 Pharmacodynamic Modelling - Performance Results

Parametric modelling supported in the single and multi-variable Hill model was considered given in Section 2.4.2. Least square (LSQ) curve fitting and genetic algorithm (GA), with two cost functions - Sum of square error (SSE) equation (3.5) and Mean absolute error (MAE) equation (3.6) - were used. LSQ and GA find the optimal Ce_{50} and γ parameters for the single Hill model, or $Ce_{50,prop}$, $Ce_{50,remi}$, β and γ parameters for multi-variable Hill model minimizing the respective cost function in the training dataset.

$$SSE = \sum_{i=1}^{m} (Effect(Ce_i) - BIS_i)^2 \tag{3.5}$$

$$MAE = \frac{1}{m} \sum_{i=1}^{m} |Effect(Ce_i) - BIS_i| \tag{3.6}$$

where m is the number of points of the training dataset; $Effect(Ce_i)$ is the estimated effect by the PD model of the anaesthesia on the patient; and BIS_i is the effect of the anaesthesia on the patient measured by the *BIS Vista* monitor on the i^{th} patient.

The second technique applied was SVR using a diverse combination of kernels and C values, for the three inputs configurations estimated - one drug (propofol), two drugs (propofol and remifentanil) and two drugs with nominal cardiac output in order to estimate the function $f(x)$ defined in equation (3.3). The obtained results and some observations are made below. SVR modelling was performed using polynomial, gaussian radial basis (RBF), exponential radial basis, spline

and anova spline kernel functions, C value of 1, 10, 100, 500 and 1000, and ϵ of 2.

The recorded clinical data is presented in Figure 3.4 together with BIS values, propofol and remifentanil effect-site concentration and nCO during one vascular surgery. Some of the estimated PD models for this case are also presented, including all PD models based on single and multi variable Hill equations and the models estimated using the SVR technique under a RBF kernel and C value of 10, as examples of the different PD models estimated by the various techniques.

Figure 3.4 shows top recorded BIS values (black line) and BIS estimations from the estimated PD models. Estimated BIS are from PD modelling with Hill - LSQ/GA-SSE (magenta solid line) single-drug Hill model by least square curve fitting and genetic algorithm with sum square errors cost function; Hill - SMAE (yellow solid line) single-drug Hill model by genetic algorithm with mean absolute errors cost function; Hill - MLSQ (cyan dashed line) multi-drug Hill model by least square curve fitting; Hill - MSSE (magenta dashed line) multi-drug Hill model by genetic algorithm with sum square errors cost function; Hill - MMAE (yellow dashed line) multi-drug Hill model by genetic algorithm with mean absolute errors cost function; SVR - S (blue solid line) single-drug SVR model; SVR - M (red solid line) multi-drug SVR model; SVR - MCO (green solid line) nCO adjusted multi-drug SVR model. Propofol and remifentanil predicted effect-site concentrations are shown in the middle and nCO values at the bottom.

3.5.1.1 Single-Drug (Propofol) Hill Model

Similar estimated parameters were obtained by LSQ and GA methods when modelling BIS using single-variable Hill model (effect-site propofol concentration is

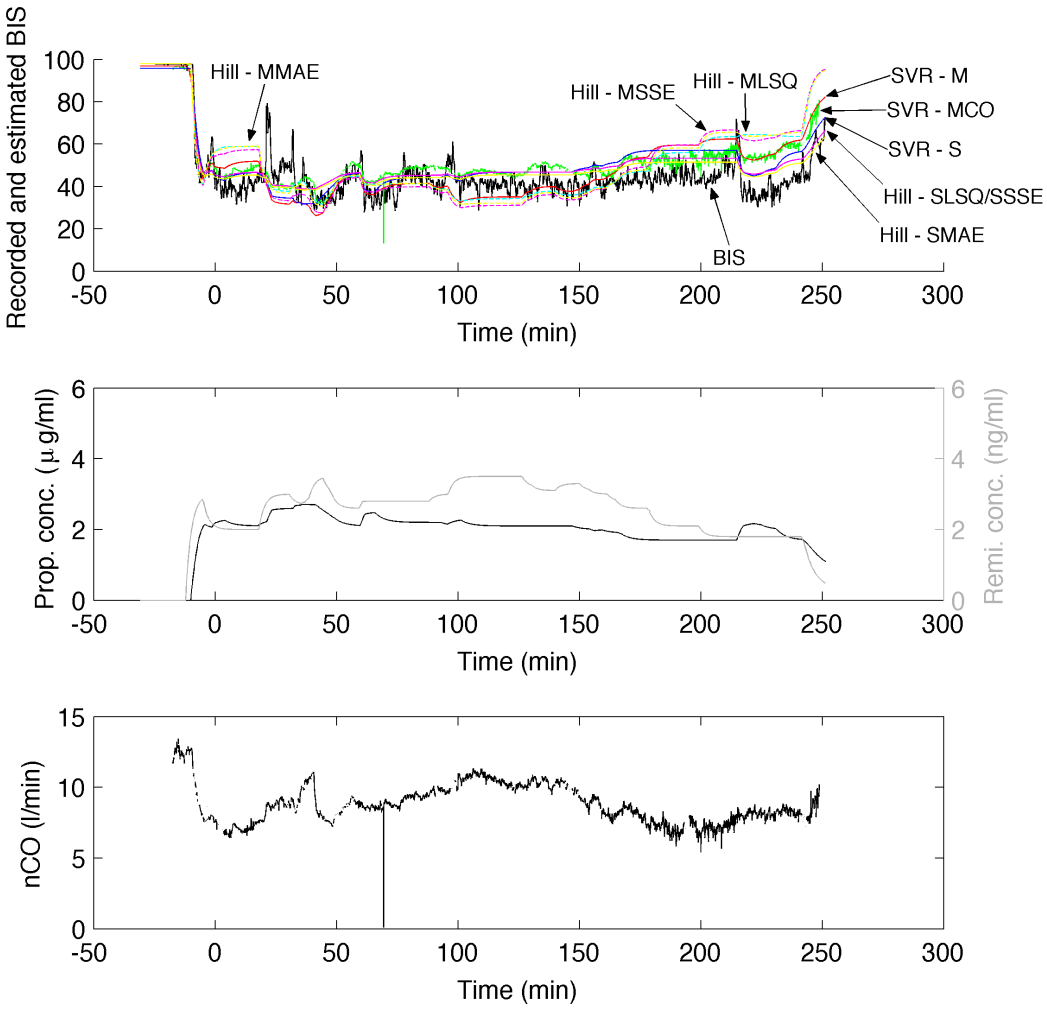

Figure 3.4: Clinical data traces and estimated PD models for case 3. Zero minute was set at 100 samples (8 minutes and 20 seconds) following BIS first reading below 60, which match the end of the training dataset and start of testing dataset.

Table 3.5: Parameters results for Hill Models.

Model	**Method**	γ	$Ce_{50}prop$	$Ce_{50}remi$	β
One Drug	LSQ	1.76 ± 0.78	2.65 ± 0.83	—	—
One Drug	GA SSE	1.76 ± 0.78	2.64 ± 0.8	—	—
One Drug	GA MAE	1.73 ± 0.7	2.7 ± 0.95	—	—
Two Drugs	LSQ	5.56 ± 7.48	5.97 ± 5.27	42.84 ± 36.17	1.5 ± 1.62
Two Drugs	GA SSE	3.11 ± 1.62	4.25 ± 2.09	23.2 ± 5.39	1.71 ± 0.87
Two Drugs	GA MAE	2.92 ± 1.4	4.52 ± 2.58	23.3 ± 5.38	1.68 ± 0.85

the only model input) (Table 3.5). LSQ and GA SSE presents the same mean absolute errors on the various sub-set of data analysed, having a 4.89 ± 1.76 training MAE and 11.89 ± 7.47 testing MAE, see Table 3.6. A smaller error (4.76 ± 1.69) is obtained in training data when the GA MAE method is used in contrast to LSQ or GA SSE, but with higher testing errors (12.17 ± 7.64).

3.5.1.2 Multi-Drug (Propofol and Remifentanil) Hill Model

When BIS modelling is performed using the multi-variable Hill model (using propofol and remifentanil effect-site concentration as inputs), different results and performances can be observed in Tables 3.5 and 3.6. The least square curve fitting method presents slightly better performance in the training dataset, but a worse performance in the testing dataset, when compared to GA methods. Also to be noted are the considerable differences that can be observed between the estimated parameters with the LSQ or GA techniques. Standard deviation of the estimated parameters is substantially smaller when a GA technique is applied in

Table 3.6: Mean absolute errors for Hill Models. MAE presented for training and testing datasets and for induction, maintenance and recovery stages of general anaesthesia.

Model	**Method**	**MAE (Training)**	**MAE (Testing)**	**MAE (Ind.)**	**MAE (Maint.)**	**MAE (Rec.)**
One Drug	LSQ	4.89 ± 1.76	11.89 ± 7.47	5.01 ± 4.64	11.47 ± 7.12	13.87 ± 10.11
One Drug	GA SSE	4.89 ± 1.76	11.88 ± 7.47	5.01 ± 4.64	11.46 ± 7.12	13.88 ± 10.11
One Drug	GA MAE	4.76 ± 1.69	12.17 ± 7.64	4.91 ± 4.68	11.75 ± 7.3	13.7 ± 10.06
Two Drugs	LSQ	4.3 ± 1.4	31.23 ± 17.7	4.33 ± 3.99	15.61 ± 11.11	21.58 ± 12.52
Two Drugs	GA SSE	4.59 ± 1.41	29.01 ± 15.98	4.55 ± 3.92	13.19 ± 8.61	19.84 ± 12.29
Two Drugs	GA MAE	4.48 ± 1.4	28.35 ± 15.46	4.46 ± 3.97	12.78 ± 8.49	18.97 ± 12.58

comparison with LSQ, with a reduction of 50% (5.27 to 2.58) to 80% (36.17 to 5.38).

3.5.1.3 Single-Drug (Propofol) SVR Model

Diverse results were obtained with the single-drug SVR modelling, having errors in the training dataset varying from 2.27 ± 0.93 to 13.57 ± 4.16 and from 8.69 ± 6.90 to 14.73 ± 6.83 in the testing dataset, depending on the kernel function and C value used. Detailed results are presented in Table 3.7, 3.8, 3.9, 3.10 and 3.11.

Analyzing modelling performance as mean absolute error (MAE) in the testing dataset, it is not clear which is the best choice for kernel function and C value, as the kernel function with the best performance also presents bad performances for different C values, and the same can be observed in relation to C value.

Performance in terms of training and testing error of single-drug SVR modelling compared with parametric Hill modelling is highly dependent in the kernel function and C value used, and no inference can be easily obtained from it.

3.5.1.4 Multi-Drug (Propofol and Remifentanil) SVR Model

As with the single-drug SVR modelling, varied results were obtained with multi-drug SVR modelling, with training errors varying between 1.93 ± 0.79 and 13.37 ± 4.37m and testing errors from 10.80 ± 4.86 to 53.27 ± 69.74, having the same outcome when compared to the multi-drug Hill modelling. Detailed results are presented in Table 3.12, 3.13, 3.14, 3.15 and 3.16.

However in this case, it is clear that the polynomial kernel function presents the worst performance in terms of mean absolute errors in the testing dataset, and

Table 3.7: Mean absolute errors for SVR Models for one drug model structure, kernel and C value. %SV is the percentage of support vectors. MAE presented for training and testing datasets and for induction, maintenance and recovery stages of general anaesthesia.

kernel	**C**	**% SV**	**MAE (Training)**	**MAE (Testing)**	**MAE (Ind.)**	**MAE (Maint.)**	**MAE (Rec.)**
anovaspline1	1	84 ± 9	9,05 ± 4,63	11,73 ± 5,38	12,72 ± 11,27	11,52 ± 5,28	11,03 ± 6,63
anovaspline1	10	65 ± 11	4,11 ± 1,32	12,56 ± 6,92	1,46 ± 1,91	12,22 ± 6,66	12,13 ± 9,09
anovaspline1	100	62 ± 13	3,68 ± 1,23	12,7 ± 7,57	0,47 ± 1,2	12,29 ± 7,24	13,01 ± 10,16
anovaspline1	500	61 ± 13	3,36 ± 1,14	12,71 ± 8,23	0,24 ± 1,09	12,23 ± 7,86	13,68 ± 10,84
anovaspline1	1000	60 ± 13	3,21 ± 1,09	12,81 ± 8,66	0,14 ± 1,07	12,31 ± 8,28	13,95 ± 11,1

Table 3.8: Mean absolute errors for SVR Models for one drug model structure, kernel and C value. %SV is the percentage of support vectors. MAE presented for training and testing datasets and for induction, maintenance and recovery stages of general anaesthesia.

kernel	**C**	**% SV**	**MAE (Training)**	**MAE (Testing)**	**MAE (Ind.)**	**MAE (Maint.)**	**MAE (Rec.)**
erbf	1	90 ± 7	13,57 ± 4,16	14,73 ± 6,83	17,66 ± 10,55	14,7 ± 6,93	12,13 ± 6,73
erbf	10	68 ± 11	3,89 ± 1,23	12,07 ± 6,49	1,7 ± 1,66	11,71 ± 6,25	12,07 ± 8,68
erbf	100	61 ± 12	2,79 ± 0,97	12,02 ± 7,7	0,49 ± 1,1	11,51 ± 7,36	13,3 ± 10,61
erbf	500	56 ± 11	2,38 ± 0,93	12,13 ± 7,91	0,36 ± 1,1	11,56 ± 7,57	13,49 ± 10,84
erbf	1000	55 ± 12	2,27 ± 0,93	12,21 ± 7,9	0,35 ± 1,08	11,63 ± 7,56	13,54 ± 10,83

Table 3.9: Mean absolute errors for SVR Models for one drug model structure, kernel and C value. %SV is the percentage of support vectors. MAE presented for training and testing datasets and for induction, maintenance and recovery stages of general anaesthesia.

kernel	**C**	**% SV**	**MAE (Training)**	**MAE (Testing)**	**MAE (Ind.)**	**MAE (Maint.)**	**MAE (Rec.)**
poly	1	70 ± 13	6,02 ± 1,47	8,69 ± 6,9	5,15 ± 3,6	8,3 ± 6,72	11,99 ± 6,04
poly	10	64 ± 12	3,67 ± 1,24	14,01 ± 11,56	0,74 ± 1,22	13,55 ± 11,25	13,44 ± 10,22
poly	100	63 ± 11	3,63 ± 1,23	14,46 ± 11,75	0,38 ± 1,16	13,99 ± 11,45	13,89 ± 10,72
poly	500	63 ± 11	3,63 ± 1,23	14,59 ± 12,17	0,35 ± 1,13	14,12 ± 11,87	13,92 ± 10,73
poly	1000	63 ± 11	3,62 ± 1,23	14,59 ± 12,17	0,35 ± 1,13	14,12 ± 11,87	13,92 ± 10,73

Table 3.10: Mean absolute errors for SVR Models for one drug model structure, kernel and C value. %SV is the percentage of support vectors. MAE presented for training and testing datasets and for induction, maintenance and recovery stages of general anaesthesia.

kernel	**C**	**% SV**	**MAE (Training)**	**MAE (Testing)**	**MAE (Ind.)**	**MAE (Maint.)**	**MAE (Rec.)**
rbf	1	87 ± 7	10,05 ± 3,88	12,71 ± 5,67	13,46 ± 9,64	12,54 ± 5,57	11,48 ± 6,93
rbf	10	68 ± 11	4,3 ± 1,36	12,72 ± 6,88	1,62 ± 2,31	12,4 ± 6,61	12,21 ± 9,05
rbf	100	66 ± 13	4,01 ± 1,31	12,84 ± 7,2	0,59 ± 1,14	12,47 ± 6,89	12,56 ± 9,68
rbf	500	64 ± 14	3,91 ± 1,28	12,99 ± 7,43	0,46 ± 1,25	12,6 ± 7,13	12,99 ± 9,87
rbf	1000	63 ± 13	3,87 ± 1,27	13,01 ± 7,52	0,46 ± 1,26	12,6 ± 7,22	13,12 ± 9,94

Table 3.11: Mean absolute errors for SVR Models for one drug model structure, kernel and C value. %SV is the percentage of support vectors. MAE presented for training and testing datasets and for induction, maintenance and recovery stages of general anaesthesia.

kernel	**C**	**% SV**	**MAE (Training)**	**MAE (Testing)**	**MAE (Ind.)**	**MAE (Maint.)**	**MAE (Rec.)**
spline	1	84 ± 9	9,05 ± 4,63	11,73 ± 5,38	12,72 ± 11,27	11,52 ± 5,28	11,03 ± 6,63
spline	10	65 ± 11	4,11 ± 1,32	12,56 ± 6,92	1,46 ± 1,91	12,22 ± 6,66	12,13 ± 9,09
spline	100	62 ± 13	3,68 ± 1,23	12,7 ± 7,57	0,47 ± 1,2	12,29 ± 7,24	13,01 ± 10,16
spline	500	61 ± 13	3,36 ± 1,14	12,71 ± 8,23	0,24 ± 1,09	12,23 ± 7,86	13,68 ± 10,84
spline	1000	60 ± 13	3,21 ± 1,09	12,81 ± 8,66	0,14 ± 1,07	12,31 ± 8,28	13,95 ± 11,1

that, in general, the Gaussian radial basis, exponential radial basis are the kernel functions with better performances, independent of the C value. If focusing only on the results for only these two kernel functions, opposite performance results are observed for each kernel in relation to C value, performance increases with the increase of C value in the case of the exponential radial basis, and decreases for the Gaussian radial basis kernel function.

3.5.1.5 nCO Adjusted Multi-Drug (Propofol and Remifentanil) SVR Model

When multi-drug and nCO SVR modelling was applied to the clinical data, training errors between 1.59 ± 0.27 and 16.31 ± 4.25 and testing errors from 9.45 ± 3.63 to 76.11 ± 109.37 were obtained. As for the multi-drug SVR modelling, the polynomial kernel function presented the worst performance and the Gaussian and exponential radial basis kernel functions had the best performances. The relation between the value of the C value and the kernel function is the same as observed in the previous modelling case, with the exception of the combination of the exponential radial basis kernel function and the C value of 1, which has a better performance than any other models obtained with the kernel. Detailed results are presented in Table 3.17, 3.18, 3.19, 3.20 and 3.21.

If focusing only on modelling results for the Gaussian and exponential radial basis kernel functions, the nCO adjusted multi-drug modelling seems to have better performance when compared to multi-drug modelling, but that advantage disappears with increase of the C value.

Table 3.12: Mean absolute errors for SVR Models for two drugs model structure, kernel and C value. %SV is the percentage of support vectors. MAE presented for training and testing datasets and for induction, maintenance and recovery stages of general anaesthesia.

kernel	**C**	**% SV**	**MAE (Training)**	**MAE (Testing)**	**MAE (Ind.)**	**MAE (Maint.)**	**MAE (Rec.)**
anovaspline1	1	79 ± 9	7,78 ± 4,11	12,47 ± 5,87	10,52 ± 10,21	12,1 ± 5,74	12,27 ± 8,16
anovaspline1	10	64 ± 9	3,8 ± 1,23	13,31 ± 7,17	1,04 ± 1,2	12,8 ± 6,95	13,84 ± 9,61
anovaspline1	100	60 ± 10	3,3 ± 1,09	13,91 ± 8,16	0,44 ± 0,94	13,31 ± 7,96	14,69 ± 9,52
anovaspline1	500	55 ± 9	2,93 ± 0,98	14,94 ± 10,61	0,26 ± 0,83	14,23 ± 10,42	16,15 ± 10,99
anovaspline1	1000	54 ± 10	2,79 ± 0,93	15,9 ± 11,87	0,2 ± 0,8	15,15 ± 11,66	16,78 ± 12,25

Table 3.13: Mean absolute errors for SVR Models for two drugs model structure, kernel and C value. %SV is the percentage of support vectors. MAE presented for training and testing datasets and for induction, maintenance and recovery stages of general anaesthesia.

kernel	**C**	**% SV**	**MAE (Training)**	**MAE (Testing)**	**MAE (Ind.)**	**MAE (Maint.)**	**MAE (Rec.)**
erbf	1	90 ± 6	13,37 ± 4,37	13,65 ± 5,9	17,85 ± 10,96	13,52 ± 5,92	12 ± 7,11
erbf	10	67 ± 11	3,8 ± 1,18	12,45 ± 6,69	1,74 ± 1,25	11,93 ± 6,48	13,45 ± 9,07
erbf	100	52 ± 11	2,5 ± 0,89	12,08 ± 7,19	0,49 ± 0,87	11,46 ± 6,94	13,59 ± 9,44
erbf	500	46 ± 11	2,05 ± 0,8	11,81 ± 7,15	0,4 ± 0,82	11,16 ± 6,91	13,47 ± 9,22
erbf	1000	45 ± 11	1,93 ± 0,79	11,74 ± 7,09	0,4 ± 0,82	11,09 ± 6,84	13,4 ± 9,15

Table 3.14: Mean absolute errors for SVR Models for two drugs model structure, kernel and C value. %SV is the percentage of support vectors. MAE presented for training and testing datasets and for induction, maintenance and recovery stages of general anaesthesia.

kernel	**C**	**% SV**	**MAE (Training)**	**MAE (Testing)**	**MAE (Ind.)**	**MAE (Maint.)**	**MAE (Rec.)**
poly	1	66 ± 11	4,38 ± 1,31	32,32 ± 36,47	2,11 ± 2,34	30,87 ± 37,18	32,33 ± 15,57
poly	10	59 ± 12	3,4 ± 1,2	30,98 ± 33,51	0,49 ± 0,94	29,84 ± 33,78	26,29 ± 14,99
poly	100	58 ± 11	3,19 ± 1,12	32,86 ± 40,66	0,32 ± 0,92	31,79 ± 40,59	25,28 ± 19,87
poly	500	58 ± 11	3,1 ± 1,11	46,54 ± 59,67	0,28 ± 0,91	44,61 ± 59,61	39,14 ± 37,1
poly	1000	57 ± 11	3,07 ± 1,12	53,27 ± 69,74	0,28 ± 0,91	50,51 ± 69,34	50,23 ± 50,74

Table 3.15: Mean absolute errors for SVR Models for two drugs model structure, kernel and C value. %SV is the percentage of support vectors. MAE presented for training and testing datasets and for induction, maintenance and recovery stages of general anaesthesia.

kernel	**C**	**% SV**	**MAE (Training)**	**MAE (Testing)**	**MAE (Ind.)**	**MAE (Maint.)**	**MAE (Rec.)**
rbf	1	84 ± 8	8,87 ± 4,13	10,8 ± 4,86	12,16 ± 9,94	10,45 ± 4,73	11,9 ± 7,25
rbf	10	65 ± 11	4,17 ± 1,28	12,2 ± 6,74	1,56 ± 1,39	11,74 ± 6,49	13,22 ± 9,29
rbf	100	64 ± 9	3,83 ± 1,22	12,69 ± 7,24	0,71 ± 1,12	12,22 ± 6,99	13,28 ± 9,6
rbf	500	62 ± 9	3,65 ± 1,2	13,64 ± 7,54	0,6 ± 1,11	13,08 ± 7,33	14,64 ± 10,16
rbf	1000	61 ± 10	3,58 ± 1,19	14,26 ± 7,82	0,55 ± 1,06	13,61 ± 7,6	15,93 ± 11,15

Table 3.16: Mean absolute errors for SVR Models for two drugs model structure, kernel and C value. %SV is the percentage of support vectors. MAE presented for training and testing datasets and for induction, maintenance and recovery stages of general anaesthesia.

kernel	**C**	**% SV**	**MAE (Training)**	**MAE (Testing)**	**MAE (Ind.)**	**MAE (Maint.)**	**MAE (Rec.)**
spline	1	79 ± 9	7,78 ± 4,11	12,47 ± 5,87	10,52 ± 10,21	12,1 ± 5,74	12,27 ± 8,16
spline	10	64 ± 9	3,8 ± 1,23	13,31 ± 7,17	1,04 ± 1,2	12,8 ± 6,95	13,84 ± 9,61
spline	100	60 ± 10	3,3 ± 1,09	13,91 ± 8,16	0,44 ± 0,94	13,31 ± 7,96	14,69 ± 9,52
spline	500	55 ± 9	2,93 ± 0,98	14,94 ± 10,61	0,26 ± 0,83	14,23 ± 10,42	16,15 ± 10,99
spline	1000	54 ± 10	2,79 ± 0,93	15,9 ± 11,87	0,2 ± 0,8	15,15 ± 11,66	16,78 ± 12,25

Table 3.17: Mean absolute errors for SVR Models for two drugs with nCO model structure, kernel and C value. %SV is the percentage of support vectors. MAE presented for training and testing datasets and for induction, maintenance and recovery stages of general anaesthesia.

kernel	**C**	**% SV**	**MAE (Training)**	**MAE (Testing)**	**MAE (Ind.)**	**MAE (Maint.)**	**MAE (Rec.)**
anovaspline1	1	79 ± 7	7,46 ± 2,13	13,76 ± 6,28	9,02 ± 4,78	13,13 ± 6,49	16,19 ± 19,6
anovaspline1	10	59 ± 10	3,72 ± 1,19	13,67 ± 7,57	1 ± 0,86	12,91 ± 7,47	18,1 ± 24,54
anovaspline1	100	51 ± 10	3,04 ± 0,95	14,15 ± 7,47	0,29 ± 0,67	13,26 ± 7,32	19,59 ± 26,7
anovaspline1	500	47 ± 10	2,63 ± 0,74	16,19 ± 9,23	0,2 ± 0,64	15,16 ± 9,05	21,43 ± 25,16
anovaspline1	1000	45 ± 10	2,46 ± 0,66	18,06 ± 12,65	0,17 ± 0,62	16,98 ± 12,41	22,28 ± 24,82

Table 3.18: Mean absolute errors for SVR Models for two drugs with nCO model structure, kernel and C value. %SV is the percentage of support vectors. MAE presented for training and testing datasets and for induction, maintenance and recovery stages of general anaesthesia.

kernel	**C**	**% SV**	**MAE (Training)**	**MAE (Testing)**	**MAE (Ind.)**	**MAE (Maint.)**	**MAE (Rec.)**
erbf	1	90 ± 6	16,31 ± 4,25	10,4 ± 4,11	25,72 ± 9,83	10,19 ± 4,07	11,03 ± 6,24
erbf	10	64 ± 9	3,92 ± 1,11	13,08 ± 6,2	2,19 ± 1,12	12,53 ± 5,99	14,06 ± 8,6
erbf	100	47 ± 10	2,28 ± 0,61	12,47 ± 6,7	0,56 ± 0,58	11,81 ± 6,47	14,17 ± 8,67
erbf	500	41 ± 9	1,72 ± 0,36	12,16 ± 6,79	0,4 ± 0,47	11,46 ± 6,57	14,05 ± 8,53
erbf	1000	39 ± 8	1,59 ± 0,27	12,08 ± 6,75	0,4 ± 0,44	11,37 ± 6,53	14,02 ± 8,51

Table 3.19: Mean absolute errors for SVR Models for two drugs with nCO model structure, kernel and C value. %SV is the percentage of support vectors. MAE presented for training and testing datasets and for induction, maintenance and recovery stages of general anaesthesia.

kernel	**C**	**% SV**	**MAE (Training)**	**MAE (Testing)**	**MAE (Ind.)**	**MAE (Maint.)**	**MAE (Rec.)**
poly	1	64 ± 10	4,4 ± 1,24	32,5 ± 34,73	2,41 ± 2,24	30,7 ± 35,47	38,85 ± 47,81
poly	10	53 ± 10	3,13 ± 1,01	33,79 ± 38,18	0,45 ± 0,55	31,65 ± 38,52	44,32 ± 109,69
poly	100	50 ± 10	2,82 ± 0,87	38,36 ± 44,21	0,23 ± 0,6	35,32 ± 43,52	57,27 ± 184,55
poly	500	49 ± 10	2,71 ± 0,82	60,65 ± 76,83	0,21 ± 0,6	57,09 ± 77,37	71,55 ± 167,94
poly	1000	48 ± 10	2,68 ± 0,81	76,11 ± 109,37	0,2 ± 0,58	70,95 ± 110,09	101,61 ± 277,06

Table 3.20: Mean absolute errors for SVR Models for two drugs with nCO model structure, kernel and C value. %SV is the percentage of support vectors. MAE presented for training and testing datasets and for induction, maintenance and recovery stages of general anaesthesia.

kernel	**C**	**% SV**	**MAE (Training)**	**MAE (Testing)**	**MAE (Ind.)**	**MAE (Maint.)**	**MAE (Rec.)**
rbf	1	85 ± 6	11,7 ± 3,96	9,45 ± 3,63	18,41 ± 9,69	9,15 ± 3,64	10,95 ± 6,37
rbf	10	61 ± 10	4,17 ± 1,26	12,37 ± 6,73	1,72 ± 1,22	11,85 ± 6,52	13,96 ± 9,22
rbf	100	57 ± 11	3,63 ± 1,19	12,8 ± 7,38	0,57 ± 0,8	12,28 ± 7,16	14,13 ± 9,39
rbf	500	55 ± 11	3,4 ± 1,1	13,75 ± 7,82	0,44 ± 0,75	13,17 ± 7,63	15,2 ± 9,57
rbf	1000	54 ± 10	3,32 ± 1,07	14,14 ± 8,14	0,39 ± 0,74	13,5 ± 7,92	16,09 ± 10,53

Table 3.21: Mean absolute errors for SVR Models for two drugs with nCO model structure, kernel and C value. %SV is the percentage of support vectors. MAE presented for training and testing datasets and for induction, maintenance and recovery stages of general anaesthesia.

kernel	**C**	**% SV**	**MAE (Training)**	**MAE (Testing)**	**MAE (Ind.)**	**MAE (Maint.)**	**MAE (Rec.)**
spline	1	79 ± 7	7,46 ± 2,13	13,76 ± 6,28	9,02 ± 4,78	13,13 ± 6,49	16,19 ± 19,6
spline	10	59 ± 10	3,72 ± 1,19	13,67 ± 7,57	1 ± 0,86	12,91 ± 7,47	18,1 ± 24,54
spline	100	51 ± 10	3,04 ± 0,95	14,15 ± 7,47	0,29 ± 0,67	13,26 ± 7,32	19,59 ± 26,7
spline	500	47 ± 10	2,63 ± 0,74	16,19 ± 9,23	0,2 ± 0,64	15,16 ± 9,05	21,43 ± 25,16
spline	1000	45 ± 10	2,46 ± 0,66	18,06 ± 12,65	0,17 ± 0,62	16,98 ± 12,41	22,28 ± 24,82

3.5.2 Results of the Model Adequacy Index

The MAI was assessed for all the models obtained using the SVR modelling technique. For the pharmacodynamic models obtained using either single-drug Hill Model or multi-drug Hill, the MAI was not assessed as these are parametric models based on a sigmoid curve which complies with all the BIS characteristics to which the MAI was developed to assess compliance.

Tables 3.22 to 3.26 presents a summary of the obtained MAI for all the Pharmacodynamic SVR models grouped by model structure, kernel and C value. It shows the minimum, maximum, mean and standard deviation (SD) of the MAI for each group of 42 estimated Pharmacodynamic SVR models as well totals per model structure and kernel.

The overall MAI minimum and maximum obtained were 24% and 100%, respectively, while the mean value was 52%. Similar results are obtained when considering the results per model structure, and no difference is observed between the three model structures.

Analysing the results per kernel, only the RBF kernel has the maximum MAI of 100% and a mean above 90% while the remaining kernels do not present any MAI above 60%. While the exponential radial basis function (ERBF) kernel presents the MAI's highest minimum and the smallest standard deviation of all the kernels used, its mean value is 59% and never achieves higher values of compliance above 60%. This is due mainly to an extremely low value of Deviation, reflecting the inability of the estimated Pharmacodynamic SVR models achieving the BIS values of zero in high concentrations of propofol, as presented in figure 3.5.

Table 3.22: Summary of Model Adequacy Index (MAI) results

	One Drug				Two Drugs				Two Drugs with nCO				Total			
	Min	Max	Mean	SD	Min	Max	Mean	SD	Min	Max	Mean	SD	Min	Max	Mean	SD
anovaspline1	36%	60%	43%	5%	26%	51%	36%	4%	25%	43%	35%	4%	25%	60%	38%	5%
1	39%	60%	44%	5%	36%	42%	38%	1%	27%	43%	37%	2%	27%	60%	40%	5%
10	38%	53%	41%	3%	35%	40%	37%	1%	34%	40%	37%	1%	34%	53%	38%	3%
100	38%	60%	43%	5%	26%	47%	37%	4%	26%	40%	35%	3%	26%	60%	38%	5%
500	38%	60%	43%	5%	26%	51%	35%	5%	25%	40%	33%	4%	25%	60%	37%	7%
1000	36%	52%	42%	4%	26%	43%	34%	5%	25%	40%	33%	4%	25%	52%	36%	6%

Table 3.23: Summary of Model Adequacy Index (MAI) results

	One Drug				Two Drugs				Two Drugs with nCO				Total			
	Min	Max	Mean	SD	Min	Max	Mean	SD	Min	Max	Mean	SD	Min	Max	Mean	SD
erbf	58%	60%	59%	0%	55%	60%	59%	1%	55%	60%	59%	1%	55%	60%	59%	1%
1	58%	60%	59%	0%	58%	60%	59%	0%	57%	60%	59%	1%	57%	60%	59%	0%
10	59%	60%	59%	0%	58%	60%	59%	0%	58%	60%	59%	0%	58%	60%	59%	0%
100	58%	60%	59%	0%	57%	60%	59%	0%	56%	60%	59%	1%	56%	60%	59%	1%
500	58%	60%	59%	0%	56%	60%	59%	1%	55%	60%	59%	1%	55%	60%	59%	1%
1000	58%	60%	59%	0%	55%	60%	59%	1%	55%	60%	59%	1%	55%	60%	59%	1%

Table 3.24: Summary of Model Adequacy Index (MAI) results

	One Drug				Two Drugs				Two Drugs with nCO				Total			
	Min	Max	Mean	SD	Min	Max	Mean	SD	Min	Max	Mean	SD	Min	Max	Mean	SD
poly	28%	47%	34%	5%	24%	35%	30%	3%	24%	35%	30%	3%	24%	47%	31%	4%
1	30%	43%	40%	2%	26%	35%	31%	2%	26%	34%	30%	2%	26%	43%	33%	5%
10	28%	47%	33%	5%	24%	35%	31%	3%	25%	35%	30%	3%	24%	47%	31%	4%
100	28%	45%	33%	5%	24%	35%	30%	4%	24%	35%	30%	3%	24%	45%	31%	4%
500	28%	41%	33%	4%	24%	35%	30%	4%	24%	35%	30%	3%	24%	41%	31%	4%
1000	28%	41%	33%	4%	24%	35%	29%	4%	24%	35%	29%	3%	24%	41%	30%	4%

Table 3.25: Summary of Model Adequacy Index (MAI) results

	One Drug				Two Drugs			Two Drugs with nCO			Total		
	Min	Max	Mean	SD	Min	Max	Mean	SD	Min	Max	Mean	SD	Min	Max	Mean	SD
rbf	42%	100%	87%	14%	69%	99%	96%	5%	81%	100%	97%	3%	42%	100%	93%	10%
1	80%	100%	95%	5%	96%	99%	98%	1%	96%	100%	99%	0%	80%	100%	97%	3%
10	54%	100%	89%	10%	94%	99%	97%	1%	95%	99%	98%	1%	54%	100%	95%	7%
100	44%	100%	87%	13%	81%	99%	96%	4%	90%	99%	97%	2%	44%	100%	93%	9%
500	43%	100%	82%	16%	72%	99%	94%	6%	84%	99%	96%	4%	43%	100%	91%	12%
1000	42%	100%	80%	18%	69%	99%	93%	7%	81%	99%	95%	5%	42%	100%	89%	13%

Table 3.26: Summary of Model Adequacy Index (MAI) results

	One Drug				Two Drugs				Two Drugs with nCO				Total			
	Min	Max	Mean	SD	Min	Max	Mean	SD	Min	Max	Mean	SD	Min	Max	Mean	SD
spline	36%	60%	43%	5%	26%	51%	36%	4%	25%	43%	35%	4%	25%	60%	38%	5%
1	39%	60%	44%	5%	36%	42%	38%	1%	27%	43%	37%	2%	27%	60%	40%	5%
10	38%	53%	41%	3%	35%	40%	37%	1%	34%	40%	37%	1%	34%	53%	38%	3%
100	38%	60%	43%	5%	26%	47%	37%	4%	26%	40%	35%	3%	26%	60%	38%	5%
500	38%	60%	43%	5%	26%	51%	35%	5%	25%	40%	33%	4%	25%	60%	37%	7%
1000	36%	52%	42%	4%	26%	43%	34%	5%	25%	40%	33%	4%	25%	52%	36%	6%

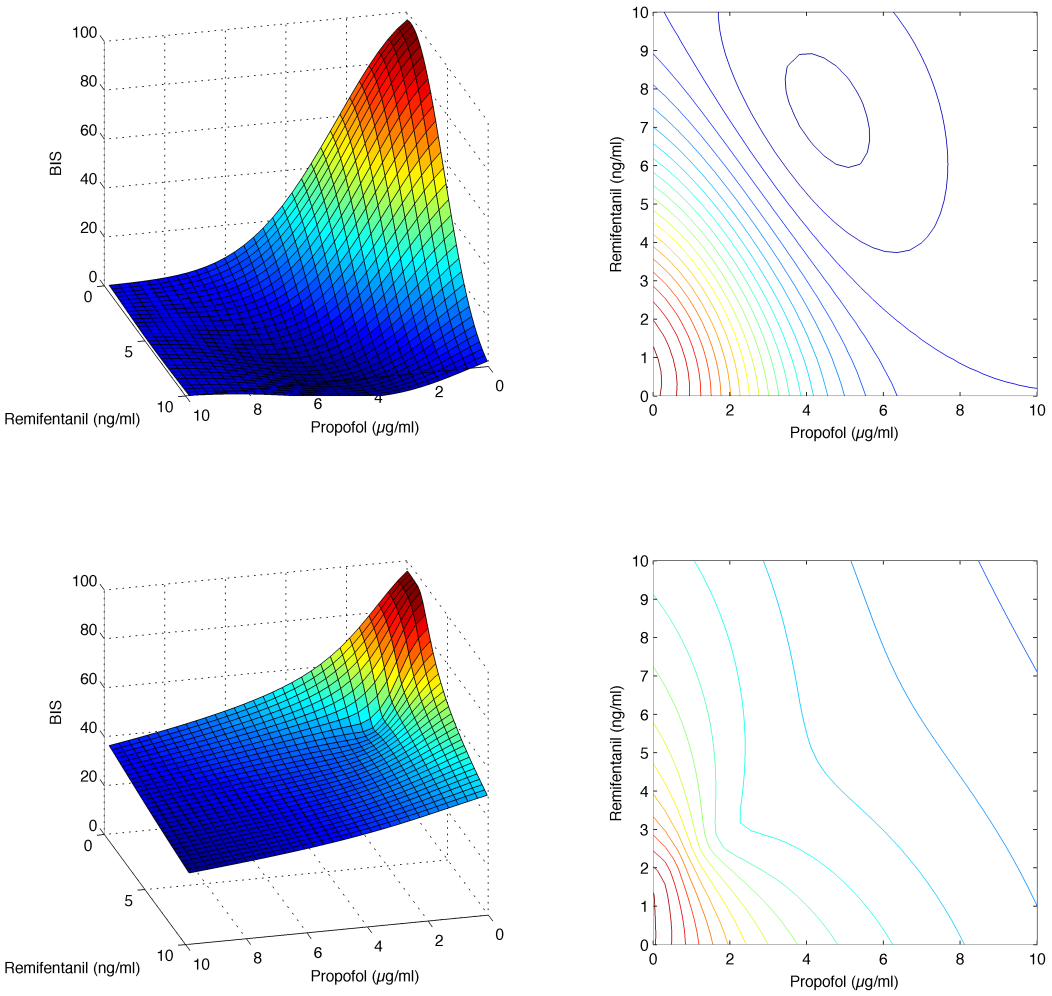

Figure 3.5: Effect surfaces (left) and contour plot (right) for case 3 estimated multi-drug SVR model with C value of 10 and rbf kernel (top line) or erbf kernel (bottom line), obtained from 4096 points evaluated to assess model adequacy index.

Regardless of all three model structures implemented showing similar MAI results considering all Pharmacodynamic SVR models estimated, if only the models estimated with a RBF kernel function are considered, an adequacy difference arises between model structures. The adequacy of the estimated models increases with the complexity of the model structures, having the one drug model the lowest adequacy of 87% ± 14%, and the two drugs with nCO the highest with 97% ± 3%.

Finally, looking at the detail of Tables 3.22 to 3.26, it is possible to observe that the Pharmacodynamic model adequacy decreases with the increase of the C values of the SVR modelling.

From these results, the most appropriate kernel would be the RBF. These results need to be analysed in conjunction with the performance results to determine the best combination of model structure, kernel and C values for Pharmacodynamic SVR modelling.

3.5.3 Comparison between Adequacy and Performance of the SVRs

In this Subsection we will focus our analysis of the suitability of SVR as a PD modelling technique in the performance of the estimated models in terms of MAE in the training and testing datasets, which is presented in Tables 3.7 to 3.21 while considering model adequacy. The best estimated Pharmacodynamic model would be the one which presented the highest adequacy, assessed by the highest MAI, and the best performance, assessed by the lowest training and testing MAE.

With the consideration of the results presented in the previous subsection, it

can be established that only SVRs with an RBF kernel present an acceptable adequacy level for the intended PD modelling. From Tables 3.7 to 3.21 it is possible to observe that the training MAE decreases with the increase of the C value. There is a significant training MAE decrease between the C values of 1 and 10, in all the RBF SVR structures implemented, but much smaller with the remaining C values. In contrast with the training MAE behaviour, the testing MAE increases with the increase of the C values, however no significant change is observed for the C values of 1 and 10, and their values are similar within the various C values used.

When taking into consideration these observations with the observation that the adequacy decreases with the increase of the C value, in the previous subsection, it can be asserted that the model estimated though the SVR technique with the RBF kernel and C value of 10, is the most suitable as an SVR PD model. This assertion is obtained by considering the described observation, it is necessary to compromise between the model adequacy and performance.

3.6 Discussion

3.6.1 Hill Models

The results for the modelling of BIS using the single and multi-variable Hill models are presented in Tables 3.5 and 3.6.

From the three techniques used to estimate Hill equation's parameters, GA with MAE as cost function proved to be the most appropriate. This is reflected by smaller training and testing errors in conjunction with the smaller standard

deviation on the Hill model parameters. The smaller standard deviation on the model parameters indicates that GA produce a model with smaller inter-patients variability, which is an advantage for the generalization of the models.

When comparing the single with the multi-variable Hill model, it is observed that the modelling of the clinical effect of the anaesthetic drugs using the multi-variable Hill presents a better, *i.e.* smaller, training error, but a considerably worse performance in the testing data.

In contrast with the SVR modelling technique, all the estimated Hill models have full adequacy as Pharmacodynamic models, which is insured by the parametric nature of the technique and the limits established for the Hill parameters.

3.6.2 SVR Models

As described in Section 3.5, the performance of the estimated SVR models is highly diverse and dependent on the model structure, kernel and C values, and therefore there is no clear better model in terms of performance. However when the Pharmacodynamic model adequacy requirement is taken in to consideration, a few features become evident.

As stated in Section 3.5 only the estimated models using a RBF kernel can be considered as adequate Pharmacodynamic models, and when adequacy and performance are analysed in conjunction, it can be concluded that the C value of 10 is the most suitable for the necessary compromise between adequacy and performance.

The observation that adequacy decreases with the increase of the C value can be explained by the fact that a high C value estimates a model with smaller

margins, forcing a high number of samples to be matched by the estimated model. As the BIS signal is noisy, this can create a model that is too sensitive.

For the combination of RBF kernel with a C value of 10, all three SVR structures implemented present a similar performance, however adequacy is improved with the increased complexity of the SVR structure. Therefore, the Pharmacodynamic models estimated though the SVR technique with a RBF kernel, C value of 10 and with the two drugs plus the cardiac output as model inputs, has the best adequacy.

3.6.3 Comparison between Hill Models and SVR Models

From the performance and adequacy analysis of the various estimated SVR Models, the models using the RBF kernel and the C value of 10 are the most suitable as a PD model. The performance of two of these SVR models can be compared with the performance of the PD models obtained through the Hill equation. For the SVR structure of two drugs with nCO information, a direct comparison to Hill models is not admissible since they do not consider nCO information.

In the first case, where the anaesthetic effect is modelled based solely on the effect-site concentration of propofol, one drug model, we can observe from Tables 3.6, 3.7, 3.8, 3.9, 3.10 and 3.11 that the SVR technique presents a smaller training error compared with all three estimation methods used on the Hill equation structure. However, the testing error is slightly higher, although with a smaller standard deviation.

The second model structure which allows direct comparison between the Hill and SVR modelling techniques is the case where the anaesthetic effect is modelled

based on the effect-site concentrations of propofol and remifentanil. As in the previous case, the SVR technique has a smaller training error compared with the Hill methods. However the performance results obtained on the testing dataset are considerably better in the PD models estimated using the SVR technique. The mean absolute error in the testing data for the SVR technique (using RBF kernel and a C of 10) was 12.2 $\pm$ 6.74 (mean $\pm$ SD) against 28.35 $\pm$ 15.46 and 31.23 $\pm$ 17.7 with the Hill structure. This result suggests that the SVR technique has a better generalization property than the Hill model, and is capable of extracting more information from the training data, namely on the synergetic interaction between the drugs.

While a better performance is obtained by the SVR modelling technique, these models do not present a 100% adequacy as a PD model in contrast with the Hill modelling techniques. However the estimated SVR models compared in this section do present a high level of adequacy (see Tables 3.22 to 3.26) and this can be adjusted with minor model output post-processing.

3.6.4 nCO adjusted Support Vector Regression Model

One of the SVR model structures used in this study makes use of the cardiac output information in addition to the effect-site concentrations of propofol and remifentanil. Tables 3.12 to 3.26 show that its performance and adequacy is similar to the case where the SVR model structures incorporate only the two effect-site concentrations (with RBF kernel and a C value of 10).

No significant performance differences can be found between these two model structures for the remaining C values with RBF kernel. Adequacy of the SVR

model structure using the nCO information also decreased with the increase of the C values, as in the case of the SVR model structure using only the effect-site concentrations of propofol and remifentanil. However, the adequacy decrease in relation to the C value increase with the SVR model structure using the nCO information, is smaller than that of the SVR model structure with two drugs without the nCO information.

As previously discussed, the nCO may have an important role to play in the PK/PD modelling. This is based on previous studies where a strong correlation between propofol requirements and nCO was found in vascular patients and in published studies such as Kurita *et al.*[35] where an inverse relation between nCO and plasmatic propofol concentration in swine is demonstrated. Considering this and that the effect-site concentration used as inputs for the PD models are estimated through a PK model solely dependent on the infusion of propofol and patients' weight, which does not account for change in the nCO, it was considered relevant to incorporate it in the PD modelling.

Considering the above, in our opinion it would be appropriate to have the nCO in consideration when constructing a controller for the induction and maintenance of intravenous anaesthesia. The inclusion of nCO in the control law will make it more robust to disturbances and might present a better performance when compared to a controller without these considerations.

3.7 Summary

In this chapter, we have studied the modelling of the effect of anaesthetic drugs in patients under general anaesthesia during surgery. Two modelling approaches

were applied to establish PD models. The first approach consisted of creating a parametric model based on the published equation of Hill. Support vector regressors were used in the second approach as a non-parametric technique which would enable the incorporation of others variables in the modelling process such as cardiac output.

From our results we can conclude that the SVR modelling technique with an RBF kernel presents a better performance compared to the parametric Hill modelling technique, for PD modelling based on predicted effect-site concentrations of propofol and remifentanil. However one needs to be aware that the SVR modelling technique does not have a 100% adequacy in contrast with the Hill modelling technique.

It was also found that incorporating the cardiac output in the modelling process using the SVR modelling technique has not reduced the performance of the estimated Pharmacodynamic models and has improved the adequacy. This is of extreme importance from a clinical perspective, since the PK models are based on estimated and not real drug concentrations (which are impossible to measure online). It is well proven that variations in nCO change the drugs' metabolism (its PK characteristics) [35], therefore a model that can predict PK and subsequent PD changes has a positive impact on the description of drug effect. Research has shown that patient heamodynamic alterations have an impact on the BIS index in response to alterations of propofol PK [29]. The inclusion of nCO allows for the SVR structure model to adjust itself to changes in the PK of the drugs during a surgical procedure, and will allow for a better control of the drug effect (in this case the EEG response measured by BIS). This adds great refinement to the traditional PK/PD model and would also allow automatic adjustment of propofol

infusion rates as the cardiac output falls. This may happen, for example, during major haemorrhage which is a major adverse effect of surgery.

Chapter 4

Control of Anaesthesia using PK and PD models

4.1 Introduction

Due to the advantages of automatic closed-loop control, in this chapter, the aim is to implement closed-loop control for the anaesthesia model. The performance of controllers is ensured by optimization and tested by simulation. For the PK/PD model used in this thesis, while an existing anaesthesia PK model is utilized, the parameters of the PD model are especially obtained from clinical data collected from 42 patients presented in Chapter 3.

Following the same design procedure, these tailor-made controllers can be re-designed for other patients as long as clinical data have been collected. In the PK/PD model, the co-administration of both propofol and remifentanil is investigated. To realize the drug administration, it is proposed to use two strategies: two fuzzy PID controllers and one fuzzy PID controller with scaling factors. For

each group of strategies, linear PID controller, type-1 (T1) fuzzy PID controllers and interval type-2 (IT2) fuzzy PID controllers are designed. To draw a distinction from existing IT2 fuzzy PID controllers, IT2 fuzzy PID controllers is combined with GA. All PID gains, scaling factors and parameters of membership functions are optimized by GA in an offline manner subject to a performance index (cost function) which quantifies the performance of the controllers. A BIS training profile is employed for training purposes which sets different local targets for regulation considering the real anaesthesia situation. The trained PID control strategies are tested with a testing profile to verify their performance in unseen working conditions. Comparisons are made among all controllers to demonstrate the characteristics of each control strategy.

The following sections are organized in this sequence: in Section 4.2, a multivariable anaesthesia model used in this chapter is described; in Section 4.3, the control background of linear PID controller, T1 fuzzy PID controllers and IT2 fuzzy PID controllers is introduced; in Section 4.4, all the control strategies and overall procedure and necessary information of the simulation are discussed; in Section 4.5, the simulation results are provided and comparison and analysis are carried out; finally, in Section 4.6, a conclusion for this chapter is drawn.

4.2 Multivariable Anaesthetic Modelling

In this section, a anaesthetic model with two drugs is introduced. As shown in Figure 4.1, the anaesthesia model consists of the target controlled infusion (TCI) system, the PK model, and the PD model, where Cpt_{prop} and Cpt_{remi} are plasma concentration targets, I_p and I_r are infusion rates, Ce_{prop} and Ce_{remi} are

effect-site concentrations, and the subscript *prop* and *remi* are for propofol and remifentanil, respectively. Details of each TCI and PK modules are described in Subsection 2.4.1.2 and 2.4.1, respectively. The PD module is a two drugs Hill-based PD model as described in Section 2.4.2 and its parameters obtained as described in Chapter 3.

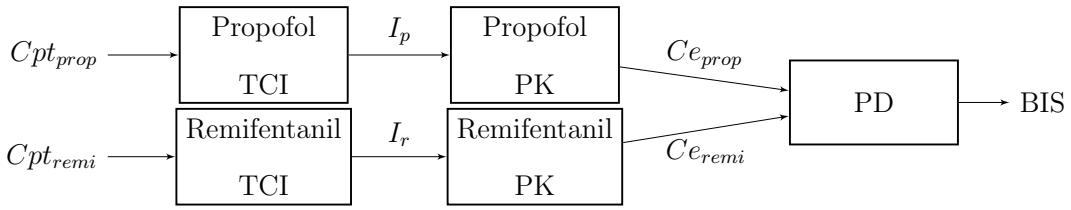

Figure 4.1: A block diagram of multivariable anaesthesia model.

4.3 PID Controllers

In this section, 3 types of PID controllers, namely linear PID controller, T1 fuzzy PID controller and IT2 fuzzy PID controller, are introduced. These 3 types of PID controllers are employed to regulate the output BIS index of the anaesthesia model.

4.3.1 Linear PID controller

A linear PID controller is shown in Figure 4.2, which consists of 3 elements, namely proportional, integral and derivative blocks. The output of the linear

PID controller in discrete time is given as

$$u(t_k) = K_P e(t_k) + K_I \sum_{i=0}^{k} e(t_i)\Delta t_k + K_D \frac{e(t_k) - e(t_{k-1})}{\Delta t_k}, \tag{4.1}$$

where $t_k = k\Delta t_k, k = 0, 1, 2, \ldots,$ is the sampling time; Δt_k is the interval of sampling time; $e(t_k) \in \Re$ is the input; $u(t_k) \in \Re$ is the output; $K_P \in \Re$, $K_I \in \Re$ and $K_D \in \Re$ are constant proportional, integral and derivative gains, respectively, to be determined.

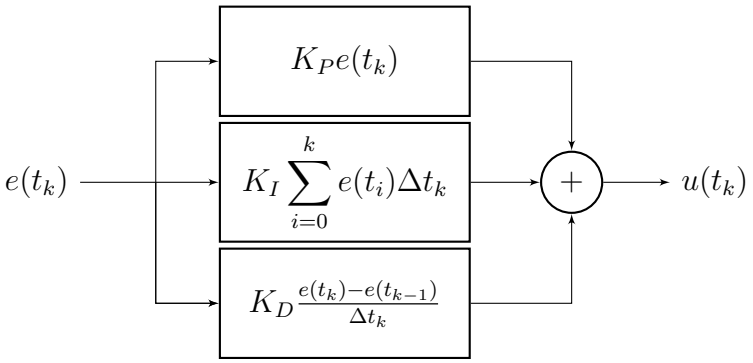

Figure 4.2: A block diagram of linear PID controller.

4.3.2 Type-1 Fuzzy PID Controller

In view of the linear PID controller [6], as the proportional, integral and derivative gains are constant, it is not able to handle well a highly nonlinear system. It motivates the use of T1 fuzzy PID controller [12, 13] of which the gains change according to the operating domains. By applying different sets of gains in different operating domains, a more appropriate PID controller is employed to deal with the nonlinear system resulting in an improvement of control performance.

A T1 fuzzy PID control system is shown in Figure 4.3, which consists of a T1

fuzzy PID controller and a patient's model (detailed in Figure 4.1) connected in a closed loop. Unlike the linear PID controller having a set of constant gains, the T1 fuzzy PID controller has a fuzzy inference system providing a set of feedback gains through a reasoning process according to the operating condition.

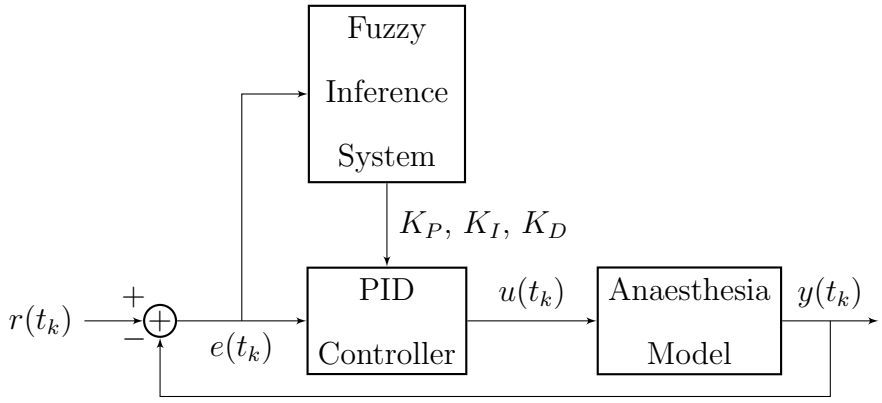

Figure 4.3: A block diagram of fuzzy PID control system.

The behavior of the fuzzy inference system is governed by a set of fuzzy rules of the following format:

$$\begin{aligned} &\text{Rule } i\text{: IF } x_1(t) \text{ is } M_1^i \text{ AND } \cdots \text{ AND } x_\Psi(t) \text{ is } M_\Psi^i \\ &\text{THEN } y(\mathbf{x}(t)) = y_i, \end{aligned} \tag{4.2}$$

where $x_j(t)$, $j = 1, 2, \ldots, \Psi$, is a linguistic variable; M_j^i, $j = 1, 2, \ldots, \Psi$, is the fuzzy term corresponding to the linguistic variable x_j in the i^{th} rule; Ψ is a positive integer; $y(\mathbf{x}(t))$ is the output of the fuzzy inference system; and y_i is the singleton membership function corresponding to the i^{th} rule. The inferred output

is given as

$$y(\mathbf{x}(t)) = \sum_{i=1}^{p} w_i(\mathbf{x}(t)) y_i, \tag{4.3}$$

where

$$\mathbf{x}(t) = \begin{bmatrix} x_1(t) & x_2(t) & \cdots & x_\Psi(t) \end{bmatrix},$$

$$\sum_{i=1}^{p} w_i(\mathbf{x}(t)) = 1, \tag{4.4}$$

$$w_i(\mathbf{x}(t)) \geq 0 \; \forall \; i, \tag{4.5}$$

$$w_i(\mathbf{x}(t)) = \frac{\prod_{l=1}^{\Psi} \mu_{M_l^i}(\mathbf{x}(t))}{\sum_{k=1}^{p} \prod_{l=1}^{\Psi} \mu_{M_l^k}(\mathbf{x}(t))} \; \forall \; i, \tag{4.6}$$

where $p > 0$ denotes the number of rules; $w_i(\mathbf{x}(t))$ is the normalized grade of membership; $\mu_{M_\alpha^i}(\mathbf{x}(t))$, $\alpha = 1, 2, \ldots, \Psi$, is the grade of membership corresponding to the fuzzy term M_α^i.

The output of the fuzzy inference system equation (4.3) is employed to replace the gains of the linear PID controller turning it to become a T1 fuzzy PID controller. More precisely, 3 fuzzy inference systems are required to implement a T1 fuzzy PID controller. The outputs of the 3 fuzzy inference systems will be employed as K_P, K_I and K_D. Consequently, the PID gains are no longer constant but dependent on the operating condition characterized by the membership functions.

4.3.3 Interval Type-2 Fuzzy PID Controller

Type-2 (T2) fuzzy sets [25, 30, 36, 37] demonstrate a superior characteristic handing uncertainties compared with the T1 fuzzy sets. Uncertainties are captured by the lower and upper membership functions which form the footprint of uncertainty (FOU). A T2 fuzzy inference system can be considered as a set of infinite number of T1 fuzzy inference systems. Consequently, a T2 fuzzy inference system is able to outperform the T1 fuzzy inference system in terms of reasoning and generalization capability. In general, the defuzzification process for general T2 fuzzy sets is computational demanding. By using IT2 fuzzy sets [43], the computational demand can be significantly reduced.

By employing interval fuzzy sets for the T1 fuzzy inference system equation (4.3), it becomes an IT2 fuzzy inference system. The behaviour of an IT2 fuzzy inference system is described by a set of rules of the following format:

$$\begin{aligned} &\text{Rule } i\text{: IF } x_1(t) \text{ is } \tilde{M}_1^i \text{ AND } \cdots \text{ AND } x_\Psi(t) \text{ is } \tilde{M}_\Psi^i \\ &\text{THEN } y(\mathbf{x}(t)) = \tilde{y}_i, \end{aligned} \tag{4.7}$$

$$W_i(\mathbf{x}(t)) = \left[\begin{array}{cc} \underline{w}_i(\mathbf{x}(t)), & \overline{w}_i(\mathbf{x}(t)) \end{array} \right], \tag{4.8}$$

$$\tilde{y}_i = \left[\begin{array}{cc} \underline{y}_i, & \overline{y}_i \end{array} \right], i = 1, 2, \ldots, p, \tag{4.9}$$

where

$$\underline{w}_i(\mathbf{x}(t)) = \prod_{\alpha=1}^{\Psi} \underline{\mu}_{\tilde{M}_\alpha^i}(\mathbf{x}(t)) \geq 0, \tag{4.10}$$

$$\overline{w}_i(\mathbf{x}(t)) = \prod_{\alpha=1}^{\Psi} \overline{\mu}_{\tilde{M}_\alpha^i}(\mathbf{x}(t)) \geq 0, \tag{4.11}$$

$$\overline{\mu}_{\tilde{M}_\alpha^i}(\mathbf{x}(t)) \geq \underline{\mu}_{\tilde{M}_\alpha^i}(\mathbf{x}(t)) \geq 0, \tag{4.12}$$

$$\overline{w}_i(\mathbf{x}(t)) \geq \underline{w}_i(\mathbf{x}(t)) \geq 0, \tag{4.13}$$

$$\overline{y}_i \geq \underline{y}_i \geq 0, \forall\, i, \tag{4.14}$$

in which $\underline{w}_i(\mathbf{x}(t))$, $\overline{w}_i(\mathbf{x}(t))$, $\underline{\mu}_{\tilde{M}_\alpha^i}(\mathbf{x}(t))$ and $\overline{\mu}_{\tilde{M}_\alpha^i}(\mathbf{x}(t))$ denote the lower grade of membership, upper grade of membership, lower membership function and upper membership function, respectively. Using the center-of-set type reducer, the inferred output of the IT2 fuzzy inference system is given as

$$y(\mathbf{x}(t)) = \bigcup_{\tilde{w}_i(\mathbf{x}(t)) \in W_i(\mathbf{x}(t)), y_i \in \tilde{y}_i} \frac{\sum_{i=1}^{p} \tilde{w}_i(\mathbf{x}(t)) y_i}{\sum_{i=1}^{p} \tilde{w}_i(\mathbf{x}(t))} = \left[\begin{array}{cc} y_l, & y_r \end{array} \right], \tag{4.15}$$

where y_l and y_r can be obtained using the Karnik-Mendel (KM) algorithms [42].

The final defuzzified output is given by

$$y(\mathbf{x}(t)) = \frac{y_l + y_r}{2}. \tag{4.16}$$

The IT2 fuzzy PID control system[18] can be represented by Figure 4.3 as well of which the PID gains are given by the outputs of 3 IT2 fuzzy inference systems.

4.4 Simulation Design

In this section, the simulation environment is presented. First, we design the training profiles and testing profiles which all controllers need to deal with. The purpose of selected target profiles is described. Then different control strategies are provided for comparison. For fuzzy control strategies, the approach to determine fuzzy rules is explained. Finally, the procedure of using GA for optimization is described, and a performance index is designed as the cost function for optimization.

4.4.1 Target Profiles

A training profile as shown in Figure 4.4, which is a series of BIS values required for an appropriate DOA, is employed for the training of the PID control strategies using GA. It defines the target BIS values in different periods that a PID control strategy has to achieve. After the training, a testing profile as shown in Figure 4.5 is employed to verify whether or not the trained PID control strategies are able to control the BIS value to reach some targets subject to different operating

conditions.

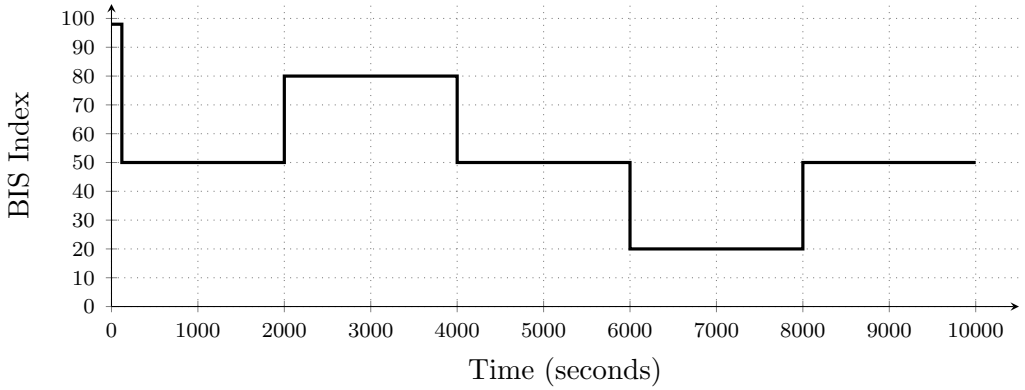

Figure 4.4: Training profile.

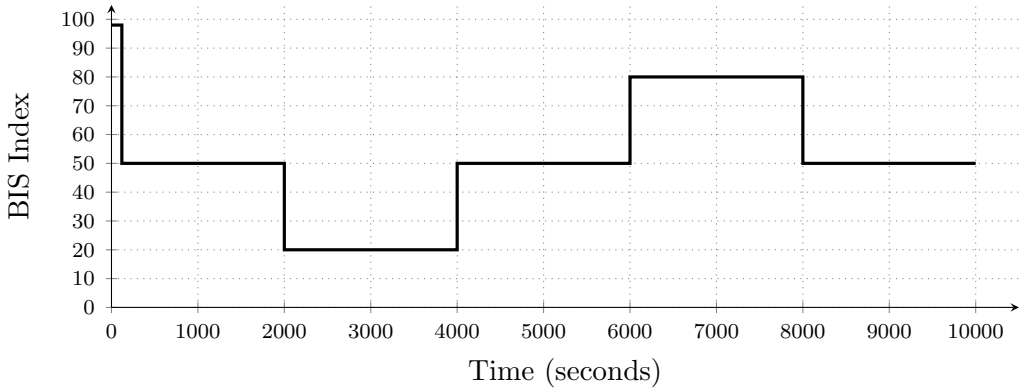

Figure 4.5: Testing profile.

Clinically, the induction process starts with $\text{BIS}(t_k) = 98$. As a result, the initial condition for the simulation is $\text{BIS}(0) = 98$ and the target profile begins by $\text{BIS}_t(t_k) = 98$, where $\text{BIS}_t(t_k)$ is the target BIS at sampling time t_k. At $t_k = 120$ seconds, the induction is executed and $\text{BIS}_t(t_k) = 50$. Since the induction period is short when compared with the maintenance period, there is not much differ-

ence during induction in terms of control performance between various control strategies. Thus, we use two linear PID controllers for two drugs to drive the BIS from 98 to 50. By trial and error, the PID gains are predefined, and it is guaranteed that BIS(1000) is around 50 and the maintenance process starts from $t_k = 1000$ seconds.

At $t_k = 1000$ seconds, designed controllers replace the predefined controller to achieve the maintenance process. For a suitable anaesthesia, it is required that $\text{BIS}_t(t_k) = 50$ and an acceptable range is $\text{BIS} \in [40, 60]$. Hence, the control objective is to maintain the BIS value within $[40, 60]$. In order to make the control difficult enough to test various control strategies, more targets are added into the profiles such as $\text{BIS}_t(t_k) = 80, t_k \in [2000, 4000)$ and $\text{BIS}_t(t_k) = 20, t_k \in [6000, 8000)$ in Figure 4.4.

As for the recovery process, since it is not allowed take the drug out of patients, the cease of controllers is the only and fastest option. These will also not exist an overshoot because the target BIS is the maximum value. Therefore, all controllers will perform the same at this stage. It is not necessary to design controllers for the recovery process which is thus not included in the target profiles. It is noted that although the induction process is not under comparison, we cannot ignore it. The reason is that it is difficult to find all model parameters describing the state of $\text{BIS}(t_k) = 50$. On the other hand, the parameters for $\text{BIS}(t_k) = 98$ are known and it is easy to start from this initial condition.

4.4.2 Control Strategies

This chapter, follows the objective of comparing different control strategies to achieve a better control performance. All six control strategies are listed in Table 4.1. These six cases can be separated into two groups: in the two-controller Cases 1 to 3 and one-controller Cases 4 to 6. In the two-controller cases, we control each drug with an independent PID controller offering control outputs $u_p(t_k)$ and $u_r(t_k)$. In one-controller cases, however, the control output of the PID controller is divided into two control outputs by two scaling factors α_r and α_p. Apparently, the parameters of these two divided controllers are constrained by the ratio of these two factors. Theoretically, this constraint leads to conservativeness and makes the performance worse than the performance in two-controller cases. Nevertheless, one-controller cases have fewer parameters to be determined resulting in lower computational demand, faster convergence in the training process and lower implementation cost for the PID control strategies.

Table 4.1: Six cases of PID control strategies.

Case	Description
1	two linear PID controllers
2	two T1 fuzzy PID controllers
3	two IT2 fuzzy PID controllers
4	one linear PID controller with scaling factors
5	one T1 fuzzy PID controller with T1 fuzzy scaling factors
6	one IT2 fuzzy PID controller with IT2 fuzzy scaling factors

In each of these two groups, we have the following control strategies: linear PID controllers, T1 fuzzy PID controllers, and IT2 fuzzy PID controllers. For fuzzy PID controllers, the block diagram of BIS index regulation using two controllers and one controller with scaling factors are shown in Figure 4.6 and Figure 4.7, respectively. Referring to the figures, $r(t)$ denotes the desired BIS target value, $y(t_k)$ is the output BIS value from the anaesthesia model, $e(t_k)$ denotes the difference between the desired target and actual BIS value at time t_k, i.e. $e(t_k) = r(t_k) - y(t_k)$. The PID gains (K_{P_1}, K_{I_1}, K_{D_1}, K_{P_2}, K_{I_2} and K_{D_2}) and scaling factors (α_r and α_p) are decided by the fuzzy inference systems. The PID controller will generate the control signals $u_p(t_k)$ and $u_r(t_k)$ for BIS regulation where $u_p(t_k)$ and $u_r(t_k)$ are Cpt_{prop} and Cpt_{remi} in Figure 4.1.

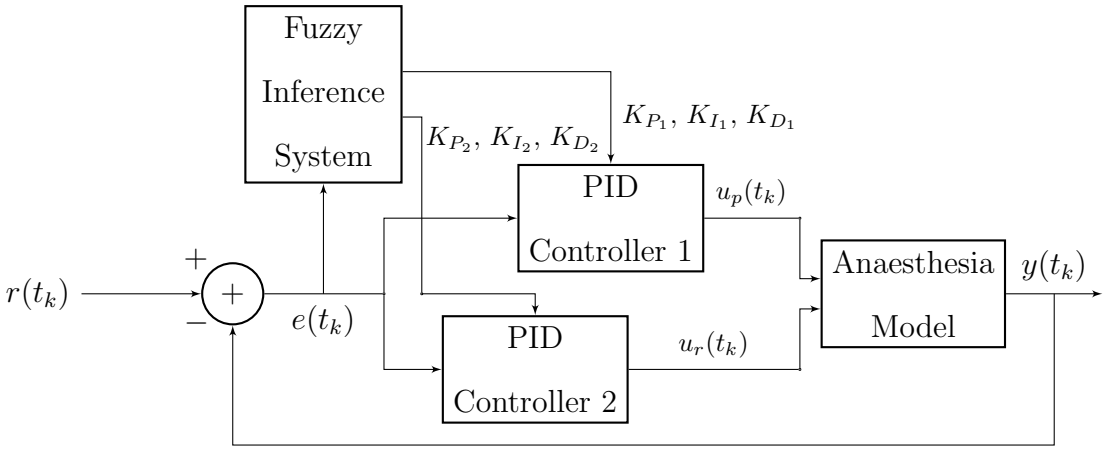

Figure 4.6: BIS index regulation using two fuzzy PID controllers.

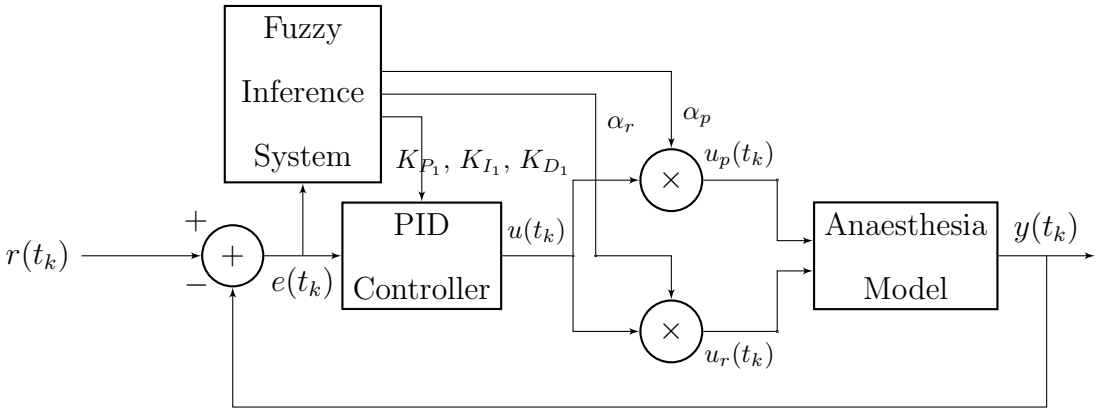

Figure 4.7: BIS index regulation using one fuzzy PID controller with scaling factors.

4.4.3 Fuzzy Rules

T1 and IT2 fuzzy PID controllers are discussed in subsections 4.3.2 and 4.3.3, respectively. While the number of fuzzy rules and the shape of membership function are predefined, the parameters of input and output membership functions

are optimized by GA.

In this chapter, the shape of membership functions is defined as a triangular shape for simplicity. The triangular IT2 membership functions are shown in Figure 4.8. For each input IT2 membership functions, the lower and upper membership functions are characterized by seven points p_1 to p_7 which are to be optimized by GA. As for the T1 fuzzy PID controller, each input membership function is characterized by three points p_1 to p_3 which are to be optimized by GA. For both the T1 and IT2 fuzzy PID controllers, their output membership functions are T1 and IT2 singleton membership functions whose values are to be determined by GA.

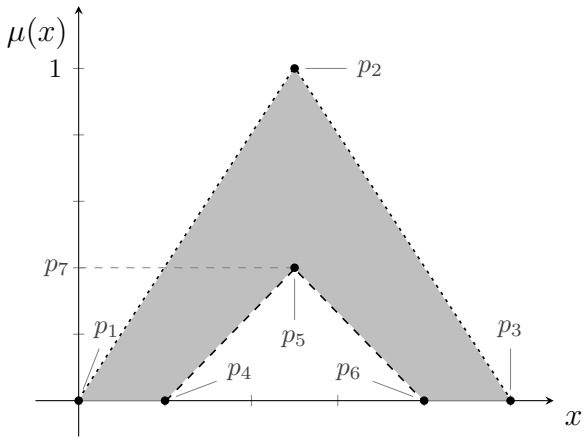

Figure 4.8: An example of IT2 membership functions. Dashed line: lower membership function. Dotted line: Upper membership function. Grey area: footprint of uncertainty.

In fact, from the determination of membership functions and fuzzy rules, we can find the relation between these control strategies: solutions for linear PID controllers can be implemented by T1 fuzzy PID controllers, and solutions for

T1 fuzzy PID controllers can be implemented by IT2 fuzzy PID controllers. In other words, linear PID controller is a subset of T1 fuzzy PID controller, and T1 fuzzy PID controller is a subset of IT2 fuzzy PID controller. By adding some constraints on the membership functions and consequents in fuzzy rules, IT2 fuzzy PID controllers can be reduced to T1 fuzzy PID controllers, and T1 fuzzy PID controllers can be reduced to linear PID controllers.

Three rules are employed for each fuzzy inference system. The premise of each rule takes only one linguistic variable, i.e., $\Delta\text{BIS}(t_k) = \text{BIS}_t(t_k) - \text{BIS}(t_k)$ where $\text{BIS}_t(t_k)$ is the target BIS value at time t_k and $\text{BIS}(t_k)$ is the actual BIS value. Three linguistic terms, namely negative (N), zero (Z), and positive (P), are employed to characterize the premise variable $\Delta\text{BIS}(t_k)$. More rules can be used to partition the universe of discourse for a better result. However, it will lead to slower convergence of training and more computational burden. Additionally, the rate of change of $\Delta\text{BIS}(t_k)$ can also be treated as another linguistic variable together with $\Delta\text{BIS}(t_k)$. Likewise, it will cause more fuzzy rules and parameters which increases the computational burden and defers the convergence.

From the above discussion, triangular membership functions and three rules are employed for both T1 and IT2 fuzzy PID controllers. In the GA optimization, the triangular shape and sequence of membership functions of three rules should be guaranteed. For the sequence, specifically, the same point in membership functions corresponding to linguistic terms N, Z and P should be in ascending order (except p_7). For example, $Np_2 < Zp_2 < Pp_2$, where Np_2, Zp_2, and Pp_2 are points p_2 for membership functions corresponding to linguistic terms N, Z and P, respectively.

Another condition which needs to be ensured is that at least one rule is fired

for $\Delta\text{BIS}(t_k) \in [-100, 100]$. Between two adjacent membership functions, as long as they intersect with each other, there exists one rule to be fired. On the left-hand side of membership function N and the right right-hand side of membership function P, there are two approaches to ensure this condition. One is defining $Np_2 = -100$ and $Pp_2 = 100$, and another is defining $Np_1 = Np_4 = -\infty$ and $Pp_3 = Pp_6 = +\infty$. It can be found that solutions from the first approach can be implemented by the second approach. In other words, the second approach is more general than the first approach. Hence, the second method is adopted. For that reason, N and P are two shoulder-shape membership functions which can be treated as a special case of triangular membership functions. In this approach, it is guaranteed that at least one rule is fired for $\Delta\text{BIS}(t_k) \in (-\infty, +\infty)$, although only $[-100, 100]$ is concerned practically. Note that under this method the equalities $Np_1 = Np_4 = Np_2$ and $Pp_3 = Pp_6 = Pp_2$ are temporarily employed in the optimization.

4.4.4 Parameters Optimization

The PID gains, scaling factors and membership functions are optimized by GA subject to a cost function reflecting the control performance. Due to the disparity of each training, GA is run 10 times for each case of PID control strategy as shown in Table 4.1. The best set of parameters for each control strategy for each run of GA is recorded for further comparison, analysis and practical application. Statistical information including the worst, mean and best costs and the standard deviation for the 10 runs are collected. Among the 10 runs for each PID control strategy, the best set of parameters given by the best cost is used to implement

the corresponding PID controller. During the optimization, the lower and upper bounds (LB and UB) of PID gains and scaling factors are listed in Table 4.2, which are determined by trial and error for good control performance.

Table 4.2: Lower and upper bounds of parameters

K_{P_1}, K_{P_2}		K_{I_1}, K_{I_2}		K_{D_1}, K_{D_2}	
LB	UB	LB	UB	LB	UB
-10	0	-0.1	0	-10	0
α_p		α_r			
LB	UB	LB	UB		
0	1	0	1		

Due to a large number of variables and the highly nonlinear cost function (defined in the following subsection 4.4.5), especially for fuzzy PID controllers, GA may not be able to reach the global optimal solution. To speed up the training process, the initial population for fuzzy PID controllers is defined based on knowledge of the PID control strategy. It is known that the linear PID controller is a subset of T1 fuzzy PID controller, and the T1 fuzzy PID controller is a subset of IT2 fuzzy PID controller. It is thus reasonable that the best set of PID gains for linear PID controllers obtained by GA is employed as the initial PID gains for T1 fuzzy PID controllers for all rules. As a result, initially, the T1 fuzzy controller is equivalent to a linear PID controller. Similarly, the best set of PID gains and membership function parameters obtained for T1 fuzzy PID controller is employed as the initial set of PID gains and membership function parameters for IT2 fuzzy PID controller. That is to say, the "knowledge" of the PID control

strategy is utilized such that GA starts with a considerably good initial condition. In this way, although there is still the same number of variables to be trained, GA only needs to utilize the additional parameters and new structures (fuzzy rules and membership functions) provided by fuzzy PID controllers in order to obtain a better cost value.

4.4.5 Performance Index

The performance index is used to judge whether the control objective is achieved and show the merits of various control strategies. Different performance indices can be selected such as settling time, overshoot, steady error, mean absolute error (MAE), and mean square error (MSE). For the GA optimization, a well-defined performance index is required as the cost function. All parameters of the controllers are optimized by minimizing the cost function. In this chapter, the following index J is presented mainly based on MAE:

$$\begin{aligned} J = \frac{1}{n+1}\sum_{k=0}^{n}\Bigg(&\lambda_1|\Delta\mathrm{BIS}(t_k)| + \lambda_2|\frac{\Delta\mathrm{BIS}(t_k)-\Delta\mathrm{BIS}(t_{k-1})}{T}| \\ &+ \lambda_3|\frac{Cpt_{prop}(t_k)-Cpt_{prop}(t_{k-1})}{T}| \\ &+\lambda_4|\frac{Cpt_{remi}(t_k)-Cpt_{remi}(t_{k-1})}{T}|\Bigg) \\ &+ \lambda_5|\frac{\sum_{k=0}^{n}(Cpt_{prop}(t_k))}{\sum_{k=0}^{n}(Cpt_{prop}(t_k)+Cpt_{remi}(t_k))} - 0.5|, \end{aligned} \tag{4.17}$$

where $t_k = kT, k = 0, 1, 2, \ldots, n$, is the sampling time, and n is a positive integer; T is the sampling period; $\Delta\mathrm{BIS}(t_k) = \mathrm{BIS}_t(t_k) - \mathrm{BIS}(t_k)$, $\mathrm{BIS}_t(t_k)$ is the target BIS value at time t_k, and $\Delta\mathrm{BIS}(t_{-1}) = 0$; $Cpt_{prop}(t_k)$ and $Cpt_{remi}(t_k)$ are plasma concentration targets of propofol and remifentanil, respectively, and

$Cpt_{prop}(t_{-1}) = Cpt_{prop}(t_0)$, $Cpt_{remi}(t_{-1}) = Cpt_{remi}(t_0)$; $\lambda_1, \lambda_2, \ldots, \lambda_5$ are predefined weights.

In the cost function equation (4.17), the first term is MAE which aims at minimizing the difference between the current BIS value and its target. Unlike settling time, overshoot and steady error, MAE and MSE record the error information through all simulation periods which reflect more comprehensive properties of performance. The reason to choose MAE instead of MSE is that MSE amplifies the effect of large errors and then the optimization tries to minimize large errors which results in oscillation. On the other hand, MAE keeps the original weights on large and small errors leading to a mild and smooth response.

The three terms after the first term of equation (4.17) are the rate of change of $\Delta\text{BIS}(t_k)$, $Cpt_{prop}(t_k)$ and $Cpt_{remi}(t_k)$, respectively, which are designed to give a smooth response. The last term is to reduce the difference of the concentration of two drugs because they are equally important for different purposes during the anaesthesia. Serious differences in either of these two drugs will not provide an adequate anaesthesia.

4.5 Simulation Results

In this section, the simulation of the control of anaesthesia using the anaesthesia model in Figure 4.1 is implemented. Different control strategies in Table 4.1 are applied to regulate the BIS using the training profiles shown in Figure 4.4 for training and their control performance are verified by testing profiles shown in Figure 4.5. PID gains, parameters of scaling factors and membership functions are optimized by GA according to the cost function (4.17). Comparisons of per-

formance are made between the six cases. It should be noted that the simulation was carried out in discrete time. The PK model in equation (4.1) was discretized using the zero-order-hold (ZOH) assumption.

A real-coded GA available from Matlab global optimization toolbox is employed for the training. The control parameters of GA are listed in Table 4.3.

Table 4.3: Control parameters of GA.

Parameter	Value
Number of iterations	200
Size of population	100
Selection	Stochastic uniform selection function
Elitism	Elitism is implemented. The best two chromosomes are guaranteed to survive to the next population.
Crossover	Scattered crossover.
Crossover fraction	0.8
Mutation	Gaussian mutation.
Stopping criterion	It stops if the weighted average relative change in the best fitness function value over 100 generations is less than or equal to 10^{-6}.

The parameters in equation (4.17) are defined as follows: $n = 1000$, $T = 10$ seconds, $\lambda_1 = \lambda_5 = 1, \lambda_2 = \lambda_3 = \lambda_4 = 20$. It is worth mentioning that although the weight λ_1 is not the largest, the MAE is still the main contribution to the

total cost. The bounds of parameters in Table 4.2 are adopted for the training process of GA. By running GA 10 times for each case in Table 4.1, it obtains the statistical information of the cost J as shown in Table 4.4.

Table 4.4: The cost J from running GA 10 times

Case	Description	Best	Worst	Std	Mean
1	2 linear PID	4.0546	6.0544	0.6915	4.7190
2	2 T1 PID	3.8913	4.0479	0.0439	3.9273
3	2 IT2	3.8606	3.8899	0.0091	3.8825
4	1 linear PID with s.f.	4.0585	4.0594	0.0003	4.0587
5	1 T1 PID with T1 fuzzy with s.f.	3.9544	3.9780	0.0073	3.9696
6	1 IT2 PID with IT2 fuzzy with s.f.	3.9264	3.9437	0.0060	3.9380

Referring to Table 4.4, comparing with Cases 1 to 3, Case 3 offers the best cost and Case 2 comes second which comples with the theory. The same rank can be found in Cases 4 to 6. Comparing Cases 1 and 4, two-controller case is better than one-controller case, which can be also proved by comparing Cases 2 and 5, and Cases 3 and 6. The reason is that one-controller case has the constraint on the ratio of control signals between two drugs while two-controller case does not have such constraint. One-controller case is a subset of two-controller case. Although one-controller case performs worse, it has fewer parameters to be determined and thus reduces the computational demand and implementation cost of PID control strategy.

In spite of the "Best" cost, the "Std" (standard deviation) is descending from linear PID controllers to IT2 fuzzy PID controller except in Case 4. It provides

the information that the convergence gets easier for fuzzy PID controllers. The reason is that we use the best set of parameters in previous cases as the initial populations in subsequent training. It also indicates that the improvement becomes more and more difficult, and thus 10 times running offers similar results. The "Std" for two-controller cases is larger than the corresponding one-controller cases, which implies that the convergence for two-controller cases is harder due to more variables to be trained.

The best sets of parameters and membership functions are shown in Table 4.5 to Table 4.14. Corresponding membership functions are exhibited in Figure 4.9 to Figure 4.12. From the obtained membership functions, it can be summarized that points $|Np_2|$ and $|Pp_2|$ are preferred to be around 20 related to the training profiles we define in Figure 4.4. Considering that the only linguistic variable is $\Delta\text{BIS}(t_k)$ and the maximum change of $\text{BIS}_t(t_k)$ is ± 30 in the training profile, it is reasonable to choose $\Delta\text{BIS}(t_k) \in [-30, 30]$ as an estimated domain where the PID controllers work suggests that the fuzzy blending should start from around ± 20. For the IT2 membership functions of IT2 fuzzy PID controllers in Figure 4.10 and Figure 4.12 after training, it was found that the lower and upper membership functions are very close to each other such as membership functions of N and Z in Figure 4.10. The values of points (p_1 to p_7) associated with the IT2 membership functions are shown in Tables 4.9 and 4.14.

Table 4.5: Best set of parameters for two PID controllers

K_{P_1}	K_{I_1}	K_{D_1}
-0.0531	-0.0004	-0.0028
K_{P_2}	K_{I_2}	K_{D_2}
-0.2203	-0.0012	-0.0910

Table 4.6: Best set of parameters for two T1 fuzzy PID controllers

Rule	K_{P_1}	K_{I_1}	K_{D_1}
N	-0.0531	-0.0002	-0.5027
Z	-1.8031	-0.0004	-4.0368
P	-2.5531	-0.0004	-0.0028
	K_{P_2}	K_{I_2}	K_{D_2}
N	-0.2203	-0.0012	-0.0910
Z	-0.2203	-0.0012	-1.5909
P	-7.5162	-0.0012	-0.5910

Table 4.7: Best set of membership functions for two T1 fuzzy PID controllers

Rule	p_1	p_2	p_3
N	$-\infty$	-19.0370	7.0855
Z	-7.1950	5.7480	13.1011
P	-1.1593	19.0370	$+\infty$

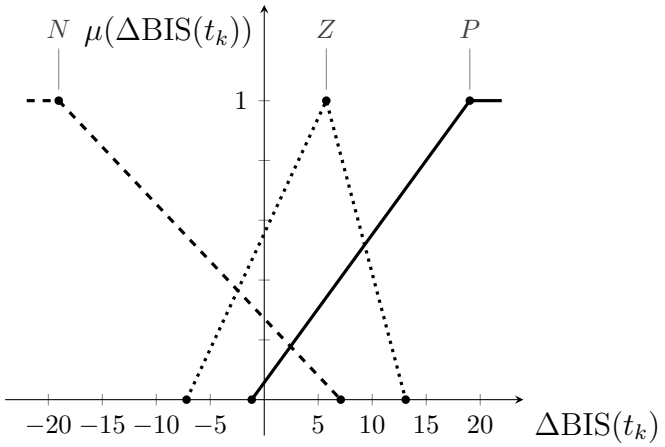

Figure 4.9: Membership functions for two T1 fuzzy PID controllers. Dashed line: membership function N. Dotted line: membership function Z. Solid line: membership function P.

Table 4.8: Best set of parameters for two IT2 fuzzy PID controllers

Rule	K_{P_1}	K_{I_1}
N	$[-0.0531, -0.0530]$	$[-0.0002, -0.0002]$
Z	$[-1.8031, -1.8022]$	$[-0.0004, -0.0004]$
P	$[-2.5531, -2.5481]$	$[-0.0020, -0.0020]$
	K_{D_1}	K_{P_2}
N	$[-0.5027, -0.4399]$	$[-0.2203, -0.2203]$
Z	$[-6.5368, -6.5352]$	$[-0.2203, -0.2203]$
P	$[-0.0013, -0.0013]$	$[-7.5162, -3.7581]$
	K_{I_2}	K_{D_2}
N	$[-0.0012, -0.0012]$	$[-0.0910, -0.0451]$
Z	$[-0.0012, -0.0012]$	$[-1.5909, -1.5870]$
P	$[-0.0012, -0.0012]$	$[-0.5910, -0.5310]$

Table 4.9: Best set of membership functions for two IT2 fuzzy PID controllers

Rule	p_1	p_2	p_3	p_4
N	$-\infty$	-19.0371	7.0975	$-\infty$
Z	-7.2069	5.7480	13.4781	-7.1951
P	-1.4565	19.0371	$+\infty$	-1.1593
	p_5	p_6	p_7	
N	-19.0371	7.0856	0.9990	
Z	5.7480	13.1011	0.9990	
P	19.0371	$+\infty$	0.8135	

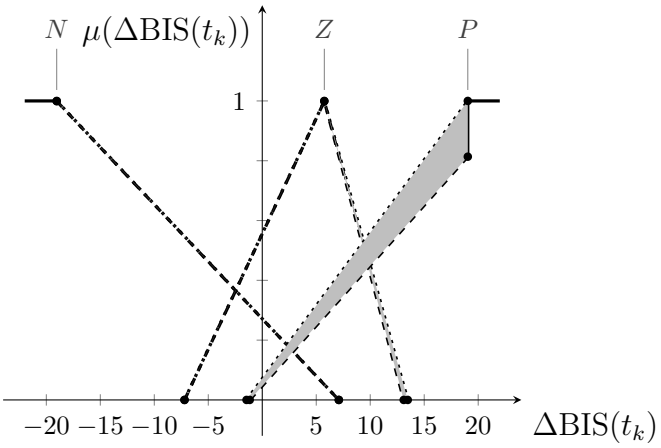

Figure 4.10: Membership functions for two IT2 fuzzy PID controllers. Dashed line: lower membership functions. Dotted line: upper membership functions. Solid line: the shoulder of membership functions.

Table 4.10: Best set of parameters for one PID controller

K_{P_1}	K_{I_1}	K_{D_1}	α_p	α_r
-0.9267	-0.0061	-0.6068	0.0598	0.1869

Table 4.11: Best set of parameters for one T1 fuzzy PID controller with T1 fuzzy scaling factors

Rule	K_{P_1}	K_{I_1}	K_{D_1}	α_p	α_r
N	-0.8642	-0.0061	-0.5443	0.0665	0.2189
Z	-1.7068	-0.0054	-9.6913	0.0725	0.1869
P	-8.6575	-0.0061	-6.6119	0.0602	0.1947

Table 4.12: Best set of membership functions for one T1 fuzzy PID controller with T1 fuzzy scaling factors

Rule	p_1	p_2	p_3
N	$-\infty$	-24.6107	-10.1748
Z	-11.4184	-6.9156	1.8562
P	-9.1078	24.6107	$+\infty$

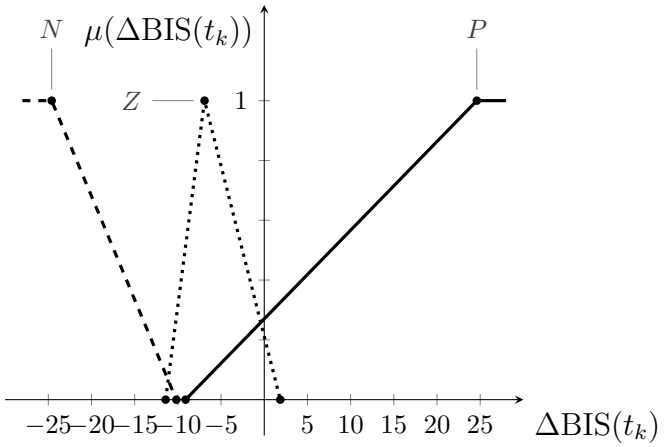

Figure 4.11: Membership functions for one T1 fuzzy PID controller with T1 fuzzy scaling factors. Dashed line: membership function N. Dotted line: membership function Z. Solid line: membership function P.

Table 4.13: Best set of parameters for one IT2 fuzzy PID controller with IT2 fuzzy scaling factors

Rule	K_{P_1}	K_{I_1}
N	$[-0.8642, -0.8372]$	$[-0.0061, -0.0061]$
Z	$[-1.7068, -1.6635]$	$[-0.0032, -0.0031]$
P	$[-8.6575, -8.6575]$	$[-0.0061, -0.0059]$
	K_{D_1}	α_p
N	$[-0.5443, -0.5273]$	$[0.0665, 0.0742]$
Z	$[-9.6913, -9.6393]$	$[0.1037, 0.1248]$
P	$[-7.2369, -7.2228]$	$[0.0563, 0.0594]$
	α_r	
N	$[0.2189, 0.2204]$	
Z	$[0.2162, 0.2407]$	
P	$[0.2045, 0.2728]$	

Table 4.14: Best set of membership functions for one IT2 fuzzy PID controller with IT2 fuzzy scaling factors

Rule	p_1	p_2	p_3	p_4
N	$-\infty$	-24.6105	-5.0849	$-\infty$
Z	-13.6412	-6.9156	2.2345	-13.6302
P	-9.1233	24.6105	$+\infty$	-9.1078
	p_5	p_6	p_7	
N	-24.6105	-7.0984	0.9990	
Z	-6.9156	1.8562	0.9990	
P	24.6105	$+\infty$	0.9990	

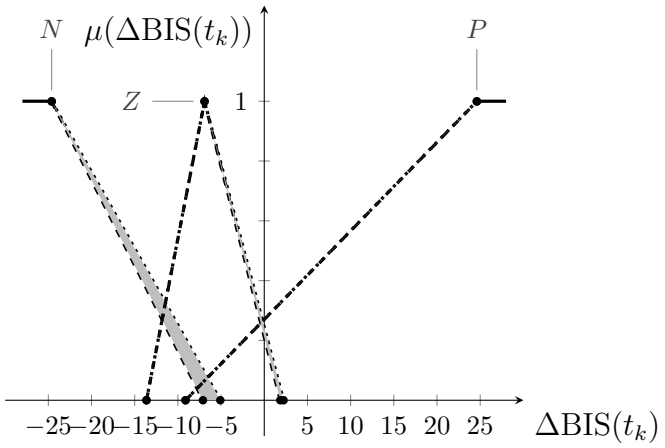

Figure 4.12: Membership functions for one IT2 fuzzy PID controllers with IT2 fuzzy scaling factors. Dashed line: lower membership functions. Dotted line: upper membership functions. Solid line: the shoulder of membership functions.

By applying the best sets of parameters to the training profile of BIS, the time

responses of BIS and corresponding drug concentration information are shown in Figure 4.13 to Figure 4.18 for Cases 1 to 6, respectively. By applying the best sets of parameters to the testing profile of BIS, the ones for the testing profile are exhibited in Figure 4.19 to Figure 4.24. The green line is drawn by $\mathrm{BIS}(t_k) = \mathrm{BIS}_t(t_k) \pm 2$. Despite BIS value during general anaesthesia is aimed to be with the 40 to 60 band, from the practical clinical point of view, the acceptable range of BIS is $[\mathrm{BIS}_t(t_k) - 5, \mathrm{BIS}_t(t_k) + 5]$. Therefore, if BIS is stabilized within the region bounded by the lower and upper green lines, the performance will be more than acceptable.

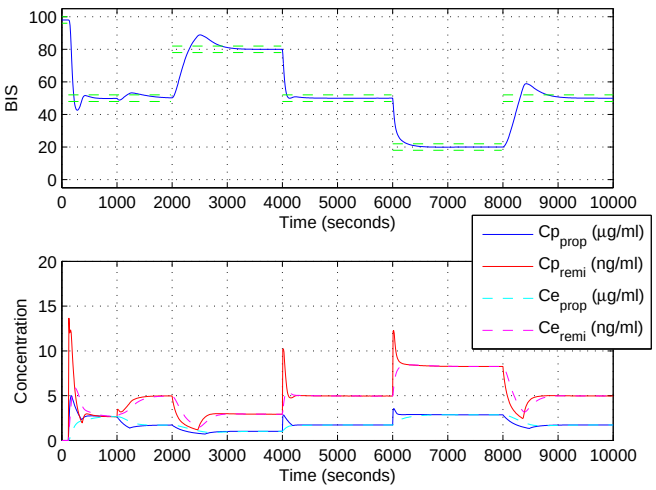

Figure 4.13: BIS and drug concentration for training profile by two PID controllers.

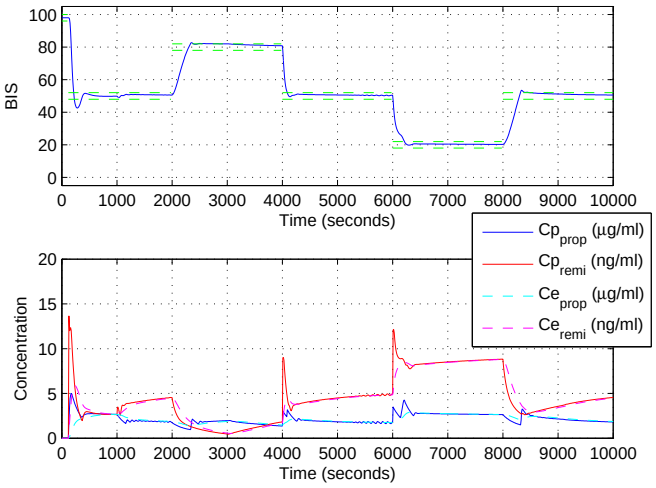

Figure 4.14: BIS and drug concentration for training profile by two T1 fuzzy PID controllers.

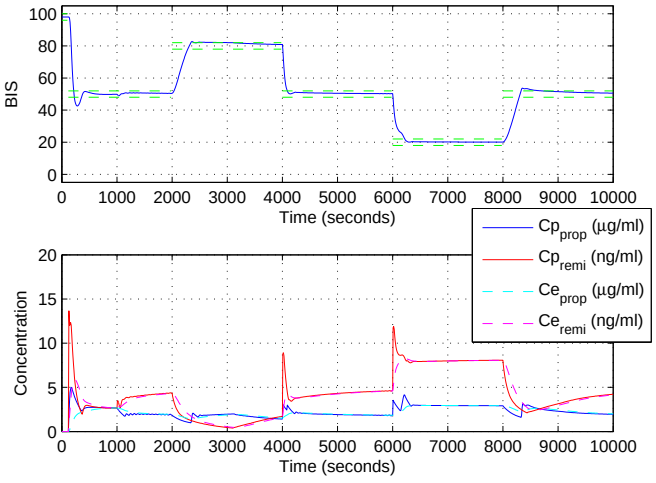

Figure 4.15: BIS and drug concentration for training profile by two IT2 fuzzy PID controllers.

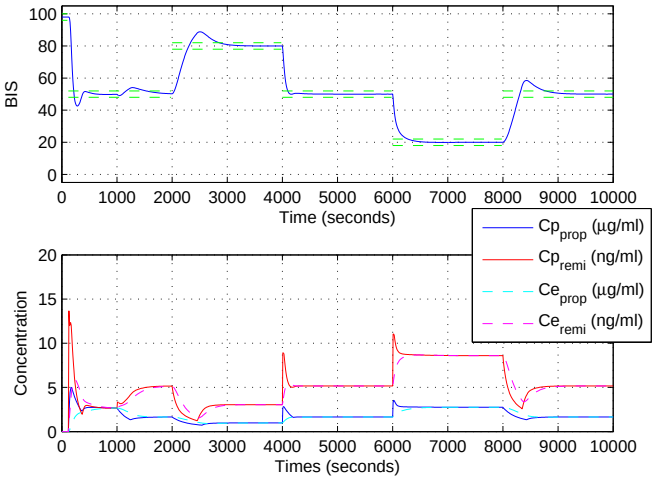

Figure 4.16: BIS and drug concentration for training profile by one PID controller with scaling factors.

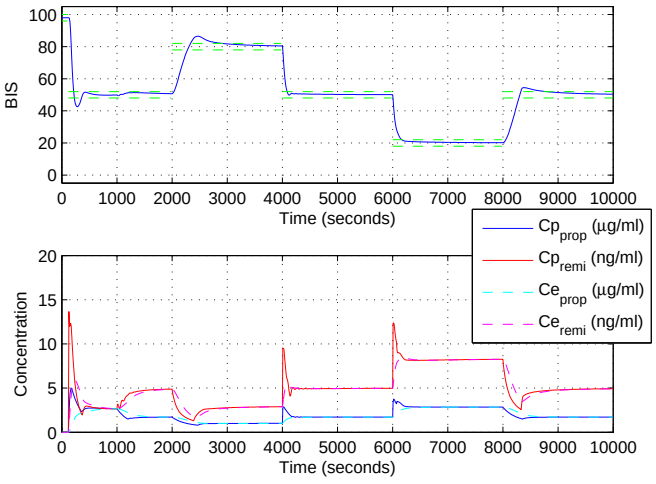

Figure 4.17: BIS and drug concentration for training profile by one T1 fuzzy PID controller with T1 fuzzy scaling factors.

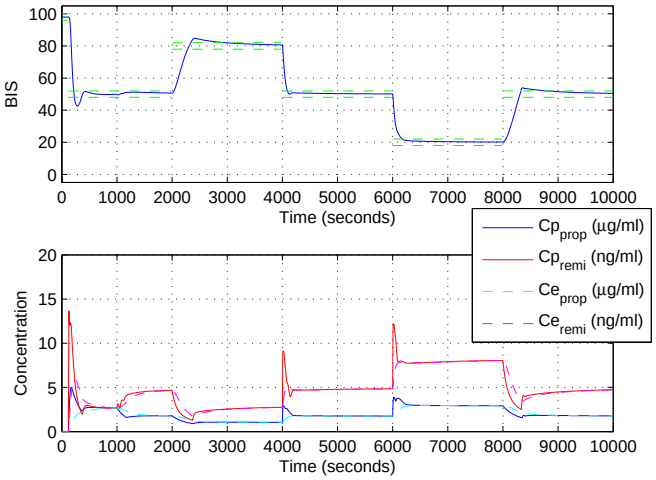

Figure 4.18: BIS and drug concentration for training profile by one IT2 fuzzy PID controller with IT2 fuzzy scaling factors.

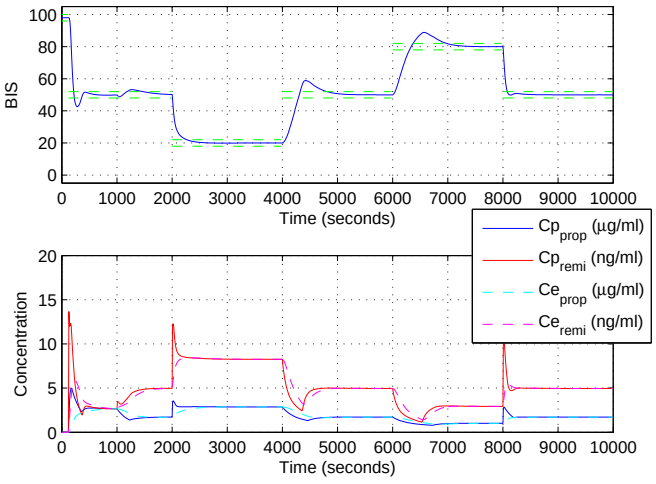

Figure 4.19: BIS and drug concentration for testing profile by two PID controllers.

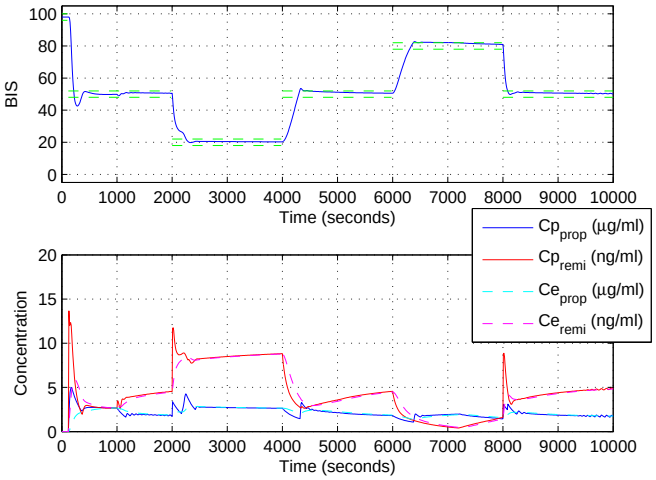

Figure 4.20: BIS and drug concentration for testing profile by two T1 fuzzy PID controllers.

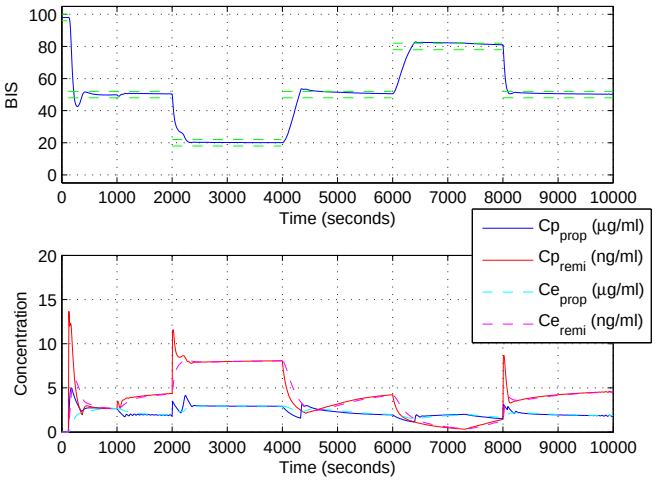

Figure 4.21: BIS and drug concentration for testing profile by two IT2 fuzzy PID controllers.

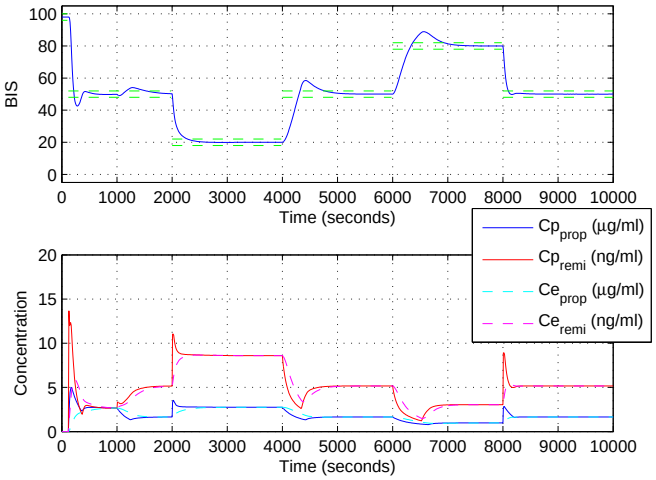

Figure 4.22: BIS and drug concentration for testing profile by one PID controller with scaling factors.

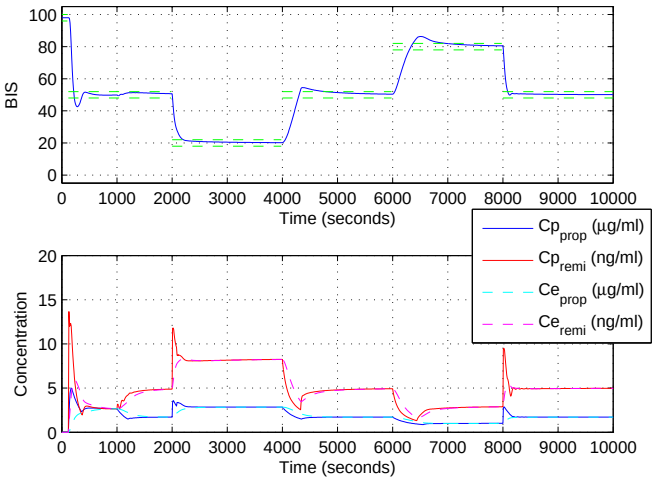

Figure 4.23: BIS and drug concentration for testing profile by one T1 fuzzy PID controller with T1 fuzzy scaling factors.

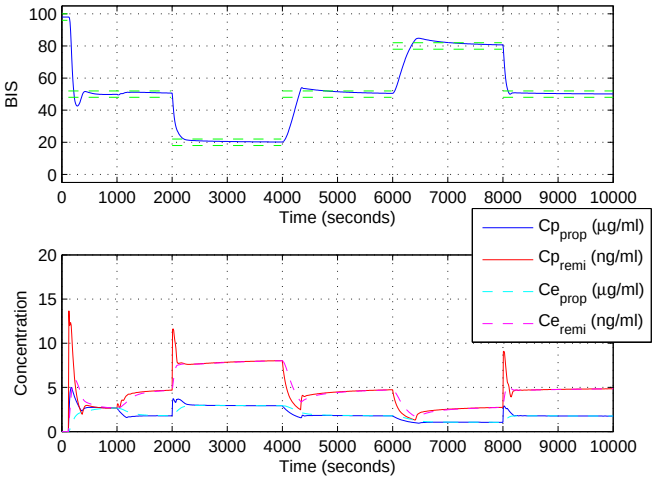

Figure 4.24: BIS and drug concentration for testing profile by one IT2 fuzzy PID controller with IT2 fuzzy scaling factors.

The figures show that all cases of PID control strategies succeed in tracking the BIS targets and maintaining BIS values. In terms of control performance, while the linear PID controllers have less steady error, fuzzy PID controllers have less overshoot and settling time. Since there is no rigorous requirement on small steady error, fuzzy PID controllers are preferable in that they are able to keep the BIS values within the regions bounded by the green lines with less overshoot and settling time. Both training and testing profiles demonstrate the same characteristics as discussed for the corresponding control strategies. Recalling a common controller with two linear PID controllers and predefined parameters is used to achieve the induction process for all cases, the proposed PID control strategies kick in at the start of the maintenance process. The switching point in the induction and maintenance process occurs at 1000 seconds which results in a small vibration.

The lower panels of Figure 4.19 to Figure 4.24 show the behavior of drug concentration. It can be seen that both Cp and Ce of propofol and remifentanil are adjusted by controllers according to target profiles. More importantly, they are adjusted in advance to decrease the overshoot. This is mainly because all controllers are based on PID control strategy, whose abilities are inherited. In addition, the total amount of remifentanil is larger than propofol, which illustrates that the remifentanil is more favorable to the stabilization of BIS than the propofol. This might be due to the faster acting time of remifentail comparatively to propofol. Although the total amount of remifentanil is larger, the cost function takes the difference of the amount of two drugs into consideration such that serious bias to remifentanil is avoided. Even though the slight bias towards remifentanil can be noticed overall the propofol and remifentanil Ce reached are within acceptable clinical boundaries even when the BIS target was set at 20, a value inferior to the safe interval of 40 to 60.

Overall, from a clinical point of view the results and performance obtained are acceptable, considering the lack of significant overshoot, the stability of the controller response and the ability to achieve the desired targets in a short time with clinically acceptable Ce. The controller also provided the expected response when the value of BIS target increased, and it stops the infusion of anaesthetic drugs and only restarts its infusion to avoid an overshot.

When the PID control strategies with the best set of parameters (offering the best cost of J) are employed to regulate the BIS value using the testing profile in Figure 4.5, their cost values are listed in Table 4.15. The rank of which is identical to the sequence of cost values from the training profile. It indicates that the advantage of fuzzy PID controller over linear PID controller exists not only

in the training profile, but also in various target profiles.

Table 4.15: The cost J for the testing profile

Case	1	2	3
Cost	4.1175	3.9888	3.9745
Case	4	5	6
Cost	4.1228	4.0408	4.0166

4.6 Summary

In this chapter, drug administration for anaesthesia has been realized by various PID control strategies. From the multivariable anaesthesia model with propofol and remifentanil based on 42 patients' clinical data constructed on Chapter 3, simulations have been conducted to regulate the output BIS value governed by this model using six control strategies including linear PID controllers, T1 fuzzy PID controllers and IT2 fuzzy PID controllers. These six strategies are separated into two groups, namely two controllers and one controller with scaling factors, to handle the co-administration of two drugs. Parameters of these controllers have all been optimized by GA subject to a performance index quantitatively measuring the control performance. In order to make the control sophisticated, target profiles have been designed for BIS regulation. Different target profiles have been utilized to test and verify the performance of controllers.

It has been demonstrated that the IT2 fuzzy PID controllers offer the best performance, and that the T1 fuzzy PID controllers come second.

Chapter 5

Conclusions and Future work

5.1 Conclusions

In this thesis PK/PD modelling able to describe the effect of anaesthetic drugs and automatic control of general anaesthesia was studied. A PK/PD model describing propofol and remifentanil interactions and their real clinical effect measured as BIS index were obtained through Hill and SVR-based techniques from clinical data obtained at King's College Hospital. Automatic control design for general anaesthesia was also proposed and tested based on the Hill-based PK/PD model obtained.

In order to achieve these a clinical platform for data recording was assembled in the operating theatre. This platform enabled the recording of a variety of clinical signals for a significant number of surgeries throughout the duration of this research project. The recorded data was analyzed and parameters of Hill's PD model were estimated by GA using different cost functions and least squares curve fitting method. Additional research performed with the aim of obtaining a more accurate PD model using SVR techniques with the consideration of different kernel functions and different model structure including additional information

such as nCO. As the SVR-based PD model is a non-parametric model an evaluation function to measure the modelling performance and validity of the developed SVR-based PD model was developed. SVR-based PD models have shown good performance results and adequacy depending on the kernel function.

A realistic PK/PD model is a requirement for developing automatic/advisor control structures for anaesthetic drugs, since all work has to be done in simulation, before it can be tested in animal or human patients. Therefore, the SVR model structure shows a great potential for practical implementation, both as simulation (learning) tool for clinicians and also as a basis for the development of an advisor control system for drug infusion for general anaesthesia under surgery.

One of the applications of these models is a simulation structure (incorporating alarms) that can help to train clinicians in the PK/PD changes and the effect of intravenous drugs. Disturbances can be used to simulate adverse and unexpected events (or just unstable situations), and in this way predict the effect of haemodynamic changes as well as concentration changes on the patients brain response.

The traditional PID controller, type-1 fuzzy PID controller and interval type-2 fuzzy PID controller were studied in this thesis. These control methodologies were designed and tested based on the PK/PD model within the patient's parameters. A fitness function to measure the regulation performance of BIS index value was generated allowing the use of GA to determine the controller gains by optimizing it.

The PK/PD model was generated from real clinical data based upon a typical PD modelling approach and a proposed SVR-based technique allowing incorporation of additional information. These are employed to describe the dynamics of a

patient's body responding to the anaesthetic drugs, propofol and remifentanil. A closed-loop system for drug administration such that BIS index can be controlled formed by the PK/PD model and a controller was evaluated.

5.2 Future work

As all the clinical data used in the project has been collected from one operating theatre with one anaesthesiologist, the type of surgeries and group of patient tends to be quite homogeneous. Having additional clinical data is an objective that should be followed in the future to improve PD models. All the data has been recorded as part of usual anaesthetic practice, however for the benefit of PD modelling, a clinical dataset incorporating unusual concentrations of anaesthetic and its effect would be of great value.

Even through it is not possible to perform online measurements of accurate anaesthetic drugs concentrations, all the PD modelling has been performed under estimated concentration, therefore obtaining actual drugs concentrations would be valuable.

In the future, further investigations can be carried out to control a general and non-parametric multivariable anaesthesia model rather than the model with parameters obtained from a specific group of patients.

Appendix A

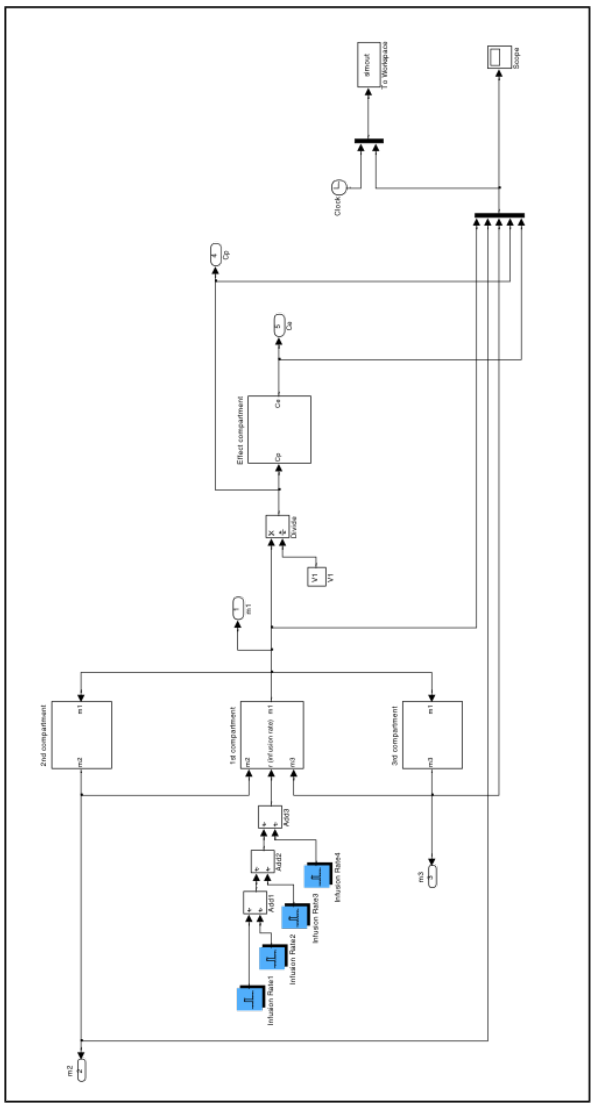

Figure 1: Implemented pharmacokinetic model.

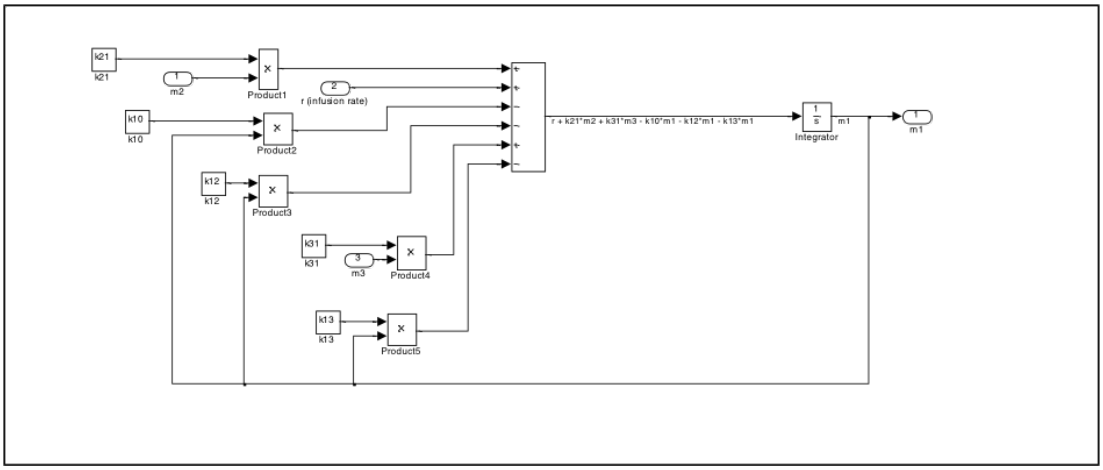

Figure 2: First compartment.

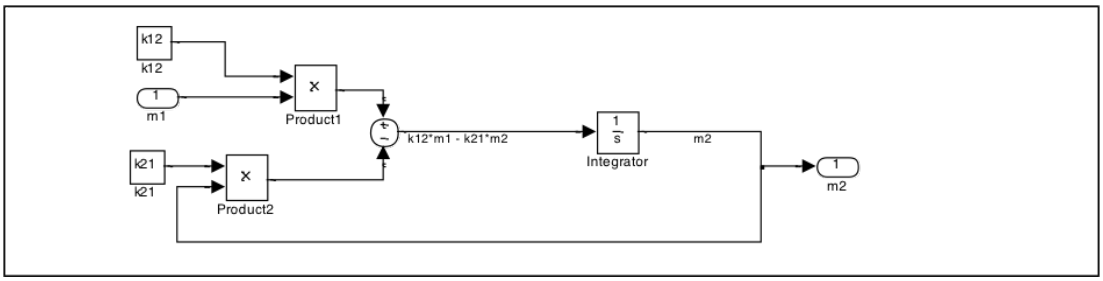

Figure 3: Second compartment.

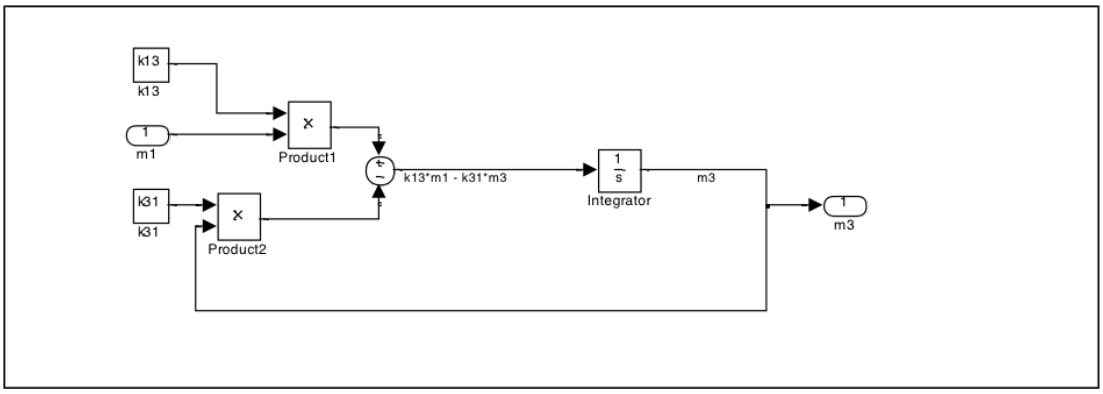

Figure 4: Third compartment.

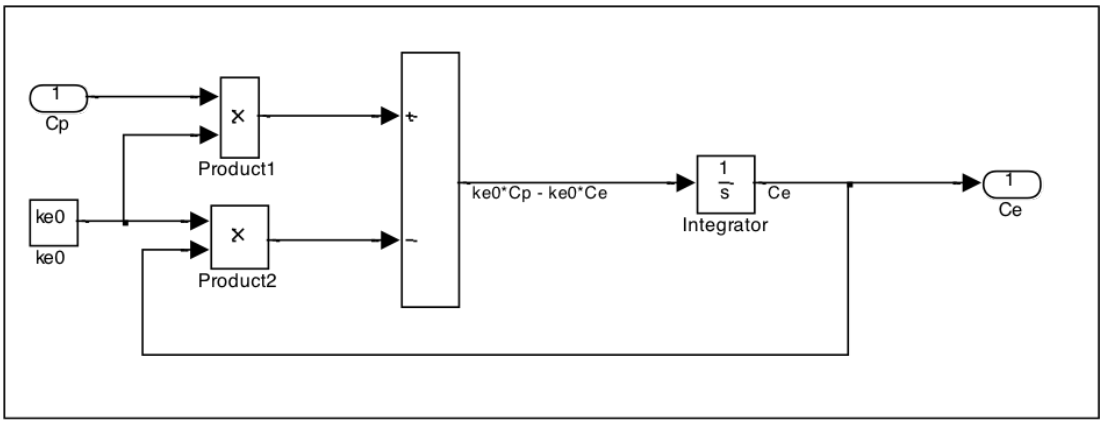

Figure 5: Effect-site compartment.

References

[1] A Absalom and M Struys. *An overview of TCI & TIVA*. Academia Press, 2007.

[2] A R Absalom, N Sutcliffe, and G N Kenny. Closed-loop control of anesthesia using bispectral index - Performance assessment in patients undergoing major orthopedic surgey under combined general and regional anesthesia. *Anesthesiology*, **96**[1]:67–73, 2002.

[3] Divya Agrawal, Sanjeev Kumar, Amod Kumar, Satinder Gombar, Anjan Trikha, and Sneh Anand. Design of an assistive anaesthesia drug delivery control using knowledge based systems. *Knowledge-Based Systems*, **31**[0]:1–7, 2012.

[4] J M Alvis, J G Reves, J A Spain, and L C Sheppard. Computer-assisted continuous infusion of the intravenous analgesic fentanyl during general anesthesia–an interactive system. *IEEE Trans Biomed Eng*, **32**[5]:323–329, 1985.

[5] J. A. Anderson. Reversal agents in sedation and anesthesia: a review. *Anesth Prog*, **35**[2]:43–7, 1988. Anderson, J A eng 1988/03/01 Anesth Prog. 1988 Mar-Apr;35(2):43-7.

[6] Kiam Heong Ang, Gregory Chong, and Yun Li. PID control system analysis, design, and technology. *IEEE Transactions on Control Systems Technology*, **13**[4]:559–576, Jul. 2005.

[7] H Araujo, D Green, and C S Nunes. Propofol requirements during BIS monitored total intravenous anesthesia, the influence of cardiac output (CO) on the pharmacokinetic model. In *Proceedings of the 3rd World Congress of Total Intravenous Anesthesia and Target Controlled Infusion*, 2011.

[8] Stéphane Bibian, Craig R. Ries, Mihai Huzmezan, and Guy Dumont. Introduction to automated drug delivery in clinical anesthesia. *European Journal of Control*, **11**[6]:535–557, 2005.

[9] N Bressan, A Castro, S Bras, H P Oliveira, L Ribeiro, D A Ferreira, L Antunes, P Amorim, and C S Nunes. Synchronization software for automation in anesthesia. *2007 Annual International Conference of the Ieee Engineering in Medicine and Biology Society, Vols 1-16*, pages 5298–5301 6760, 2007.

[10] J Bruhn, T W Bouillon, L Radulescu, A Hoeft, E Bertaccini, and S L Shafer. Correlation of approximate entropy, bispectral index, and spectral edge frequency 95 (SEF95) with clinical signs of "anesthetic depth" during coadministration of propofol and remifentanil. *Anesthesiology*, **98**[3]:621–627, 2003.

[11] Carefusion. Carefusion website. `http://www.carefusion.co.uk/medical-products/infusion/alaris-system/alaris_pk_syringe_pump.aspx`. Accessed: 2014-04.

[12] James Carvajal, Guanrong Chen, and Haluk Ogmen. Fuzzy PID controller: Design, performance evaluation, and stability analysis. *Information Sciences*, **123**[3]:249–270, Apr. 2000.

[13] Şaban Çetin and Ali Volkan Akkaya. Simulation and hybrid fuzzy-PID control for positioning of a hydraulic system. *Nonlinear Dynamics*, **61**[3]:465–476, Aug. 2010.

[14] Covidien. Covidien website - adult cardiac monitoring. `http://www.covidien.com/pace/pages.aspx?page=ClinicalEducation/Event/259958`. Accessed: 2014-04.

[15] Covidien. Covidien website - brain-monitoring monitors. `http://www.covidien.com/rms/products/brain-monitoring/monitors`. Accessed: 2014-04.

[16] Rachael Croft and Stephen Washington. Induction of anaesthesia. *Anaesthesia & Intensive Care Medicine*, **13**[9]:401–406, 2012.

[17] T. De Smet, M. M. Struys, M. M. Neckebroek, K. Van den Hauwe, S. Bonte, and E. P. Mortier. The accuracy and clinical feasibility of a new bayesian-based closed-loop control system for propofol administration using the bispectral index as a controlled variable. *Anesthesia and Analgesia*, **107**:1200–1210, 2008.

[18] Xinyu Du and Hao Ying. Derivation and analysis of the analytical structures of the interval type-2 fuzzy-PI and PD controllers. *IEEE Transactions on Fuzzy Systems*, **18**[4]:802–814, Aug. 2010.

[19] Guy A. Dumont, Arturo Martinez, and J. Mark Ansermino. Robust control of depth of anesthesia. *International Journal of Adaptive Control and Signal Processing*, **23**[5]:435–454, 2009.

[20] Mohammad El-Bardini and Ahmad M. El-Nagar. Direct adaptive interval type-2 fuzzy logic controller for the multivariable anaesthesia system. *Ain Shams Engineering Journal*, **2**[34]:149–160, 2011.

[21] R K Ellerkmann, M Soehle, T M Alves, V M Liermann, I Wenningmann, H Roepcke, S Kreuer, A Hoeft, and J Bruhn. Spectral entropy and bispectral index as measures of the electroencephalographic effects of propofol. *Anesthesia and Analgesia*, **102**[5]:1456–1462, 2006.

[22] E Gepts, F Camu, I D Cockshott, and E J Douglas. Disposition of Propofol Administered as Constant Rate Intravenous Infusions in Humans. *Anesthesia and Analgesia*, **66**[12]:1256–1263, 1987.

[23] P. Grieder, A. Gentilini, M. Morari, and T.W. Schnider. Robust adaptive control of hypnosis during anesthesia. In *Proceedings of the 23rd Annual International Conference of the IEEE Engineering in Medicine and Biology Society*, **2**, pages 2055–2058, 2001.

[24] Wassim M. Haddad, Tomohisa Hayakawa, and James M. Bailey. Adaptive control for nonlinear compartmental dynamical systems with applications to clinical pharmacology. *Systems & Control Letters*, **55**[1]:62–70, 2006.

[25] Hani Hagras. Type-2 FLCs: a new generation of fuzzy controllers. *IEEE Computational Intelligence Magazine*, **2**[1]:30–43, Feb. 2007.

[26] Jin Oh Hahn, Guy A. Dumont, and J. Mark Ansermino. Robust closed-loop control of hypnosis with propofol using WAVCNS index as the controlled variable. *Biomedical Signal Processing and Control*, **7**[5]:517–524, 2012.

[27] Christopher Hawthorne and Nick Sutcliffe. Total intravenous anaesthesia. *Anaesthesia & Intensive Care Medicine*, **14**[3]:129–131, 2013.

[28] N. H. Holford and L. B. Sheiner. Kinetics of pharmacologic response. *Pharmacol Ther*, **16**[2]:143–66, 1982. Holford, N H Sheiner, L B eng GM 26676/GM/NIGMS NIH HHS/ GM20872/GM/NIGMS NIH HHS/ Research Support, U.S. Gov't, P.H.S. Review ENGLAND 1982/01/01 Pharmacol Ther. 1982;16(2):143-66.

[29] D M Honan, P J Breen, J F Boylan, N J McDonald, and T D Egan. Decrease in bispectral index preceding intraoperative hemodynamic crisis: evidence of acute alteration of propofol pharmacokinetics. *Anesthesiology*, **97**[5]:1303–1305, 2002.

[30] Robert John and Simon Coupland. Type-2 fuzzy logic: A historical view. *IEEE Computational Intelligence Magazine*, **2**[1]:57–62, Feb. 2007.

[31] Scott D. Kelley. *Monitoring Consciousness: Using the Bispectral Index During Anesthesia - A Pocket Guide for Clinicians*. Covidien, second edition, 2010.

[32] S. E. Kern, G. Xie, J. L. White, and T. D. Egan. A response surface analysis of propofol-remifentanil pharmacodynamic interaction in volunteers. *Anesthesiology*, **100**:1374–1381, 2004.

[33] Dae Woo Kim, Jin Deok Joo, Jang Hyeok In, Yeon Su Jeon, Hong Soo Jung, Kyeong Bae Jeon, Jae Sik Park, and Jin Woo Choi. Comparison of the recovery and respiratory effects of aminophylline and doxapram following total intravenous anesthesia with propofol and remifentanil. *Journal of Clinical Anesthesia*, **25**[3]:173–176, 2013.

[34] I. Kissin. A concept for assessing interactions of general anesthetics. *Anesthesia and Analgesia*, **85**:204–210, 1997.

[35] T Kurita, K Morita, T Kazama, and S Sato. Influence of cardiac output on plasma propofol concentrations during constant infusion in swine. *Anesthesiology*, **96**[6]:1498–1503, 2002.

[36] H. K. Lam, Hongyi Li, Christian Deters, H Wuerdemann, E Secco, and Kaspar Althoefer. Control design for interval type-2 fuzzy systems under imperfect premise matching. *IEEE Trans. Industrial Electronics*, **61**[2]:956–968, Feb. 2014.

[37] H. K. Lam and L. D. Seneviratne. Stability analysis of interval type-2 fuzzy-model-based control systems. *IEEE Trans. Syst., Man and Cybern., Part B: Cybernetics*, **38**[3]:617–628, Jun. 2008.

[38] LiDCO. Lidco website. `http://www.lidco.com/clinical/downloads/library.php`. Accessed: 2014-04.

[39] J. Liu, H. Singh, and P. F. White. Electroencephalographic bispectral index correlates with intraoperative recall and depth of propofol-induced sedation. *Anesthesia and Analgesia*, **84**:185–189, 1997.

[40] Mahdi Mahfouf, Catarina S. Nunes, Derek A. Linkens, and John E. Peacock. Modelling and multivariable control in anaesthesia using neural-fuzzy paradigms: Part II. Closed-loop control of simultaneous administration of propofol and remifentanil. *Artificial Intelligence in Medicine*, **35**[3]:207–213, 2005.

[41] B Marsh, M White, N Morton, and G N Kenny. Pharmacokinetic model driven infusion of propofol in children. *Br J Anaesth*, **67**[1]:41–48, 1991.

[42] Jerry M Mendel. Type-2 fuzzy sets and systems: an overview. *IEEE Computational Intelligence Magazine*, **2**[1]:20–29, Jun. 2007.

[43] Jerry M Mendel, Robert Ivor John, and Feilong Liu. Interval type-2 fuzzy logic systems made simple. *IEEE Transactions on Fuzzy Systems*, **14**[6]:808–821, Dec. 2006.

[44] Ronald D Miller. *Miller's anesthesia*. Churchill Livingstone, New York, 6th ed edition, 2005.

[45] C F Minto, T W Schnider, T D Egan, E Youngs, H J Lemmens, P L Gambus, V Billard, J F Hoke, K H Moore, D J Hermann, K T Muir, J W Mandema, and S L Shafer. Influence of age and gender on the pharmacokinetics and pharmacodynamics of remifentanil. I. Model development. *Anesthesiology*, **86**[1]:10–23, 1997.

[46] C F Minto, T W Schnider, T G Short, K M Gregg, A Gentilini, and S L Shafer. Response surface model for anesthetic drug interactions. *Anesthesiology*, **92**[6]:1603–1616, 2000.

[47] Iain Moppett. Inhalational anaesthetics. *Anaesthesia & Intensive Care Medicine*, **9**[12]:567–572, 2008.

[48] Eric P. Mortier and Michel M.R.F. Struys. Monitoring the depth of anaesthesia using bispectral analysis and closed-loop controlled administration of propofol. *Best Practice & Research Clinical Anaesthesiology*, **15**[1]:83–96, 2001.

[49] Kannan Moudgalya. *Digital Control*. Wiley-Interscience, 2007.

[50] C S Nunes and T F Mendonça. Modelling propofol and remifentanil pharmacodynamic interaction using two different pharmacokinetic models: a comparative study. *Cadernos de Matematica*, 2005.

[51] D A Ohara, D K Bogen, and A Noordergraaf. The Use of Computers for Controlling the Delivery of Anesthesia. *Anesthesiology*, **77**[3]:563–581, 1992.

[52] H. Panagopoulos, K.J. Astrom, and T. Hagglund. Design of PID controllers based on constrained optimisation. *IEEE Proceedings of Control Theory and Applications*, **149**[1]:32–40, 2002.

[53] V. Sartori, P.M. Schumacher, T. Bouillon, M. Luginbuehl, and M. Morari. On-line estimation of propofol pharmacodynamic parameters. In *IEEE-EMBS 2005. 27th Annual International Conference of the Engineering in Medicine and Biology Society*, pages 74–77, 2005.

[54] T W Schnider, C F Minto, P L Gambus, C Andresen, D B Goodale, S L Shafer, and E J Youngs. The influence of method of

administration and covariates on the pharmacokinetics of propofol in adult volunteers. *Anesthesiology*, **88**[5]:1170–1182, 1998.

[55] Jiann Shing Shieh, Ming Hsien Kao, and Chien Chiang Liu. Genetic fuzzy modelling and control of bispectral index (BIS) for general intravenous anaesthesia. *Medical Engineering & Physics*, **28**[2]:134–148, 2006.

[56] Alex J Smola and Bernhard Schölkopf. A tutorial on support vector regression. *Statistics and Computing*, **14**[3]:199–222, 2004.

[57] Kristian Soltesz, Jin Oh Hahn, Tore Hägglund, Guy A. Dumont, and J. Mark Ansermino. Individualized closed-loop control of propofol anesthesia: a preliminary study. *Biomedical Signal Processing and Control*, **8**[6]:500–508, November 2013.

[58] Michel M. Struys, T. De Smet, S. Greenwald, A. R. Absalom, S. Bingé, and E. P. Mortier. Performance evaluation of two published closed-loop control systems using bispectral index monitoring: a simulation study. *Anesthesiology*, **100**:640–647, 2004.

[59] Michel M. Struys, Eric P. Mortier, and Tom De Smet. Closed loops in anaesthesia. *Best Practice & Research Clinical Anaesthesiology*, **20**[1]:211–220, 2005.

[60] C H Ting, R H Arnott, D A Linkens, and A Angel. Migrating from target-controlled infusion to closed-loop control in general anaesthesia. *Comput Methods Programs Biomed*, **75**[2]:127–139, 2004.

[61] H E Vereecke, P M Vasquez, E W Jensen, O Thas, R Vandenbroecke, E P Mortier, and M M Struys. New composite index based on midlatency auditory evoked potential and electroencephalographic parameters to optimize correlation with propofol effect site concentration: comparison with bispectral index and solitary used fast extracting auditory evoked po. *Anesthesiology*, **103**[3]:500–507, 2005.

[62] Per Westrin. 6 intravenous and inhalational anaesthetic agents. *Bailliere's Clinical Anaesthesiology*, **10**[4]:687–715, 1996.